

Dissertation zur Erlangung des Doktorgrades
der Fakultät für Chemie und Pharmazie
der Ludwig-Maximilians-Universität München

Analysis and control of the manufacturing process and
the release properties of PLGA microparticles for
sustained delivery of a poorly water-soluble drug

Kerstin Vay

aus

Eberbach (Deutschland)

2012

Erklärung

Diese Dissertation wurde im Sinne von § 7 der Promotionsordnung vom 28. November 2011 von Herrn Prof. Dr. Wolfgang Frieß betreut.

Eidesstattliche Versicherung

Diese Dissertation wurde eigenständig und ohne unerlaubte Hilfe erarbeitet.

München,

.....

Dissertation eingereicht am 09.07.2012

1. Gutachter: Prof. Dr. Wolfgang Frieß

2. Gutachter: Prof. Dr. Gerhard Winter

Mündliche Prüfung am 19.09.2012

Acknowledgements

This thesis has been acquired at the Department for Pharmaceutical Development at Sandoz in Kundl under the supervision of Prof. Dr. Wolfgang Frieß and Dr. Stefan Scheler.

I want to express my deepest gratitude to Prof. Dr. Wolfgang Frieß for his scientific guidance throughout the last years and the professional input into this work. I deeply appreciated his ongoing encouragement and help especially during the last 2 years of my thesis. Furthermore I want to thank him for inviting me to different social events like skiing or hiking trips.

I am deeply indebted to Dr. Stefan Scheler for giving me the opportunity to work within this interesting project and for being the second scientific advisor in the last years. Thank you for all your support and advice, for the numerous fruitful discussions and for encouraging me to present parts of my work at scientific conferences.

Moreover I want to thank Prof. Dr. Gerhard Winter for taking over the co-referee of my work.

I am very grateful to the Department of Pharmaceutical Development at Sandoz in Kundl for the outstanding cooperation, financial support and the opportunity to work with latest technology.

I would like to thank all former and present colleagues from the research groups of Prof. Dr. Frieß and Prof. Dr. Winter. Thank you for the warm welcome and your support. Particularly I want to thank Dr. Michael Wiggendorf for the introduction into the differential scanning calorimetry.

I want to thank all members of the department of pharmaceutical development at Sandoz in Kundl for their great support throughout my PhD. Special thanks to Geli and Jürgen for their support of the practical work in the lab, to Regis, Edith, Bruno, Christian, and Günther for their analytical support, Georg for his innovative idea for preparation of SEM samples and Marion for the quick and accurate proof reading.

Furthermore I want to thank Dr. Michael Noisternig and Prof. Dr. Ulrich Griesser from the Department of Pharmaceutical Technology of the University of Innsbruck for their support in mercury intrusion porosimetry.

Besides the abovementioned persons from university and industry I want to thank my family and especially my parents for all the support and encouragement they gave me all over the years.

TABLE OF CONTENTS

CHAPTER 1.....	1
INTRODUCTION AND OBJECTIVE OF THE THESIS	1
ABSTRACT	1
1 INTRODUCTION	2
2 ENCAPSULATION PROCESSES.....	5
2.1 <i>Coacervation</i>	5
2.2 <i>Spray drying, spray congealing</i>	6
2.3 <i>Methods using supercritical fluids (SCF)</i>	7
2.4 <i>Solvent removal process</i>	7
3 THE SOLVENT REMOVAL PROCESS FOR MANUFACTURING OF PLGA MICROSPHERES ON AN INDUSTRIAL SCALE	10
3.1 <i>Influences of process parameters on the solidification rate of the microparticles</i>	12
3.2 <i>Influence of the solidification rate on particle properties</i>	13
4 OBJECTIVE OF THE THESIS	15
5 REFERENCES	16
CHAPTER 2.....	21
APPLICATION OF HANSEN SOLUBILITY PARAMETERS FOR UNDERSTANDING AND PREDICTION OF DRUG DISTRIBUTION IN MICROSPHERES	21
ABSTRACT	21
1 INTRODUCTION	22
2 MATERIALS AND METHODS.....	24
2.1 <i>Materials</i>	24
2.2 <i>Determination of the solubility of the API in PLGA by differential scanning calorimetry (DSC)</i>	24
2.3 <i>Determination of the morphological state of the drug by X-Ray powder diffractometry</i>	25
2.4 <i>Determination of the solubility</i>	25
3 RESULTS AND DISCUSSION	27
3.1 <i>Determination of the solubility parameters</i>	27
3.1.1 <i>Experimental determination</i>	27
3.1.2 <i>Estimation of the solubility parameters by group contribution methods</i>	29
3.2 <i>Estimation of the solubility of the drug substance in different solvents and in PLGA</i>	32
3.3 <i>Prediction of drug-polymer-interactions during processing based on solubility parameters and effects on the properties of the resulting microspheres</i>	36
4 CONCLUSIONS	41
5 REFERENCES	43
CHAPTER 3.....	47
CONTROL OF THE DROPLET SIZE OF THE PRIMARY EMULSION IN A SOLVENT REMOVAL PROCESS	47
ABSTRACT	47
1 INTRODUCTION	48
2 MATERIALS AND METHODS.....	49
2.1 <i>Materials</i>	49
2.2 <i>Determination of the droplet size – single particle optical sizing (SPOS)</i>	49
2.3 <i>Formation of the primary emulsion</i>	49
3 RESULTS AND DISCUSSION	50

4	CONCLUSION	56
5	REFERENCES	57

CHAPTER 459

UNDERSTANDING REFLECTION BEHAVIOR AS A KEY FOR INTERPRETING COMPLEX SIGNALS IN FBRM MONITORING OF MICROPARTICLE PREPARATION PROCESSES59

ABSTRACT	59
1 INTRODUCTION.....	60
2 MATERIALS AND METHODS	62
2.1 <i>Materials</i>	62
2.2 <i>Microparticle preparation</i>	62
2.3 <i>Methods</i>	63
2.3.1 Focused beam reflectance measurement.....	63
2.3.2 Single particle optical sizing (SPOS).....	64
2.3.3 Microscopical image analysis	64
3 RESULTS AND DISCUSSION	64
3.1 <i>Single object measurements</i>	64
3.2 <i>Measurements of monodisperse particle collectives</i>	66
3.2.1 Influence of the position of the focal point.....	73
3.2.2 Influence of the particle concentration.....	74
3.2.3 CLDs of heterodisperse particle collectives and emulsion droplets.....	76
3.3 <i>Online-monitoring of a microparticle preparation process by FBRM</i>	80
4 CONCLUSIONS	86
5 REFERENCES	88

CHAPTER 591

A DETAILED VIEW OF MICROPARTICLE FORMATION BY IN-PROCESS MONITORING OF THE GLASS TRANSITION TEMPERATURE91

ABSTRACT	91
1 INTRODUCTION.....	92
2 MATERIALS AND METHODS	93
2.1 <i>Materials</i>	93
2.2 <i>Microparticle preparation</i>	94
2.3 <i>Analytical methods</i>	94
2.3.1 Thermal analysis – Differential scanning calorimetry (DSC).....	94
2.3.2 Particle size – Single Particle Optical Sizing (SPOS)	95
2.3.3 Particle morphology characterization - Scanning electron microscopy (SEM).....	95
2.3.4 Drug distribution – Chemical Imaging.....	95
2.3.5 Drug loading and in-vitro dissolution studies –RP-HPLC	96
2.3.6 Molecular weight of PLGA – SE-HPLC.....	96
3 RESULTS AND DISCUSSION	96
3.1 <i>Effects on the glass transition temperature of the polymer</i>	96
3.2 <i>Effect of the process temperature on the particle properties</i>	100
3.2.1 Influence on the particle morphology.....	100
3.2.2 Influence on the encapsulation efficiency and molecular weight.....	104
3.2.3 Influence on the drug release rate.....	105
3.2.4 Influence of the polymer chain length	109
3.2.5 Influence of solvent removal rate	111
3.2.6 Influence of a subsequent resuspension of the particles with ethanol.....	113
4 CONCLUSIONS	116
5 REFERENCES	118

CHAPTER 6.....	121
A NOVEL METHOD FOR THE DETERMINATION OF THE INTRAPARTICULATE PORE VOLUME AND STRUCTURE OF MICROSPHERES	121
ABSTRACT	121
1 INTRODUCTION	122
2 MATERIALS AND METHODS.....	124
2.1 <i>Materials</i>	124
2.2 <i>Microparticle preparation</i>	124
2.3 <i>Analytical methods</i>	125
2.3.1 Single particle optical sensing (SPOS) - light obscuration.....	125
2.3.2 Gas pycnometry	125
2.3.3 Mercury intrusion porosimetry	126
2.3.4 Specific surface area.....	126
2.3.5 Scanning electron microscopy.....	126
3 RESULTS	126
4 DISCUSSION	132
4.1 <i>Interparticulate volume</i>	132
4.2 <i>Intraparticulate volume</i>	134
4.3 <i>Porosity profiles</i>	136
5 CONCLUSIONS	139
6 REFERENCES	140
CHAPTER 7	143
SUMMARY OF THE THESIS	143
ANNEXES	146
ABBREVIATIONS	146
LIST OF PUBLICATIONS AND PRESENTATIONS	148

CHAPTER 1

Introduction and objective of the thesis

Abstract

Poly(lactide-co-glycolide) (PLGA) microparticles as an injectable dosage form for a controlled release of peptides, proteins or poorly water soluble drugs are of considerable interest for research as well as for commercial scope since the 1970's. Also there is a variety of techniques to encapsulate a drug substance in a PLGA matrix, only few of them are successfully used for the industrial scale production of a microparticulate dosage form. One of the oldest and most common used techniques is the emulsion solvent removal technique. The properties of PLGA microparticles prepared by this technique considerably depend on the applied process parameters. Especially the rate of solidification of the liquid emulsion droplets to solid microparticles has an impact on their morphology and physico-chemical properties. The relationship between process parameters, solidification rate and the properties of the resulting microspheres and especially the control of the latter are still not fully understood. A better understanding of this interrelation is necessary for the control and up-scale of a microparticle manufacturing process.

1 Introduction

The encapsulation of drugs into a polymeric matrix can greatly enhance the drug safety and efficiency and allows modifying the release kinetics. Thus the interest and research in these controlled release dosage forms increased steadily over the past decades. Polymeric matrix systems are available e.g. for per oral (e.g. embedding the drug substance in an insoluble PVC-matrix (Duriles[®] technology)), transdermal (matrix patches) as well as for parenteral application (e.g. as monolithic implants or microspheres). The release period from these dosage forms can range from several hours to a few months.

As a large proportion of new drugs are peptides or proteins with short half-life or low molecular compounds with poor solubility, biodegradable polymer microparticles for parenteral application provide a suitable delivery strategy. With Lupron[®] Depot, a sustained release dosage form of Leuproreline acetate for the treatment of prostate cancer or endometriosis, sales of 1.97 billion US\$ were generated in 2009. In the same year with Risperdal consta[®], a drug product for the treatment of schizophrenia, sales of 1.42 billion US\$ were achieved [1]. These data underscore the commercial relevance of these dosage forms which is still increasing.

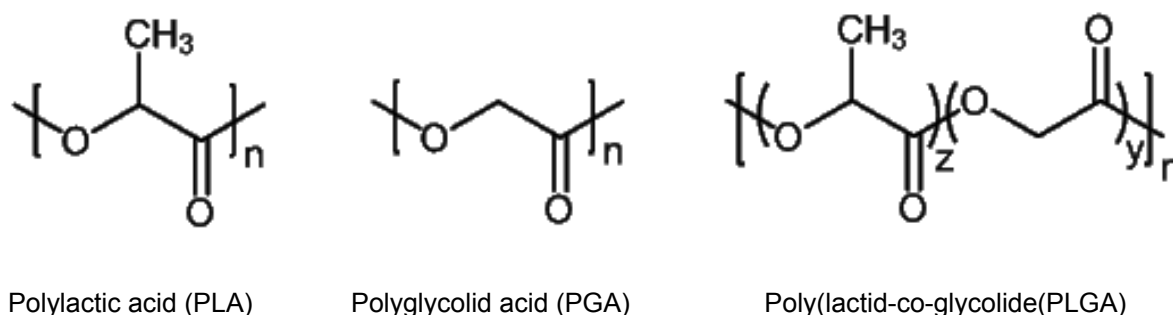
Biodegradable microparticles provide a variety of advantages like the maintenance of drug levels in a therapeutically desired range, a reduction of side effects and a decreased frequency of drug administration leading to an enhanced compliance rate [2, 3]. Especially concerning psychological diseases long acting dosage forms are able to increase the success of the treatment, as patients may be reluctant to take these medications on their own.

Biodegradable polyesters, like Poly(lactide-co-glycolide) (PLGA) are among the most often used biodegradable polymers for parenteral matrix formulations, as they are biocompatible and degrade into non-toxic oligomers and finally monomers. With PLGA different release periods can be obtained by utilizing different ratios of lactic to glycolic acid in the polymer. Higher lactic acid content leads to a prolonged release because of the enhanced hydrophobicity, whereas polymers with a higher content of glycolic acid degrade more rapidly since water can faster penetrate into the more hydrophilic polymer matrix.

In addition, there is a multitude of different methods for the manufacturing of PLGA microparticles. The appropriate choice is thereby primarily determined by the

properties of the polymer, the drug to be encapsulated and the targeted release profile. The solvent extraction evaporation method is a preferred and versatile technique. In this process a multitude of process parameters has an impact on the microparticle properties and the resulting release rate. A thorough understanding of the individual process steps is essential for the development of a product with specific characteristics. This also includes monitoring and control of the process by Process Analytical Technologies (PAT).

According to IUPAC polymer microparticles are particles of any shape or form with a size of 0.1 to 100 μm . In pharmaceutical literature the term “microparticles” is also used for particles up to 1000 μm . Two general morphologies of microparticles can be distinguished: i) microspheres, in which the drug substance is homogeneously dissolved or dispersed within a polymeric matrix and ii) microcapsules, in which a drug containing core is completely surrounded by a polymer shell; the core can be solid, liquid or gaseous. Both morphologies differ in their release behavior. The main advantage of microspheres is that severe drug burst due to a rupture of the polymer shell cannot occur. Since 1970 biodegradable polymers are designed and used for controlled release applications. One of the first and most widely used polymer groups are the polymers and copolymers of lactic and glycolic acid: PLA, PLG and PLGA (Fig. 1).



Poly(lactic acid) (PLA)

Poly(glycolic acid) (PGA)

Poly(lactid-co-glycolide) (PLGA)

Figure 1: Molecular structure of poly(lactic acid), poly(glycolic acid) and poly(lactid-co-glycolide) (PLGA)

Due to their biodegradation these polyesters do not require surgical removal and the resulting monomers, lactic and glycolic acid are two physiological occurring substances and pose no major toxicological problems. Another benefit of PLGA is that the drug release duration can be tailored from several days to more than one year, depending on the composition of the polymer, the geometry of the device, the method of preparation and the drug substance to be encapsulated. The drug release from PLGA microspheres is a complex process depending on two

mechanisms, the diffusion controlled release of the drug substance from the microspheres and the polymer erosion [4]. The initial phase of drug release, where the drug release according to a diffusion mechanism of the drug substance, is strongly dependent on the properties of the drug substance itself, e.g. its water solubility and the solubility in the polymer phase, the morphology of the polymer matrix, e.g. the porosity, the “loading of the microspheres (polymer/drug ratio) and the particle size.

In contrast to large-size PLGA devices for microspheres with less than 300 microns diameter the polymer erosion is considered to be a bulk process [5, 6]. The biodegradation is considered to be mainly a non-enzymatic hydrolytic cleavage of the ester bonds [7-9]. The hydrolytic degradation of the PLGA matrix is affected by a multitude of factors (Tab. 1).

Table 1: Factors affecting the hydrolytic behavior of biodegradable polyesters

- Water Permeability and hydrophilicity
 - Chemical composition (glycolid-lactid-ratio)
 - Crystalline or amorphous state of the polymer
 - Additives (acidic, basic, monomers, solvents, drug)
 - Mechanism of hydrolysis (autocatalytic, non-catalytic, enzymatic)
 - Device dimension
 - Porosity
 - Glass transition temperature
 - Molecular weight of the polymer
 - Physico-chemical factors (ion exchange, ionic strength, pH)
-

Source: modified from Anderson, JM [3]

The main factors are (a) the hydrolytic susceptibility of the ester bonds, (b) the diffusion coefficient of water within the matrix, (c) the diffusion rate of the chain fragments within the matrix and (d) the solubility of the oligomers in the surrounding medium. The hydrolytic degradation behaviour can be modulated by different factors, e.g. the ratio of lactic acid to glycolic acid in the copolymer. The higher the content of lactic acid moiety in the copolymer is, the slower becomes the degradation rate [10]. With a higher content of glycolic acid in the polymer, the chain cleavage can occur more easily because of the better accessibility of the glycolide-glycolide- and glycolide-lactide-bonds [11]. Furthermore, amorphous polymers or

amorphous domains in the polymer degrade faster than crystalline regions. The amorphous parts are more accessible to water than the crystalline ones and thus the degradation proceeds faster.

Besides these chemical factors also the morphology of the polymer matrix, especially the porosity can have a great influence on the degradation behaviour of PLGA microspheres. It influences not only the transport of the drug substance out of the microspheres, but also the inward transport of water and the outward transport of oligomers and monomers generated during the degradation. In addition, if the polymer matrix is very dense and degradation products accumulate inside the microspheres, the carboxylic chain ends and thus the decrease in pH can facilitate an autocatalytic degradation of the polymer [4, 12].

2 Encapsulation Processes

Numerous methods for preparation of biodegradable microspheres for parenteral application are known and the manufacturing technique has a great influence on the resulting microparticle properties, like particle size, porosity or surface morphology. For a parenteral application the diameter of the microspheres should be less than 250 μm to allow injection with needles of acceptable diameter. Furthermore the microparticles should show a good suspensibility prior to application in order to obtain stable and homogeneous suspensions for proper dosing. Apart from these considerations the process should be well controlled and easy to scale up. For the preparation of PLGA microparticles the most widely used techniques briefly described below.

2.1 Coacervation

The application of coacervation methods for the preparation of microcapsules for pharmaceutical purposes started in the 1960s, e.g. to encapsulate acetylsalicylic acid and procaine penicillin G [14, 15]. The first PLGA drug microspheres prepared by coacervation contained nafarelin, a luteinizing hormone-releasing hormone [16, 17]. The term coacervation in this context refers to the embedding of a drug substance in a polymeric matrix by phase separation. It is characterized by the appearance of a polymer-rich phase and a second phase, mainly consisting of the

solvent. In this process the drug substance is suspended or dissolved in a solution of the polymer. In case of PLGA as the polymeric component methylene chloride is a common solvent. The polymer separation as a viscous liquid phase can be induced by several methods. In simple coacervation processes the formation of the polymer-rich phase is generated by the addition of the coacervating agent, typically silicon oil. Above a critical volume fraction of the silicon oil, which depends on the given polymer concentration, the polymer molecular weight and the temperature, phase separation occurs. The forming coacervate droplets are subsequently hardened by adding a hardening agent like hexane or octamethylcyclotetrasiloxane. A drawback of this process is the problem of residual coacervating or hardening agent in the microspheres, which reduces biocompatibility. In other methods the precipitation of PLGA from a water-miscible organic phase is caused by emulsifying in a salt solution (“salting out”).

Today there are several commercially available PLGA microsphere products prepared by phase separation on the market. Decapeptyl[®] Depot (Ferring Pharmaceuticals, Suffern, New York, USA) is a PLGA microparticle formulation encapsulating Triptorelin acetate for prostate cancer endometriosis treatment. Sandostatin[®] LAR[®] (Novartis Pharma, Basel, Switzerland) contains octreotide acetate, a synthetic analogue of somatostatin. Although coacervation is mainly applied for water soluble drugs, it can be used for hydrophobic drugs as well [18].

2.2 Spray drying, spray congealing

In spray drying typically the polymer and the drug substance are dissolved, the solution is spray-atomized into a gas stream, the solvent evaporates and solid particles are formed. It can be applied to encapsulate hydrophilic as well as lipophilic drugs. The benefits of spray drying are the short manufacturing time and easy scale up [19]. Besides the process parameters like e.g. pump rate or drying time, also the concentration of the polymer – drug – solution and the solvent composition have an influence on the morphology and drug release of the resulting microspheres [20, 21]. It can be difficult to obtain spherical particles and often the microspheres are irregularly shaped [22]. Another limitation of this process is that only small particles in the lower micrometer range (<15 µm) are obtained. Furthermore the resulting microparticles are usually hollow and porous spheres, which increases drug release as the water uptake is thereby enhanced. The first

pharmaceutical application of this process for the commercial production was the encapsulation of bromocriptine in poly(L-lactic acid). Today this product is prepared with a star branched polyester poly(D,L-lactide-co-glycolide-D-glucose) and marketed under the trade name Parlodel LAR™ (Sandoz (Novartis) Pharma, Basel Switzerland) [23-25].

2.3 Methods using supercritical fluids (SCF)

A supercritical fluid is a substance either liquid or gas, above its critical temperature and critical pressure, where gases and liquids can coexist. It exhibits the flow properties of a gas and the dissolving power of a liquid. Most commonly CO₂ is used as a SCF. There are many different methods to form microparticles by using SCF [26]. As PLGA has only a limited solubility in supercritical CO₂, the supercritical fluid is normally used as an antisolvent. This principle is applied in the Supercritical Antisolvent process (SAS) or Gas Antisolvent process (GAS). The polymer and drug substance are dissolved in a liquid organic solvent, for example methylene chloride. Then the solution can be either sprayed into the supercritical CO₂ or precipitation of the microparticles is induced by injecting supercritical CO₂ into the solution phase [27, 28]. In a modified version of the SAS process, the Solution Enhanced Dispersion by Supercritical Fluids process (SEDS) the drug-polymer-solution and the SCF are sprayed together through specially designed two or three channelled nozzles. A disadvantage of this process is that large quantities of organic solvents and surfactants remain in the microspheres and that a wide size distribution of particles is obtained. A molten polymer-drug-mixture can also be saturated with SCF and then sprayed through a nozzle (the Particles from Gas Saturated Solutions process (PGSS)). The mixture is solidified by the cooling effect due to the large expansion and pressure reduction during spraying. With this process an efficient incorporation of a drug substance with a homogeneous distribution throughout the polymer matrix can be obtained [29, 30].

2.4 Solvent removal process

One of the simplest and most widely used techniques to prepare PLGA microspheres containing a hydrophobic drug is the emulsion solvent removal process [31, 32]. It consists mainly of four steps: i) formation of a solution or

dispersion of the active ingredient and the polymer in a volatile organic solvent, ii) formation of a primary emulsion by emulsifying the organic phase in a continuous (mostly aqueous) phase, iii) feeding the primary emulsion into a surplus of continuous phase and removal of the organic solvent by extraction / evaporation and iv) hardening of the emulsion droplets and finally harvesting and drying of the microparticles (Fig. 2).

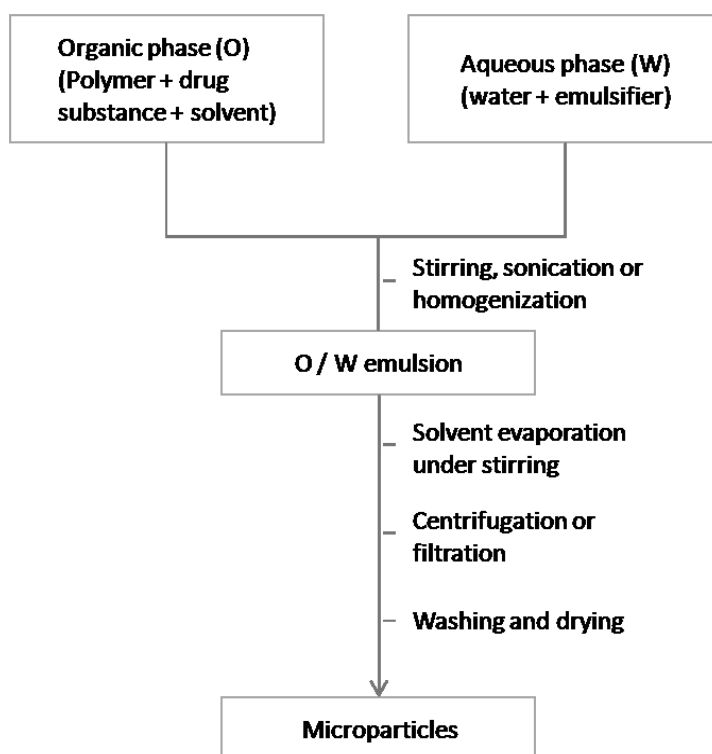


Figure 2: Schematic diagram of a common O/W emulsion solvent evaporation process

After the formation of an organic solution or dispersion containing the drug substance and the polymer this organic phase is emulsified using a stirrer, a sonicator or a homogenizer. This primary emulsion is then passed into a surplus of outer aqueous phase containing stabilizers like polyvinylalcohol, sorbitanester, polysorbate or other surface active substances. By discharging the primary emulsion into the large quantity of outer phase the organic solvent is extracted from the droplets, which implies a certain solubility of the organic solvent in the aqueous phase. The organic solvent is then released via evaporation in the gas phase. By extraction and evaporation of the organic solvent, the emulsion droplets are hardened and microspheres with a size range generally between 5 to 250 μm are obtained. The emulsification-solvent evaporation technique is mainly used for encapsulating proteins or drugs, which are insoluble or poorly soluble in water. The

release properties of the microparticles can be tailored via the employed solvents, the ratio of the dispersed to continuous phase, the viscosity of the solution, the temperature of the external phase and others [31, 33, 34]. On industrial scale this technique is used for the production of Vivitrol[®] (Cephalon, Inc., Frazer, USA) [35]. Variations of this technique include the formation of a multiple emulsion (w/o/w-method) or the utilization of an external oil phase, like paraffin oil, in case of water soluble drugs. The w/o/w-double emulsion method is especially suitable for the encapsulation of proteins, peptides, vaccines or other water soluble macromolecules to obtain microparticles with sufficient encapsulation efficiency. With an o/w-emulsion process however, the encapsulation efficiency is very low because the drug easily dissolves in the outer aqueous phase. A parenteral depot formulation with leuprorelide acetate is manufactured by the w/o/w method and is marketed under the trade name Enantone[™] (Takeda Pharmaceutical Company Limited, Osaka, Japan). For hydrophobic drugs this technique seems not beneficial. However, by adding an inner water phase in the w/o/w process the porosity of the microparticles and thus the drug release can be modified [36-38].

3 The solvent removal process for manufacturing of PLGA microspheres on an industrial scale

For the commercial production of PLGA microspheres coacervation, spray-drying and solvent extraction /evaporation are applied. Table 2 shows a selection of marketed microparticulate dosage forms and the applied encapsulation technique.

Table 2: List of marketed PLGA microparticle formulations *

Drug	Product	Distributor	Encapsulation technique
Ocreotide acetate	Sandostatin LAR [®] Depot	Novartis	Coacervation
Lanreotide acetate	Somatuline [®] Depot	Ipsen	Coacervation
Naltrexone	Vivitrol [®]	Alkermes	o/w emulsion solvent extraction
Risperidone	Risperdal [®] consta	Janssen / Alkermes Inc.	o/w emulsion solvent extraction
Leuprorelide acetate	Lupron Depot [®]	TAP Pharmaceuticals	w/o/w emulsion solvent evaporation

* modified from Kumar and Palmieri, 2010 [39]

The emulsion solvent extraction evaporation method is a straightforward method for the preparation of microspheres and most widely used on a laboratory scale. Due to the fact that the product properties are influenced by a large number of process variables (Fig. 3), the transfer from laboratory scale to commercial production is often associated with difficulties.

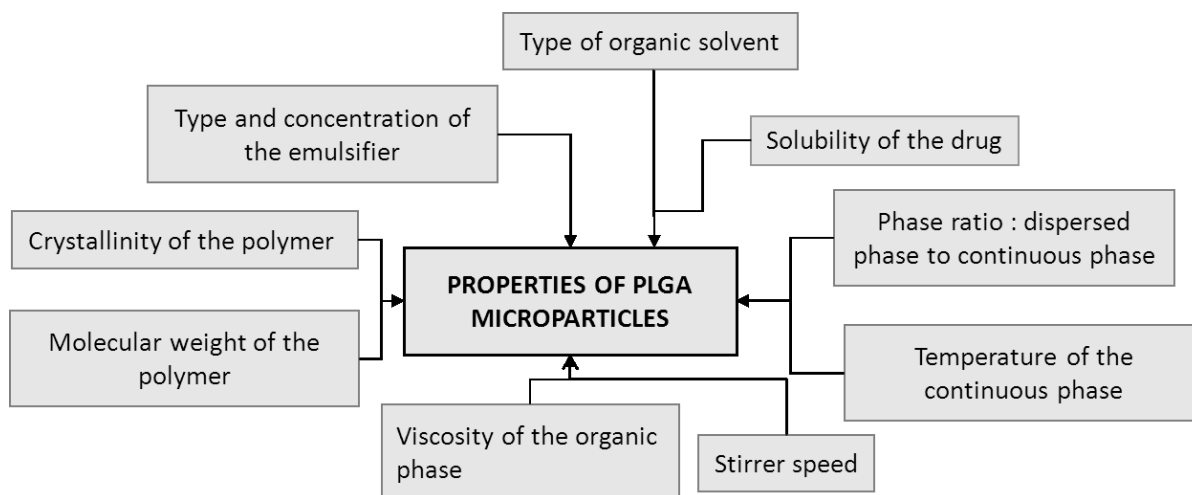


Figure 3: Parameters influencing the product properties of the resulting PLGA microparticles

For a manufacturing process of PLGA microparticles with defined composition, the properties of the resulting product will be strongly influenced by the chosen process parameters, like e.g. stirring speed, temperature of the continuous phase and others. These process parameters influence strongly the rate and time point of the transformation from liquid emulsion droplets to solid particles. This in turn has a great impact on the physico-chemical properties of the latter.

During the conversion of the liquid emulsion droplets into solid particles different events take place: (a) diffusion of the organic solvent from the embryonic particles into the aqueous medium, (b) in return diffusion of the aqueous medium in opposite direction, (c) polymer phase separation on the particle surface, (d) drug loss into the quench solution and (e) evaporation of the solvent. All these coupled events influence each other. How fast these different processes occur has an impact on the rate of solidification of the microspheres, which in turn influences the resulting particle characteristics [40].

3.1 Influences of process parameters on the solidification rate of the microparticles

Hardening of the polymer matrix occurs as the organic solvent is extracted from the emulsion droplets. The extraction process itself can be controlled by a variety of process parameters (Fig. 4). It is influenced amongst others by the ratio of dispersed phase to continuous phase, the temperature of the extraction medium, the stirring speed, the solvent exchange at the emulsion droplet – extraction medium interface and subsequent gas exchange on the surface of the external solution, the pressure in the vessel and the gas flow removing the organic solvent. The temperature is rather simple to control for a process with a constant temperature during manufacturing, but sometimes temperature ramps are applied which need to be controlled precisely [41]. As the temperature of the continuous phase is adjusted by the heating jacket of the reactor, the temperature change is delayed if the volume is increased. While the heated area changes with the second power, the volume of the quench solution is linked with the third power. Another difficulty is the flow conditions in the reactor. The agitation depends on the stirrer geometry and the stirring speed, but considering the geometry of the reactor this might not be a simple scale-up factor. Once transferred into the aqueous phase the solvent is conveyed to the interface between quench solution and head space. This mass transfer is related to the relative velocities of particles, resp. gas molecules and the fluid in the system, the viscosity of the liquid, and the solubility of the solvent in the extraction medium. The flow pattern in the reactor crucially depends on the stirrer speed and stirrer position given that the stirrer geometry does not change. A certain stirrer speed is required to obtain a mixing of the total volume in the reactor and thus to enhance the transport of the gas molecules to the liquid – gas interface. The driving force for the mass transfer from the extraction medium to the head space above is the concentration gradient on both sides. The faster the gas molecules are removed from the gaseous side of interface, e.g. by feeding air through the head space of the reactor, the faster the evaporation rate. By increasing the volume of the extraction phase the interface does not equally increase, meaning that the solvent is faster extracted from the emulsion droplets but not from the extraction medium and thus influencing the solidification rate of the droplets as described below.

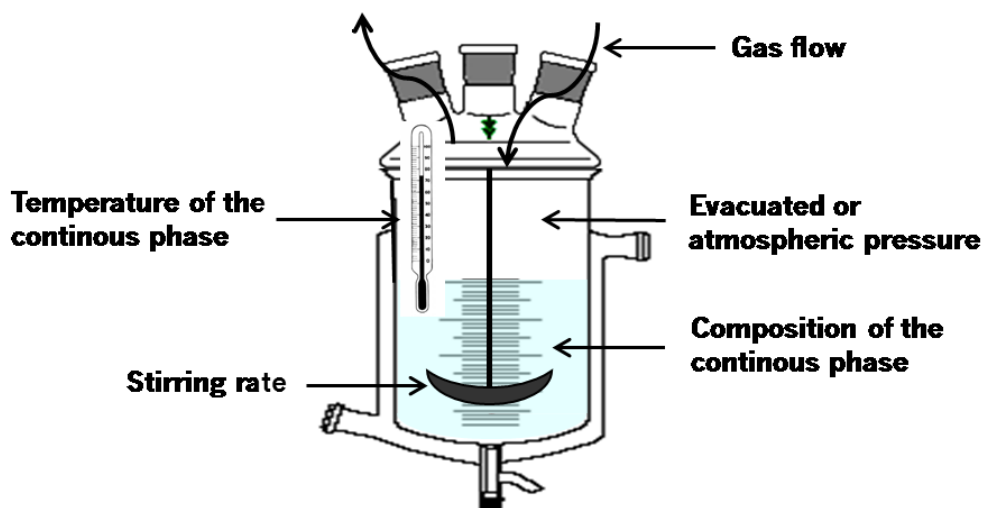


Figure 4: Process parameters influencing the rate of solvent removal from the emulsion during solvent extraction / evaporation process for PLGA microparticles.

3.2 Influence of the solidification rate on particle properties

Fast polymer precipitation results in a porous inner structure and smooth surface of the microparticles. The encapsulation efficiency is typically high, as the solid polymer film, which is formed rapidly on the particle surface, acts as a diffusion barrier for the drug [42]. In contrast, slow polymer precipitation results in a dense polymer structure, but skin formation is slower and the polymer matrix stays soft for a long time span. This allows an enhanced influx of water during solidification and the formation of water pockets leading to cavities in the dried microparticles [43].

Besides the varying drug loading of the final microspheres also their drug release depends on the formation process and the resulting particle morphology. The diffusion-controlled release is higher for porous microparticles, as the drug needs to pass to the particle surface either through the polymer matrix or through pores. Furthermore, an open porous microparticle structure can lead to a significant burst effect [44]. In return water can enter the particles through these pores and fill the inner cavities inside the particles. Degradation of the polymer matrix is accelerated from the inside by these water-filled cavities in the interior of the particle leading to a faster drug release [45].

Due to the fact that the precipitation rate has such an influence on the resulting particle characteristics, it is essential to control the parameters which affect the

solvent removal and the precipitation during microparticle processing carefully [46-48].

4 Objective of the Thesis

The goal of the thesis was to understand the mechanism of microparticle formation in an emulsion solvent extraction / evaporation process for the preparation of drug loaded PLGA microspheres on a 5 L batch scale. The model drug selected was 3-{2-[4-(6-fluor-1,2-benzisoxazol-3-yl)piperidono]ethyl}-2-methyl-6,7,8,9-tetrahydro-4H-pyrido[1,2-a]pyrimidin-4-on. It has to be considered, that the drug substance is hydrophobic and poorly water soluble and thus provides several challenges for the encapsulation and the release.

On this basis the key process parameters influencing particle morphology and their impact on the resulting drug release profiles were to be identified. In the applied emulsion solvent extraction / evaporation process the morphology and particle size distribution is the result of a primary structure formation at the beginning of the process and secondary structural changes during processing. The understanding of these processes is essential for the control of the preparation process and a prerequisite for a successful upscale to commercial manufacturing.

The main objectives of this thesis were:

- Characterization of drug-polymer interactions and evaluation of possible solvent and solvent mixtures by the Hansen solubility parameters and their impact on the resulting drug and particle morphology (**CHAPTER 2**)
- Control of the droplet of the primary emulsion in a solvent removal process (**CHAPTER 3**)
- Monitoring and understanding of the structural changes during the process by focused beam reflectance measurement (**CHAPTER 4**)
- Understanding the influence of process parameters like temperature, type of polymer and post-treatment of the particles on particle morphology (**CHAPTER 5**)
- Characterization of the microparticle morphology by determination of the porosity and the pore size distribution (**CHAPTER 6**)

5 References

- [1] Database "Newport Horizon", www.thomsonreuters.com, last access: 06.2010
- [2] Langer,R. Drug delivery and targeting. *Nature* **1998**, 392 (6679), 5-10.
- [3] Sbarbaro,J.A. Strategies to Improve Compliance with Therapy. *American Journal of Medicine* **1985**, 79 (6A), 34-37.
- [4] Anderson,J.M.; Shive,M.S. Biodegradation and biocompatibility of PLA and PLGA microspheres. *Advanced Drug Delivery Reviews* **1997**, 28 (1), 5-24.
- [5] Burkersroda,F.v.; Schedl,L.; Göpferich,A. Why degradable polymers undergo surface erosion or bulk erosion. *Biomaterials* **2002**, 23 (21), 4221-4231.
- [6] Spenlehauer,G.; Vert,M.; Benoit,J.P.; Boddaert,A. Invitro and Invivo Degradation of Poly(D,L Lactide Glycolide) Type Microspheres Made by Solvent Evaporation Method. *Biomaterials* **1989**, 10 (8), 557-563.
- [7] Anderson JM. Perspectives on the in vivo responses of biodegradable polymers. In *Biomedical application of synthetic biodegradable polymers*; Hollinger JO Ed.; CRC Press: Boca Raton, **1995**, 223-231.
- [8] Kopecek,J.; Ulbrich,K. Biodegradation of biomedical polymers. *Progress in Polymer Science* 1983, 9 (1), 1-58.
- [9] Vert,M.; Li,S.M.; Spenlehauer,G.; Guerin,P. Bioresorbability and Biocompatibility of Aliphatic Polyesters. *Journal of Materials Science-Materials in Medicine* **1992**, 3 (6), 432-446.
- [10] Beck,L.R.; Pope,V.Z.; Flowers,C.E.; Cowsar,D.R.; Tice,T.R.; Lewis,D.H.; Dunn,R.L.; Moore,A.B.; Gilley,R.M. Poly(DI-Lactide-Co-Glycolide) Norethisterone Microcapsules - An Injectable Biodegradable Contraceptive. *Biology of Reproduction* **1983**, 28 (1), 186-195.
- [11] Park,T.G. Degradation of Poly(Lactic-Co-Glycolic Acid) Microspheres - Effect of Copolymer Composition. *Biomaterials* **1995**, 16 (15), 1123-1130.
- [12] Klose,D.; Siepmann,F.; Elkharraz,K.; Krenzlin,S.; Siepmann,J. How porosity and size affect the drug release mechanisms from PLIGA-based microparticles. *International Journal of Pharmaceutics* **2006**, 314 (2), 198-206.
- [13] Arshady,R. Microspheres and microcapsules, a survey of manufacturing techniques Part II: Coacervation. *Polym Eng Sci* **1990**, 30 (15), 905-914.
- [14] Phares,R.E.; Sperandio,G.J. Coating Pharmaceuticals by Coacervation. *Journal of Pharmaceutical Sciences* **1964**, 53 (5), 515-&.

- [15] Phares,R.E.; Sperandio,G.J. Preparation of Phase Diagram for Coacervation. *Journal of Pharmaceutical Sciences* **1964**, 53 (5), 518-&.
- [16] Sanders,L.M.; Kent,J.S.; Mcrae,G.I.; Vickery,B.H.; Tice,T.R.; Lewis,D.H. Controlled Release of A Luteinizing-Hormone-Releasing Hormone Analog from Poly(D,L-Lactide-Co-Glycolide) Microspheres. *Journal of Pharmaceutical Sciences* **1984**, 73 (9), 1294-1297.
- [17] Sanders,L.M.; Kell,B.A.; Mcrae,G.I.; Whitehead,G.W. Prolonged Controlled-Release of Nafarelin, A Luteinizing-Hormone-Releasing Hormone Analog, from Biodegradable Polymeric Implants - Influence of Composition and Molecular-Weight of Polymer. *Journal of Pharmaceutical Sciences* **1986**, 75 (4), 356-360.
- [18] Leelarasamee,N.; Howard,S.A.; Malanga,C.J.; Ma,J.K.H. A Method for the Preparation of Polylactic Acid Microcapsules of Controlled Particle-Size and Drug Loading. *Journal of Microencapsulation* **1988**, 5 (2), 147-157.
- [19] Wagenaar,B.W.; Muller,B.W. Piroxicam Release from Spray-Dried Biodegradable Microspheres. *Biomaterials* **1994**, 15 (1), 49-54.
- [20] Rizi,K.; Green,R.J.; Donaldson,M.; Williams,A.C. Production of pH-Responsive Microparticles by Spray Drying: Investigation of Experimental Parameter Effects on Morphological and Release Properties. *J. Pharm. Sci.* **2011**, 100 (2), 566-579.
- [21] Rattes,A.L.R.; Oliveira,W.P. Spray drying conditions and encapsulating composition effects on formation and properties of sodium diclofenac microparticles. *Powder Technology* **2007**, 171 (1), 7-14.
- [22] Mu,L.; Feng,S.S. Fabrication, characterization and in vitro release of paclitaxel (Taxol (R)) loaded poly (lactic-co-glycolic acid) microspheres prepared by spray drying technique with lipid/cholesterol emulsifiers. *Journal of Controlled Release* **2001**, 76 (3), 239-254.
- [23] Montini M; Pedroncelli M; Tengattini F; Pagani M; Gianola D; Cortesi L; Lancranjan I; Pagani G. Medical applications of intramuscularly administered bromocriptin microspheres. In *Pharmaceutical Particulate Carriers* Marcel Dekker: New York, **1993**, 227-274.
- [24] Nerlich B; Mank R; Gustafsson J; Hörig J; Köchling W. Mikroverkapslung wasserlöslicher Wirkstoffe. [EP 579,347]. **1999**.
- [25] Petersen H; Ahlheimer M. Sustained release formulation comprising ocreotide and two or more polylactide-co-glycolide polymers. [WO 2007/071395]. **2007**. 28-6-2007.
- [26] Brich Z; Kissel T. Polyolester, deren Herstellung und Verwendung. CH 672133A5[Swiss Patent Application]. **1986**.

- [27] Bodmeier,R.; Wang,H.; Dixon,D.J.; Mawson,S.; Johnston,K.P. Polymeric Microspheres Prepared by Spraying Into Compressed Carbon-Dioxide. *Pharmaceutical Research* **1995**, *12* (8), 1211-1217.
- [28] Engwicht,A.; Girreser,U.; Muller,B.W. Critical properties of lactide-co-glycolide polymers for the use in microparticle preparation by the Aerosol Solvent Extraction System. *International Journal of Pharmaceutics* **1999**, *185* (1), 61-72.
- [29] Howdle,S.M.; Watson,M.S.; Whitaker,M.J.; Popov,V.K.; Davies,M.C.; Mandel,F.S.; Wang,J.D.; Shakesheff,K.M. Supercritical fluid mixing: preparation of thermally sensitive polymer composites containing bioactive materials. *Chemical Communications* **2001** (01), 109-110.
- [30] Jung,J.; Perrut,M. Particle design using supercritical fluids: Literature and patent survey. *Journal of Supercritical Fluids* **2001**, *20* (3), 179-219.
- [31] Mao,S.; Xu,J.; Cai,C.; Germershaus,O.; Schaper,A.; Kissel,T. Effect of WOW process parameters on morphology and burst release of FITC-dextran loaded PLGA microspheres. *International Journal of Pharmaceutics* **2007**, *334* (1-2), 137-148.
- [32] Obeidat,W.M.; Obeidat,S.M.; Alzoubi,N.M. Investigations on the Physical Structure and the Mechanism of Drug Release from an Enteric Matrix Microspheres with a Near-Zero-Order Release Kinetics Using SEM and Quantitative FTIR. *Aaps Pharmscitech* **2009**, *10* (2), 615-623.
- [33] Chung,T.W.; Huang,Y.Y.; Liu,Y.Z. Effects of the rate of solvent evaporation on the characteristics of drug loaded PLLA and PDLLA microspheres. *International Journal of Pharmaceutics* **2001**, *212* (2), 161-169.
- [34] Jeyanthi,R.; Thanoo,B.C.; Metha,R.C.; Deluca,P.P. Effect of solvent removal technique on the matrix characteristics of polylactide/glycolide microspheres for peptide delivery. *Journal of Controlled Release* **1996**, *38* (2-3), 235-244.
- [35] Whitaker,M.J.; Hao,J.Y.; Davies,O.R.; Serhatkulu,G.; Stolnik-Trenkic,S.; Howdle,S.M.; Shakesheff,K.M. The production of protein-loaded microparticles by supercritical fluid enhanced mixing and spraying. *Journal of Controlled Release* **2005**, *101* (1-3), 85-92.
- [36] Dhanaraju,M.D.; Vema,K.; Jayakumar,R.; Vamsadhara,C. Preparation and characterization of injectable microspheres of contraceptive hormones. *International Journal of Pharmaceutics* **2003**, *268* (1-2), 23-29.
- [37] Dhanaraju,M.D.; Jayakumar,R.; Vamsadhara,C. Influence of manufacturing parameters on development of contraceptive steroid loaded injectable microspheres. *Chemical & Pharmaceutical Bulletin* **2004**, *52* (8), 976-979.

- [38] Dhanaraju,M.D.; RajKannan,R.; Selvaraj,D.; Jayakumar,R.; Vamsadhara,C. Biodegradation and biocompatibility of contraceptive-steroid-loaded poly (DL-lactide-co-glycolide) injectable microspheres: in vitro and in vivo study. *Contraception* **2006**, 74 (2), 148-156.
- [39] Kumar,R.; Palmieri,M.J. Points to Consider when Establishing Drug Product Specifications for Parenteral Microspheres. *Aaps Journal* **2010**, 12 (1), 27-32.
- [40] Berkland,C.; Kim,K.K.; Pack,D.W. Fabrication of PLG microspheres with precisely controlled and monodisperse size distributions. *Journal of Controlled Release* **2001**, 73 (1), 59-74.
- [41] Yang,Y.Y.; Chia,H.H.; Chung,T.S. Effect of preparation temperature on the characteristics and release profiles of PLGA microspheres containing protein fabricated by double-emulsion solvent extraction/evaporation method. *Journal of Controlled Release* **2000**, 69 (1), 81-96.
- [42] Berkland,C.; King,M.; Cox,A.; Kim,K.; Pack,D.W. Precise control of PLG microsphere size provides enhanced control of drug release rate. *Journal of Controlled Release* **2002**, 82 (1), 137-147.
- [43] Tang,H.; Xu,N.; Meng,J.; Wang,C.; Nie,S.F.; Pan,W.S. Application of a novel approach to prepare biodegradable polylactic-co-glycolic acid microspheres: Surface liquid spraying. *Yakugaku Zasshi-Journal of the Pharmaceutical Society of Japan* **2007**, 127 (11), 1851-1862.
- [44] Cavalier,M.; Benoit,J.P.; Thies,C. The Formation and Characterization of Hydrocortisone-Loaded Poly((+/-)-Lactide) Microspheres. *Journal of Pharmacy and Pharmacology* **1986**, 38 (4), 249-253.
- [45] Schalper,K.; Harnisch,S.; Muller,R.H.; Hildebrand,G.E. Preparation of microparticles by micromixers: Characterization of oil/water process and prediction of particle size. *Pharmaceutical Research* **2005**, 22 (2), 276-284.
- [46] Bodmeier,R.; McGinity,J.W. Solvent Selection in the Preparation of Poly(DL-Lactide) Microspheres Prepared by the Solvent Evaporation Method. *International Journal of Pharmaceutics* **1988**, 43 (1-2), 179-186.
- [47] Siepmann,J.; Siepmann,F. *Microparticles Used as Drug Delivery Systems. Smart Colloidal Materials.*, 133 Ed.; Richtering,W. Ed.; Springer Berlin / Heidelberg: 2006, 15-21.
- [48] Wischke,C.; Lorenzen,D.; Zimmermann,J.; Borchert,H.H. Preparation of protein loaded poly(D,L-lactide-co-glycolide) microparticles for the antigen delivery to dendritic cells using a static micromixer. *European Journal of Pharmaceutics and Biopharmaceutics* **2006**, 62 (3), 247-253.

CHAPTER 2

Application of Hansen solubility parameters for understanding and prediction of drug distribution in microspheres ‡

Abstract

In an emulsion solvent extraction / evaporation process for the preparation of microspheres the employed solvents have a tremendous influence on the characteristics of the resulting particles. Nevertheless the solvent selection is often based on empirical data rather than on calculated values. The purpose of this investigation was to use the concept of solubility parameters for interpretation and improved understanding of solvent effects in the process of microparticle preparation. Partial solubility parameters of 3-{2-[4-(6-Fluor-1,2- benzisoxazol-3-yl) piperidino]ethyl}- 2-methyl-6,7,8,9- tetrahydro-4H-pyrido [1,2-a]pyrimidin-4-on, which was used as a model drug, were determined experimentally using an extended Hansen regression model. Poly(lactide-co-glycolide) microparticles were prepared with an emulsion solvent removal process employing methylene chloride and its mixtures with benzyl alcohol and n-butanol. It could be shown, that the encapsulation efficiency was influenced by the change of the solvent composition during the extraction process. Furthermore the solvent selection had an essential influence on the morphological state of the drug and it could be shown and explained, that by a decrease of the dissolving power a completely amorphous product was obtained.

‡ Published in International Journal of Pharmaceutics, 2011, 416 (1), p. 202-209: Vay,K.; Scheler,S.; Friess,W. Application of Hansen solubility parameters for understanding and prediction of drug distribution in microspheres.

1 Introduction

The microencapsulation of a drug substance in a polymeric matrix offers the possibility of a controlled drug release with many clinical benefits like the drug targeting to a specific location or higher compliance of the patient because of a reduced dosing frequency. There are several methods to prepare microspheres from preformed polymers and the emulsion solvent extraction / evaporation process is one of the most frequently used techniques. In this preparation process, the properties of the utilized solvents are among the primary factors determining the characteristics of the resulting microspheres [1-4]. Nearly every step of the particle formation process is affected by the solvents in a distinct way. In the first step where an organic solution of the polymer or, as in most cases, a solution of drug and polymer is formed the dissolving power of the solvent determines the upper concentration limit of the organic phase. If it is not intended to incorporate the drug as a suspension, both, drug substance and polymer should be well soluble in the organic solvent. In a second step an emulsion is formed from this solution and an aqueous phase. By feeding the emulsion into a stirred reactor containing an aqueous medium, the solvent is extracted into the external phase from where it can be evaporated in case of volatile solvents. During this process different diffusion processes take place like the transfer of the organic solvent out of and in return the non-solvent into the microspheres. This solvent exchange causes the transformation of the droplets into solid microspheres and is determined by the miscibility of the solvents and the aqueous medium. The drug, however, ideally should not be soluble in the aqueous medium otherwise it will be leached out of the particles resulting in low encapsulation efficiency [5].

A variety of different solvent parameters like volatility and boiling point, reactivity or viscosity have to be considered in order to tailor the resulting microparticle properties. Another critical factor is the toxicological safety, as a certain amount of solvent residues remains in the product and thus restricts the range of suitable solvents. However one of the most important criterions on which a suitable solvent has to be chosen is an optimum balanced affinity to the other process compounds. Often the solvent selection is based on empirical data rather than on calculated values. An initial estimate based on solubility calculations can help to optimize the

results and to minimize experimental expenditure. An established tool to estimate the solubility behaviour of a substance is the concept of solubility parameters, originally defined by Hildebrand [6]. He proposed the square root of the cohesive energy density as a numeric value to specify the solubility characteristics of a specific solvent:

$$\delta = \sqrt{\Delta H - RT / V_m} \quad (1)$$

where ΔH is the heat of vaporization, R is the gas constant, T is the temperature and V_m is the molar volume. The cohesive energy density of a liquid is the energy of vaporization per volume unit. It reflects the degree of attractive forces holding the molecules together. This amount of energy is required to separate the atoms or molecules of the material from each other and is the effect of all interatomic / -molecular interactions. Hansen subdivided the total Hildebrand value δ_t into three fractions: dispersive interactions (δ_d), polar interactions (δ_p) and hydrogen bonding (δ_h). These 3 parameters can be visualized as coordinates in a 3-dimensional diagram, which allows a good illustration of the miscibility or solubility of different materials. The smaller the distance between the coordinates of two substances is in this 3-dimensional space, the better is their mutual solubility.

In this study the principle of Hansen solubility parameters was applied to an emulsion-solvent evaporation process for the preparation of PLGA microspheres. Moldenhauer and Nairn used Hansen solubility parameters to choose alternative solvent systems for the production of microcapsules with similar properties and showed that particle characteristics and release rates could be correlated with the solubility parameters of solvent mixtures [7]. Bordes et al. applied them for the solvent substitution in a microencapsulation process with poly(ϵ -caprolactone) [8]. The objective of our work was to optimize the particle characteristics by modifying the solvent mixture of the dispersed phase. Starting with methylene chloride, which is often used in this process, binary mixtures of methylene chloride with benzyl alcohol and n-butanol were tested to analyze their influence on the morphology of the drug substance, the encapsulation efficiency and the drug release rate. Furthermore the solubility of the drug in the polymer matrix could be estimated. Experimentally determined Hansen parameters of a huge number of solvents, drug substances and other chemicals are listed in the literature. However no values can be found so far for 3-{2-[4-(6-Fluor-1,2-benzisoxazol-3-yl)piperidino]ethyl}-2-methyl-

6,7,8,9-tetrahydro-4H-pyrido[1,2-a]pyrimidin-4-on. In this study we determined these parameters experimentally and compared them with those obtained by group contribution methods according to Hoftyzer / Van Krevelen and Hoy.

2 Materials and Methods

2.1 Materials

3-{2-[4-(6-Fluor-1,2-benzisoxazol-3-yl)piperidino]ethyl}-2-methyl-6,7,8,9-tetrahydro-4H-pyrido[1,2-a]pyrimidin-4-on was obtained by Jubilant Organosys (Mysore, India) with an assay of 100.2% and 0.19% total impurities (main impurities: N-Oxide-Derivative and 9-OH-Derivative); Poly(D,L-lactide-co-glycolide) 75:25 (Resomer 755 S), Mw = 64710 Da was purchased from Boehringer Ingelheim, (Ingelheim, Germany). All solvents used were of analytical grade and were used as obtained.

2.2 Determination of the solubility of the API in PLGA by differential scanning calorimetry (DSC)

To determine the solubility the drug substance in PLGA the enthalpy of fusion of pure PLGA, drug substance and three mixtures of PLGA with 30.9%, 49.3% and 81.8% of API were measured. Approximately 2 mg were weighed in a standard aluminium pan, sealed and heated from -20 to 250 °C with a heating rate of 50° per minute in a DSC (823e/500) from Mettler Toledo (Greifensee, Switzerland). The melting peak of the drug substance at 170 °C was integrated. The heat of fusion thus obtained was plotted against the drug concentration in the mixture as described in literature [9] (Panyam et al, 2004).

To examine if the decomposition occurs the pan with pure drug substance was heated for a second time up to 250 °C. The thermogram was unchanged compared to the first one indicating that the drug substance is stable in a range between -20 and 250 °C. PLGA is described in literature to undergo no decomposition in this temperature range [10].

2.3 Determination of the morphological state of the drug by X-Ray powder diffractometry

X-ray powder diffraction (XRPD) patterns were collected with an Unisantis XMD 300 X-ray powder diffractometer (Unisantis, Georgsmarienhütte, Germany) with a position sensitive detector in parallel beam optics using the following acquisition conditions: tube anode: Cu, 40 kV, 0.8 mA; 3-43° theta/2theta; simultaneous detection of regions of 10° per step with detector resolution 1024, counting time 300 seconds per step. Samples were measured at room temperature in a standard sample holder on a rotating sample spinner.

2.4 Determination of the solubility

The solubility of on the API was determined in 17 different solvents (Table 1) by adding a surplus of drug substance in a glass vial to 5 ml solvent. The vials were sealed and shaken at room temperature for 24 hours to assure saturation. 2 ml of the saturated solution were filtered through a 1.0 µm Teflon filter and the solvent was evaporated at RT. After dissolving the residue in 0.1 N HCl, the concentration of the drug substance was determined by HPLC with a DAD detector at 235 nm and analyzed with chromeleon™ 6.7 (Dionex, Sunnyvale, California, USA). A XTerra RP 18 (20 x 3.5 mm) column was used at a flow rate 1 ml/min and an injected volume 10 µl. The mobile phase consisted of a phosphate buffer (pH 8.5) and acetonitrile at a ratio of 75:25 (v/v). The precision of this method was determined to 0.37%.

Table 1: Solubility parameters, molar volume and solubility for the API in different solvents

Solvent	δ_d [MPa ^{1/2}]	δ_p [MPa ^{1/2}]	δ_h [MPa ^{1/2}]	Molar volume V_1 [ml/mol]	API Concentration [mg/ml]
2-Propanol	15.8	6.1	16.4	76.8	5.67
Acetone	15.5	10.4	7.0	74.0	8.89
Acetonitrile	15.3	18	6.1	52.6	4.35
Benzyl alcohol	18.4	6.3	13.7	103.6	277.13
Chloroform	17.8	3.1	5.7	80.7	392.52
Diethylamine	14.9	2.3	6.1	103.2	3.21
DMSO	18.4	16.4	10.2	71.3	8.68
Ethanol	15.8	8.8	19.4	58.5	19.47
Ethylacetate	15.8	5.3	7.2	98.5	8.82
Hexanol	15.8	4.3	13.5	124.6	13.63
Methyl acetate	15.5	7.2	7.6	79.7	10.19
Methylene chloride	18.2	6.3	6.1	63.9	85.11
n-Butyl acetate	15.8	3.7	6.3	132.5	6.28
n-Hexane	14.9	0	0	131.6	0.07
Pyridine	19.0	8.8	5.9	80.9	110.37
Tetrahydrofuran	16.8	5.7	8.0	81.7	50.79
Toluene	18.0	1.4	2.0	106.8	27.88

3 Results and Discussion

3.1 Determination of the solubility parameters

3.1.1 Experimental determination

Since experimentally derived Hansen solubility parameters of 3-{2-[4-(6-Fluor-1,2-benzisoxazol-3-yl)piperidino]ethyl}-2-methyl-6,7,8,9-tetrahydro-4H-pyrido[1,2-a]pyrimidin-4-on could not be found in literature they were determined by own measurements. The total and the partial solubility parameters of a substance can be calculated from its solubility values in a series of different solvents with known cohesive energies [11]. The method is based on the rule that the more similar the parameters of two substances are, the better is their miscibility or the solubility of one substance in the other. If the parameters match exactly the solubility becomes ideal which means that the activity coefficient γ_2 which is the ratio of the ideal mole fraction solubility X_2^i and the experimental mole fraction solubility X_2 equals 1. In terms of total solubility parameters this condition is expressed by equation 2

$$\ln \gamma_2 = \ln \frac{X_2^i}{X_2} = (\delta_1 - \delta_2) \frac{V_2 \phi_1^2}{RT} \quad (2)$$

where R is the gas constant, T is the temperature at which the experiment is performed (K) and ϕ_1 is the volume fraction of the solvent. ϕ_1 can be expressed as follows:

$$\phi_1 = \frac{V_1(1 - X_2)}{V_1(1 - X_2) + V_2 X_2} \quad (3)$$

with V_1 and V_2 as the molar volumes of the solvent and the solutes, respectively. In all variables the subscript 1 refers to the solvent and the subscript 2 to the solute. On the basis of equation (2) Martin and Beerbower developed an extended regression model involving Hansen partial solubility parameters [12, 13].

$$\frac{\ln(X_2^i / X_2)}{V_2 \phi_1^2 / (RT)} = D_0 + D_1(\delta_{1d} - \delta_{2d})^2 + D_2(\delta_{1p} - \delta_{2p})^2 + D_3(\delta_{1h} - \delta_{2h})^2 \quad (4)$$

where δ_{1d} , δ_{1p} , δ_{1h} , δ_{2d} , δ_{2p} , δ_{2h} are the partial solubility parameters of the solvent and the solute, respectively. D_0 to D_3 are constants. Equation 4 can be converted into the regression equation 5.

$$\frac{\ln(X_2^i / X_2)}{V_2 \phi_1^2 / (RT)} = C_0 + C_1 \delta_{1d}^2 + C_2 \delta_{1d} + C_3 \delta_{1p}^2 + C_4 \delta_{1p} + C_5 \delta_{1h}^2 + C_6 \delta_{1h} \quad (5)$$

with

$$C_0 = D_0 + D_1 \delta_2 d_2 + D_2 \delta_2 p_2 + D_3 \delta_2 h_2 \quad (6)$$

$$C_1 = D_1 \quad (7)$$

$$C_2 = -2D_1 \delta_2 d_2 \quad (8)$$

$$C_3 = D_2 \quad (9)$$

$$C_4 = -2D_2 \delta_2 p_2 \quad (10)$$

$$C_5 = D_3 \quad (11)$$

$$C_6 = -2D_3 \delta_2 h_2 \quad (12)$$

The constant coefficients C_0 to C_6 are obtained by regressing the left hand term against the partial parameters of the solvents. Bustamante simplified the model by proving that the partial solubility parameters can also be obtained by regressing only the logarithm of the experimental mole fraction solubility X_2 against the partial solubility parameters of the solvents [14].

$$\ln X_2 = C_0 + C_1 \delta_{1d}^2 + C_2 \delta_{1d} + C_3 \delta_{1p}^2 + C_4 \delta_{1p} + C_5 \delta_{1h}^2 + C_6 \delta_{1h} \quad (13)$$

From equations 6 to 12 the partial solubility parameters δ_{2d} , δ_{2p} , and δ_{2h} are calculated as

$$\delta_{2d} = - (C_2 / 2C_1) \quad (14)$$

$$\delta_{2p} = - (C_4 / 2C_3) \quad (15)$$

$$\delta_{2h} = - (C_6 / 2C_5) \quad (16)$$

As they represent the function's maximum they can be also obtained from the zero points of the partial derivatives $\partial \ln X_2 / \partial \delta_{1(d,p,h)}$.

Seventeen different solvents were employed for this study. Their Hansen solubility parameters, molar volumes and the experimentally determined saturation concentration of 3-{2-[4-(6-Fluor-1,2-benzisoxazol-3-yl)piperidino]ethyl}-2-methyl-6,7,8,9-tetrahydro-4H-pyrido[1,2-a]pyrimidin-4-on in each solvent are listed in Table 1. The following partial solubility parameters of the drug substance were calculated from these data: $\delta_{2d} = 18.7 \text{ MPa}^{1/2}$, $\delta_{2p} = 5.4 \text{ MPa}^{1/2}$, and $\delta_{2h} = 11.6 \text{ MPa}^{1/2}$.

3.1.2 Estimation of the solubility parameters by group contribution methods

As the solubility of a material is largely determined by its chemical nature, the solubility parameters can also be calculated from its molecular structure. In this work two different approaches were chosen, on the one hand the calculation of the solubility parameters according to the group contribution method from Hoftyzer and Van Krevelen; and on the other hand according to Hoy [15] (Tab. 2).

Table 2: Comparison of the different parameters contributing to the calculated results of the applied methods.

Hoftyzer and Van Krevelen		Hoy		Experimental determination *			
<i>Parameter; derived from</i>		<i>Formula</i>		<i>Parameter; derived from</i>			
V	Calculated from density	V	Group contribution tables	V	Literature		
F _{di}	Group contribution tables	$\delta_d = \frac{\sum F_{di}}{V}$	F _{ti}	Group contribution tables	$\delta_d = \sqrt{\delta_t^2 - \delta_p^2 - \delta_h^2}$	c _{sn}	Experimentally determined
F _{pi}	Group contribution tables	$\delta_p = \frac{\sqrt{\sum F_{pi}^2}}{V}$	F _{pi}	Group contribution tables	$\delta_p = \delta_t * \left(\frac{1/\alpha * F_p}{F_t + B}\right)$		
E _{hi}	Group contribution tables	$\delta_h = \sqrt{\frac{\sum E_{hi}}{V}}$	ΔT_i	Group contribution tables	$\delta_h = \delta_t * \sqrt{\left(\frac{\alpha}{1}\right)}$		

*) Since the simplified model according to Bustamante et al (1993) [14] was used only the saturation solubility (c_s) and the molar volume are contributing to the calculation.

Method of Hoftzyer and Van Krevelen

According to Hoftzyer and Van Krevelen the partial solubility parameters can be calculated using the following equations:

$$\delta_d = \sum F_{di} / V \quad (17)$$

$$\delta_p = \sqrt{\sum F_{pi}^2} / V \quad (18)$$

$$\delta_h = \sqrt{\frac{\sum E_{hi}}{V}} \quad (19)$$

where F_{di} and F_{pi} are the group contributions to the dispersion and the polar component (F_d and F_p) of the molar attraction constant, respectively. E_{hi} is the hydrogen bonding energy per structural group in $\text{J} \cdot \text{mol}^{-1}$ and V the molar volume of the solvent in $\text{ml} \cdot \text{mol}^{-1}$. The Hansen partial solubility parameters were calculated as $\delta_d = 20.8 \text{ MPa}^{1/2}$, $\delta_p = 6.1 \text{ MPa}^{1/2}$, and $\delta_h = 9.2 \text{ MPa}^{1/2}$.

Method of Hoy

The procedure of Hoy differs in many respects from the method mentioned before. It is based on a molar attraction function (F_t), a polar component (F_p), the molar volume of the solute molecule (V), the Lyderson correction for non-ideality (Δ_T) and auxiliary equations [15]. The values obtained by this method are $\delta_d = 18.0 \text{ MPa}^{1/2}$, $\delta_p = 12.1 \text{ MPa}^{1/2}$, and $\delta_h = 5.1 \text{ MPa}^{1/2}$.

Only δ_d is within the same range as the experimental value and as calculated according to the Hoftzyer/Van Krevelen method whereas δ_p is significantly higher and δ_h significantly lower. Tracing back the calculation procedure reveals that δ_h is strongly dependent on the molar volume which is calculated in case of Hoy's method also from group contributions. The resulting computed value of $360 \text{ cm}^3/\text{mol}$ is much higher than the molar volume of $296.8 \text{ cm}^3/\text{mol}$ found in literature database [16] which is identical with the value calculated from the molecular structure (Fig. 1) by the software ACD/ChemSketch Freeware (version 10.00, Advanced Chemistry Development, Inc., Toronto, ON, Canada, www.acdlabs.com, 2006). If the cohesion parameters are recalculated with the lower molar volume the values obtained are

$\delta_d = 19.8 \text{ MPa}^{1/2}$, $\delta_p = 13.3 \text{ MPa}^{1/2}$, and $\delta_h = 12.6 \text{ MPa}^{1/2}$, with δ_h matching better the experimental value. However δ_p is still higher than determined with the other methods. This fact supports the finding that the Hoy procedure does not appear to fully separate the polar and hydrogen bonding energies [17].

Another set of values was published by Dwan'Isa et al. who computed the cohesion parameters using the software Molecular Modeling Pro [18]. These values ($\delta_d = 21.4 \text{ MPa}^{1/2}$, $\delta_p = 6.9 \text{ MPa}^{1/2}$, and $\delta_h = 9.5 \text{ MPa}^{1/2}$) are very close to those obtained with the Hoftyzer/Van Krevelen method and are most likely calculated by the same algorithm

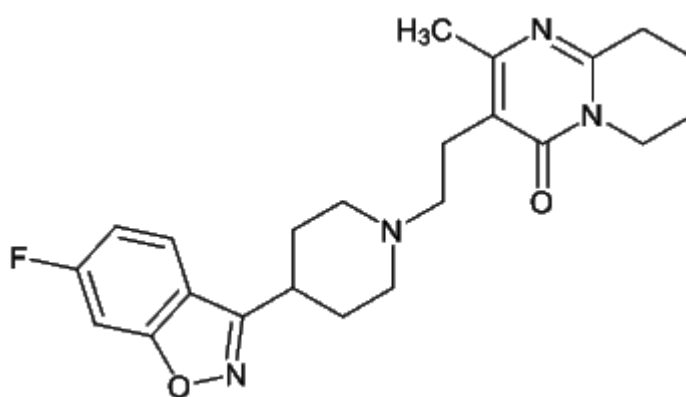


Figure 1: Molecular structure of 3-[2-[4-(6-Fluor-1,2-benzisoxazol-3-yl) piperidino]ethyl]-2-methyl-6,7,8,9-tetrahydro-4H-pyrido [1,2-a]pyrimidin-4-one

On the whole, the experimentally determined values are within a similar range as those calculated by group contribution procedures (with the exception of δ_p according to Hoy) (Tab. 3).

Table 3: Experimentally obtained and calculated partial solubility parameters

	δ_d [MPa ^{1/2}]	δ_p [MPa ^{1/2}]	δ_h [MPa ^{1/2}]
Experimental results	18.7	5.4	11.6
Calculated values (Hoftyzer, Van Krevelen)	20.8	6.1	9.2
Calculated values (Hoy)	19.8	13.3	12.9
Value derived from literature *)	21.4	6.9	9.5

*) Dwan'Isa et al., 2005 [18]

Nevertheless they are considered more reliable than those derived from molecular structure elements on the basis of empirical rules. Especially the calculated values for δ_d are extremely high and contrary to the measured solubility in less lipophilic solvents. Thus, for further considerations, only the experimental results were used.

3.2 Estimation of the solubility of the drug substance in different solvents and in PLGA

Partial solubility parameters are often represented in a three-dimensional grid, the so-called Hansen space. The mutual miscibility of two substances or the solubility of one substance within the other can be estimated from their relative coordinate positions, i.e. the Euclidean distance between both coordinate points. The smaller the distance in the diagram, the better is the mutual solubility between the two substances. Figure 2 shows the coordinate positions of the solvents listed in Table 1 and the coordinate points of the API calculated by different methods.

In such diagrams solvents and low molecular molecules are commonly depicted as single coordinate points whereas polymers are drawn as volume structures, mostly spheres. They enclose the diagram range in which solvents with good solvating or swelling properties for the polymer are located.

Schenderlein et al. used two different experimental methods and a group contribution approach to determine the center point and the interaction radius of the solubility sphere of PLGA (75:25) [19]. The following values are reported, differing especially with respect to δ_p : Swelling experiments ($\delta_d = 17.4 \text{ MPa}^{1/2}$, $\delta_p = 8.3 \text{ MPa}^{1/2}$, $\delta_h = 9.9 \text{ MPa}^{1/2}$), turbidity titration ($\delta_d = 15.8 \text{ MPa}^{1/2}$, $\delta_p = 3.5 \text{ MPa}^{1/2}$, $\delta_h = 9.1 \text{ MPa}^{1/2}$) and group contribution method ($\delta_d = 16.1 \text{ MPa}^{1/2}$, $\delta_p = 9.7 \text{ MPa}^{1/2}$, $\delta_h = 11.7 \text{ MPa}^{1/2}$). The interaction radius which was only determined by polymer swelling amounts to $7.8 \text{ MPa}^{1/2}$.

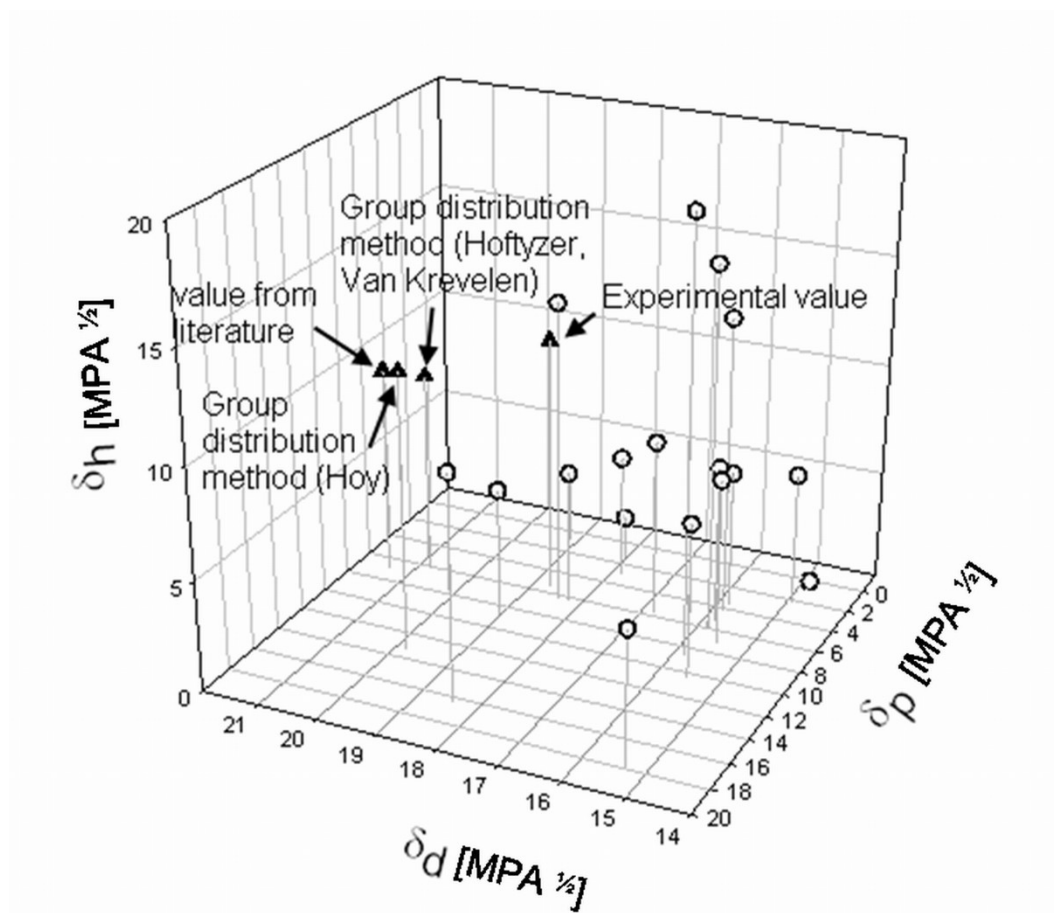


Figure 2: Position of on the drug substance (calculated and experimentally determined) and the tested solvents (Tab. 1) in a three dimensional diagram

As the experimental determination is considered to be more accurate than predictions from the molecular structure and the data obtained from swelling measurements are the most comprehensive for they provide also an interaction radius of the sphere, only these values were used for further calculations (Fig. 3).

The coordinate position of a substance with respect to a polymer solubility sphere is characterized by the ratio of the coordinates' distance to the centre of the sphere and the sphere's interaction radius. This ratio is called the Relative Energy Difference (RED) [20]. A RED less than 1.0 indicates a high affinity or solubility (coordinate position within the sphere), a RED higher than 1.0 lower affinities to the polymer (coordinate position outside the sphere) (Fig. 4).

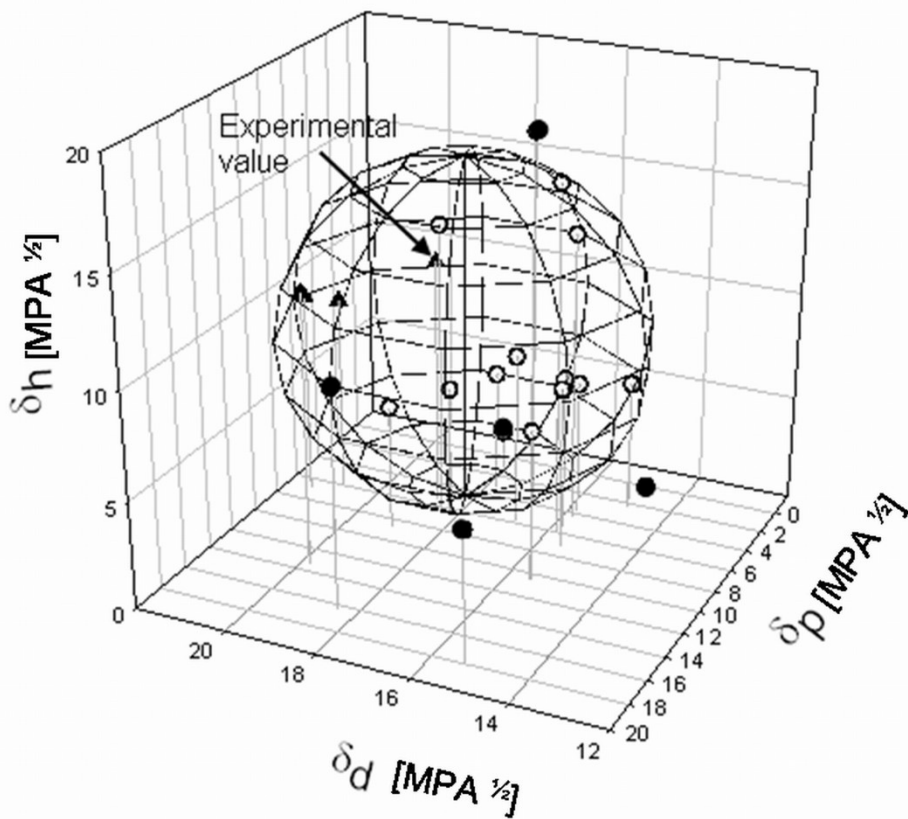


Figure 3: Solubility sphere of PLGA (75:25) and the position of the solvents (● = outside the sphere, ○ = inside the sphere) and on the drug substance (▲) in the $\delta_d - \delta_p - \delta_h$ -diagram

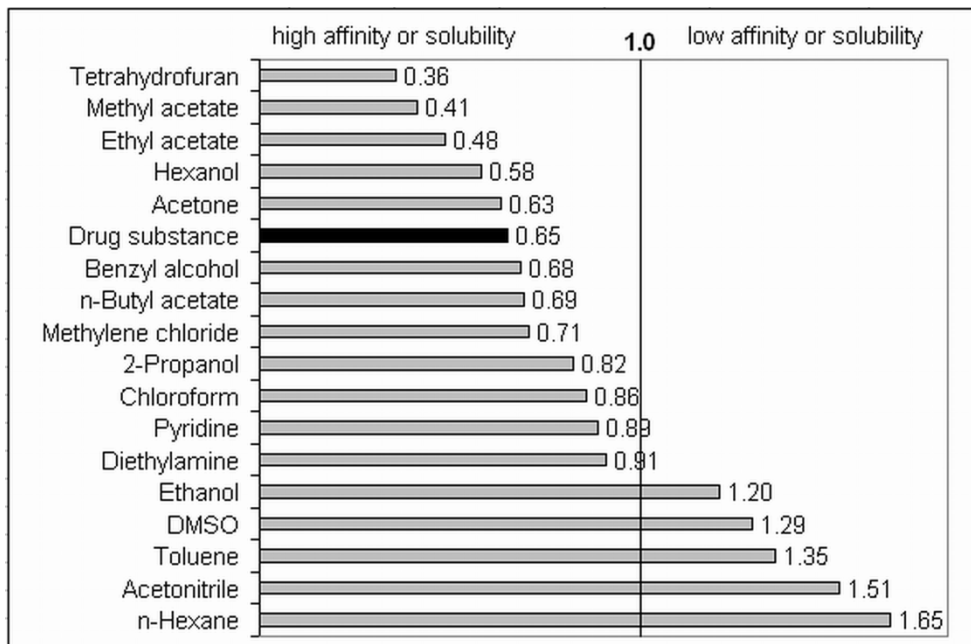


Figure 4: Relative Energy Difference between PLGA (75:25) and the analyzed solvents and the API, respectively

The distance between two coordinate points within the Hansen space $D_{(S-P)}$ is calculated by the following equation [20]:

$$D_{(S-P)} = \left[4(\delta_d \mathbf{s} - \delta_d \mathbf{p})^2 + (\delta_p \mathbf{s} - \delta_p \mathbf{p})^2 + (\delta_h \mathbf{s} - \delta_h \mathbf{p})^2 \right]^{1/2} \quad (20)$$

From the experimentally determined solubility parameters of the API and the center coordinates of the PLGA 75:25 solubility sphere taken from literature (swelling data from Schenderlein et al. [19]) a distance of 5.05 and a RED of 0.61 was calculated, which implies that the drug substance lies inside the sphere and should be soluble in the polymer to a certain extent.

The true solubility within a polymer matrix, unbiased by depositions of unsolved crystalline or amorphous substance, is hardly accessible by direct chemical analysis. A mathematical approach was made by calculating the solubility in the polymer matrix based on the regression equation 13. After $\bar{\delta}_{2d}$, $\bar{\delta}_{2p}$, and $\bar{\delta}_{2h}$ and the coefficients C_0 to C_6 are calculated they can be inserted in equation 13 together with the polymer's $\bar{\delta}_{1d}$, $\bar{\delta}_{1p}$, and $\bar{\delta}_{1h}$ to obtain X_2 as the solubility of on the drug substance in PLGA. The conversion of the mole fraction solubility into a weight/weight concentration was done on basis of the average molecular weight of a repetitive monomer unit of PLGA (75:25) (68.6 g/mol). By this method X_2 was computed as 0.0235. This corresponds to 0.144 g API per g PLGA, which is a drug load of 12.6% (w/w) in the drug/PLGA mixture.

In order to demonstrate the plausibility of these results, a second approach was tried based on differential scanning calorimetry. Microparticles with different degree of drug load as well as physical API / PLGA mixtures (0%, 30.9%, 49.3%, 81.8% and 100%) were measured and the enthalpy of fusion was calculated from the melting peak of the drug. A linear correlation could be established between the enthalpy of fusion and the drug concentration in the mixtures. Also in case of the microparticles a linear correlation function was found with almost the same slope but enthalpies being between 14 and 21 J/g lower than those of the mixtures with a corresponding drug amount. This can be explained by the fact that the drug, which is dissolved in the polymer, is not in a crystalline state and does not contribute to the enthalpy of fusion. The same applies to amorphous drug which is finely dispersed between the polymer chains and thus protected against recrystallization. From the offset between the correlation curves, we could calculate a fraction of 13-16% on the API dissolved in the polymer matrix. Taking into consideration that both, the

theoretical approach as well as the DSC measurements are afflicted with a certain error, the results are within the same range.

3.3 Prediction of drug-polymer-interactions during processing based on solubility parameters and effects on the properties of the resulting microspheres

For the microparticle preparation process three sets of solubility parameters (for the drug, the polymer and the solvent or solvent mixture) have to be considered. It is essential, that the drug substance and the polymer are soluble in the solvent of the dispersed phase. On the other hand the solvent should be soluble in the aqueous phase to some degree and extractable from the droplets to induce microparticle solidification. The solvent has to be chosen, to meet both criteria.

In pure methylene chloride the polymer and the drug substance show almost the same solubility. The distance calculated by Eq. 20 between drug substance and methylene chloride is $5.46 \text{ MPa}^{1/2}$ and between PLGA and methylene chloride it is $5.51 \text{ MPa}^{1/2}$. The solubility of both was varied by adding different co-solvents in the process. A fraction of methylene chloride was substituted by a better or a poorer solvent for the drug in order to modify the drug distribution in the polymeric phase and the degree of crystallization during the manufacturing process. This is influenced by the drug's solid state solubility [21], which in turn has an impact on the release behaviour of the resulting microspheres. Solid dispersions of poorly water soluble drugs are often used to enhance the drug dissolution and bioavailability [22, 23]. In case of a long acting dosage form a low solubility and a crystalline state of the drug is desirable.

Minghetti et al found, that the release rate of the solved drug was most quickly, when the difference between the solubility parameter of the drug and the polymer matrix was highest due to the maximum thermodynamic activity of the drug substance [24].

Furthermore co-solvents have been reported to influence the partitioning of the organic phase into the external phase and thus to affect for example drug load and release kinetics of the microspheres [25].

In the present study we investigated the impact of binary solvent mixtures on the properties of the resulting microspheres. Methylene chloride was used as the basic component in the organic phase, as it is a common solvent for the preparation of

PLGA microspheres with the advantage of simple removal by extraction and evaporation. Benzyl alcohol was added in various concentrations to enhance the dissolving power for the drug substance, whereas n-butanol was used to cause the opposite effect.

Consequently, microparticles were prepared with 10%/90% and 25%/75% mixtures of benzyl alcohol and methylene chloride (Tab. 4) and with a 25%/75% mixture of n-butanol and methylene chloride. With all solvent mixtures spherical, nonaggregated microparticles were obtained. However the particles prepared with 25% benzyl alcohol and n-butanol were not stable during storage at room temperature and agglomerated by and by.

The partial solubility parameters of benzyl alcohol differ from those of methylene chloride especially in their hydrogen bonding component. Benzyl alcohol has a lower δ_h and is a better solvent for the API. As both solvents are only poorly soluble in water with solubilities being in about the same range (benzyl alcohol: 3.9% (m/v), methylene chloride: 2.0% (m/v)) it can be assumed that the extraction process is mainly governed by different evaporation rates.

Table 4: Influence of the solvent mixture on encapsulation efficiency and drug release rate

	Ratio (w/w)	Ratio (v/v)	Encapsulation efficiency [%]	Drug released after 25 d [%]
Methylene chloride			83.6	40.2
Methylene chloride : Benzyl alcohol	90:10	88:12	85.0	52.0
Methylene chloride : Benzyl alcohol	75:25	70:30	82.9	33.8
Methylene chloride : n-Butanol	75:25	65:35	80.5	51.5

As methylene chloride (b.p. 39.8 °C) is more volatile than benzyl alcohol (b.p. 205 °C), it evaporates faster, thus shifting of the solvent ratio inside the particles (Fig. 5). It can be seen that if the process starts with a benzyl alcohol / methylene chloride ratio of 10:90 or 25:75 the solubility of the polymer in the solvent mixture, expressed as the coordinate distance in the Hansen space, decreases whereas the solubility of on the API increases during evaporation of methylene chloride. Even though the drug again becomes a little bit less soluble toward the end of the process this does not change the fact that there is a net improvement of the

drug's solubility after complete removal of methylene chloride. These contrasting changes in solubility, i.e. deterioration in case of PLGA and improvement in case of the drug, support a rapid hardening of the particles and an effective retention of the drug in the particles. At least in case of a 10:90 solvent mixture, causing a $2.6 \text{ MPa}^{1/2}$ net reduction of the drug-solvent coordinate distance during the process, improved encapsulation efficiency could be found in comparison to particles prepared with pure methylene chloride. Only a marginal change of the encapsulation efficiency even in the opposite direction was observed with a 25:75 mixture which is in a certain correlation to the much smaller intra-process distance change of only about $1 \text{ MPa}^{1/2}$. A fraction of more than 25% benzyl alcohol in the organic phase is not beneficial because multinucleated particles are formed the product is not stable and agglomerates during storage. Furthermore a high content of residual benzyl alcohol is undesirable with regard to toxicological aspects.

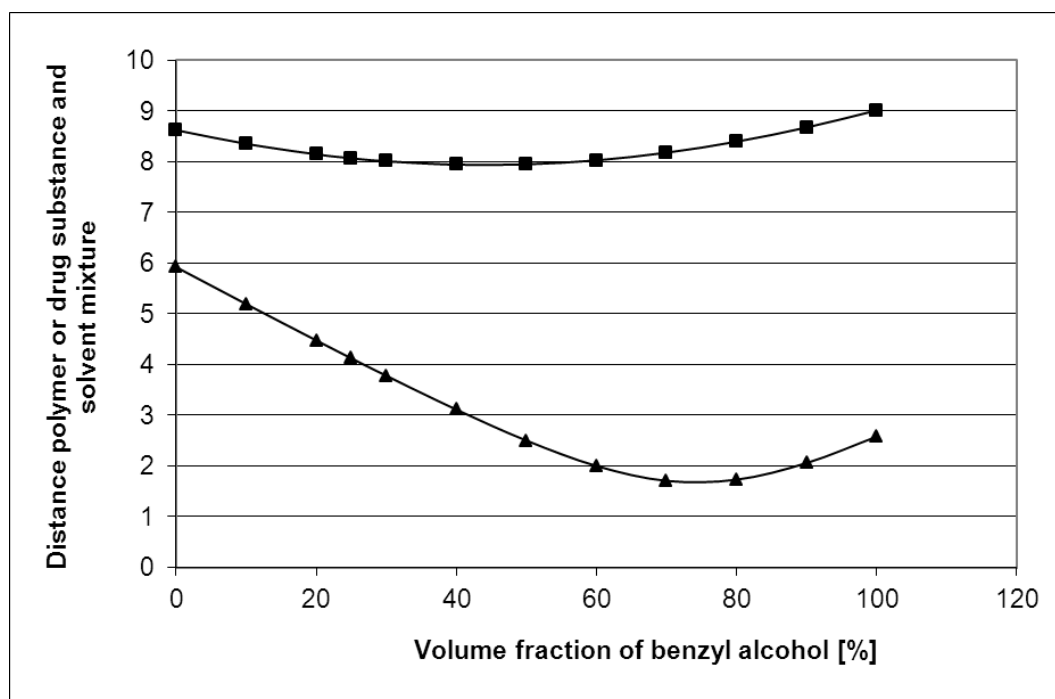


Figure 5: Distance between polymer (-■-) and API (-▲-) and solvent mixture with varying fraction (v/v) of benzyl alcohol.

As a second solvent for the preparation of the microspheres, a 25:75 n-butanol / methylene chloride mixture was employed. n-Butanol differs in its dispersion forces and hydrogen bonding component from methylene chloride and has only a low dissolving power for the API. As n-butanol (b.p. $117.7 \text{ }^\circ\text{C}$) is also less volatile than methylene chloride the same consideration as for benzyl alcohol and methylene

chloride can be made (Fig. 6). The solubility of the polymer is higher in n-butanol than in methylene chloride with a local maximum at a 60:40-mixture. It is much better than in benzyl alcohol / methylene chloride mixtures. By contrast, the solubility of the drug substance is poorer and decreases strongly from 100% methylene chloride to 100% n-butanol. Consequently a lower retention of the drug has to be expected and was confirmed by an encapsulation rate 3.1% lower than in case of a pure methylene chloride process.

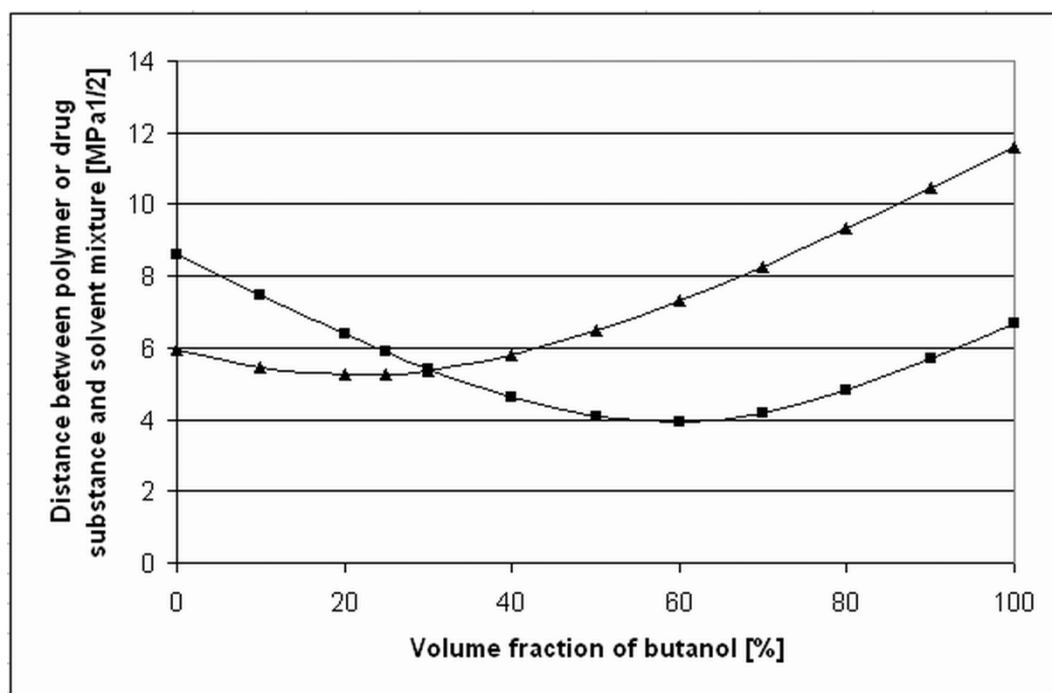


Figure 6: Distance between polymer (-■-) and API (-▲-) and solvent mixture with varying fraction (v/v) of n-butanol.

Apart from the effect on the encapsulation efficiency the solvent was found to influence also the morphology of the drug. X-ray diffraction demonstrates that in contrast to methylene chloride or its mixtures with benzyl alcohol (data not shown), which lead to a certain amount of crystalline drug, the n-butanol / methylene chloride mixture caused deposition of the drug in a totally amorphous form (Fig. 7).

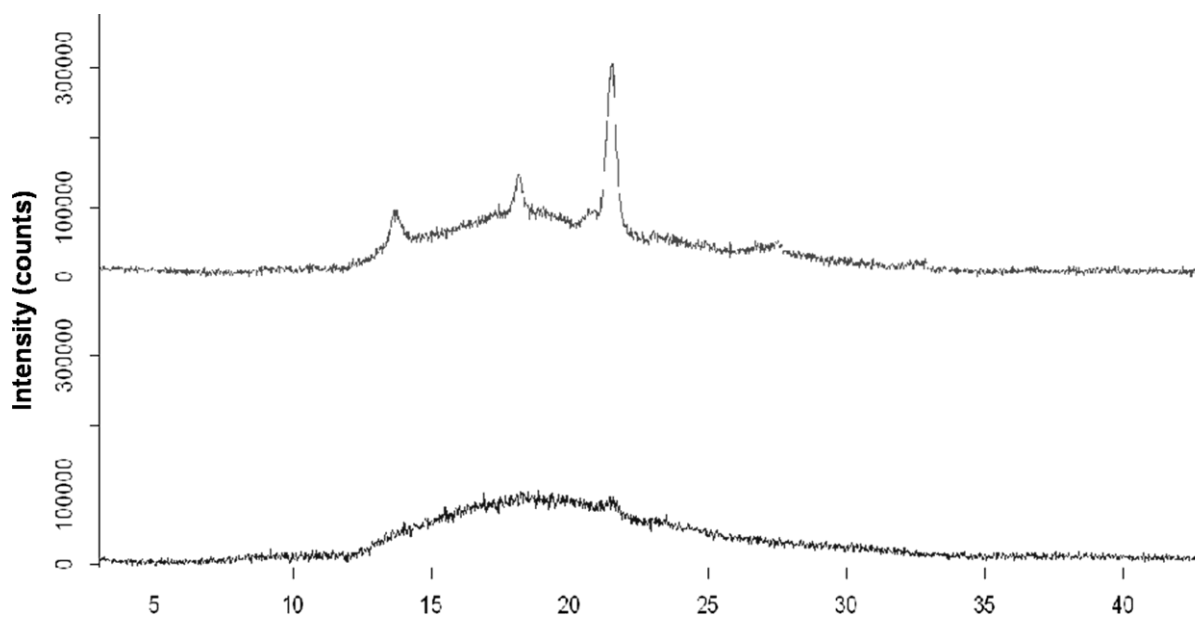


Figure 7: X-ray diffractogram of microspheres prepared with methylene chloride (top) and with a mixture of methylene chloride and n-butanol (75:25) (bottom)

When the concentration of n-butanol rises during the process as described above and thus the solubility of the drug substance in the solvent mixture inside the microspheres decreases, the partition of the drug between solvent regions and polymeric phase shifts in favour of the latter. Because the polymer acts as a crystallization inhibitor the drug will not precipitate in a crystalline but in an amorphous state. In solid dosage forms normally the most stable polymorph of a drug substance is preferred, as an amorphous drug substance is thermodynamically less stable and tends to undergo uncontrollable alterations during storage [26].

Surprisingly, in case of the studied microspheres the presence of amorphous API had about no influence on the drug release profile (Fig. 8). Regarding the drug release of the microspheres prepared with benzyl alcohol and methylene chloride also no influence could be shown. All curves were within the variation limits obtained with different batches from a pure methylene chloride process.

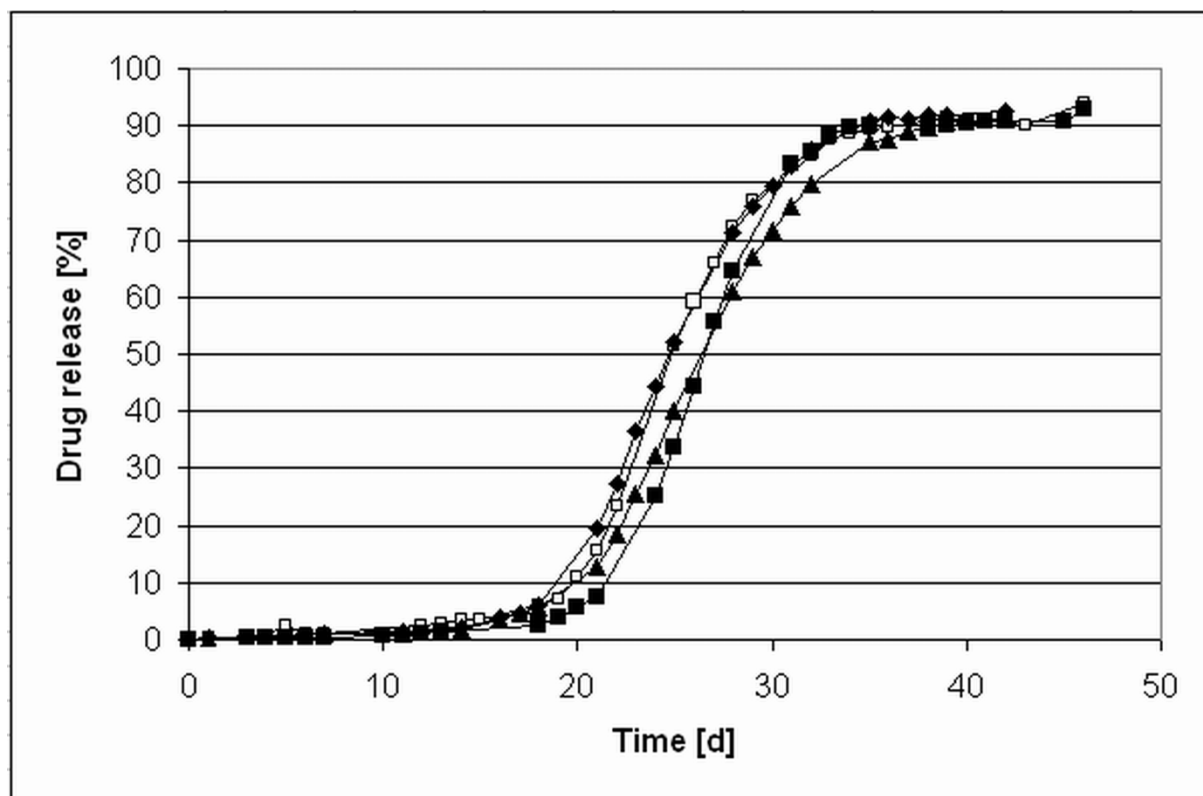


Figure 8: Drug release of microspheres prepared with different organic solvents: methylene chloride (-▲-), methylene chloride / n-butanol 75:25 (w/w) (-□-), benzyl alcohol / methylene chloride 75:25 (w/w) (-■-) and 90:10 (w/w) (-◆-)

It could be shown by DSC measurements that already on the second day of the release test the amorphous fraction had disappeared and a recrystallization peak could not be observed anymore. This indicates that the morphological state of the embedded drug is irrelevant for the release kinetics because recrystallization occurs upon the first contact with water and subsequently the drug is always released from a crystalline solid. Thus any potential recrystallization during storage is not likely to have a major impact on drug release.

4 Conclusions

The partial solubility parameters of 3-{2-[4-(6-Fluor-1,2-benzisoxazol-3-yl) piperidino]ethyl}-2-methyl-6,7,8,9-tetrahydro-4H-pyrido[1,2-a]pyrimidin-4-on were determined by three different methods, of which the experimental approach appears to provide the most reliable values. The structure of this drug substance is rather complex for the calculation by group contribution methods. For some structural elements of the molecule no values are tabulated. From the solubility parameters of

on the API and of PLGA a fraction of 12.6% of the drug was calculated to be dissolved in the polymer matrix. This order of magnitude could also be verified by DSC measurements.

Methylene chloride is one of the most commonly used solvents for the preparation of PLGA microspheres by emulsion-solvent evaporation. It is highly volatile and easily extractable from the microspheres. On the basis of partial solubility parameters two co-solvents were chosen as additional solvent components. Benzyl alcohol was selected as it enhances and n-butanol as it diminishes the dissolving power for the drug substance. Three different co-solvent / methylene chloride mixtures were analyzed with regard to their particle characteristics and drug release behaviour. The encapsulation efficiency was slightly increased if the drug became better soluble in the solvent mixture during the process and it was diminished if the extraction process led to a mixture with a lower dissolving power for the drug. Moreover, the solvent selection showed an influence on the morphology of the drug and it could be shown, that the addition of n-butanol caused an almost completely amorphous state of the API. It is remarkable, that these particles produced nearly the same drug release profile as particles, which contained the drug in a crystalline state. Recrystallization upon the first contact with dissolution medium was found to be the reason for this behaviour. Thus, microspheres which contain the drug or fractions of the drug in an amorphous state are not to be considered as prone to instabilities influencing the drug release kinetics.

5 References

- [1] Bodmeier, R.; McGinity, J.W. Solvent selection in the preparation of Poly(DL-lactide) microspheres prepared by the solvent evaporation method. *International Journal of Pharmaceutics* **1988**, *43*: 179-186.
- [2] O'Donnell, P.B.; McGinity, J.W. Preparation of microspheres by the solvent evaporation technique. *Advanced Drug Delivery Reviews* **1997**, *28*: 25 – 42.
- [3] Cho, S.W.; Song, S.H.; Choi, Y.W. Effects of solvent selection and fabrication method on the characteristics of biodegradable poly(lactide-co-glycolide) microspheres containing ovalbumin. *Archives of Pharmacal Research* **2000**, *23*: 385-390.
- [4] Moldenhauer, M.G.; Nairn, J.G. Solubility parameter effects on the microencapsulation in the presence of polyisobutylene. *Journal of controlled release* **1994**, *31*: 151-162.
- [5] Bodmeier, R.; McGinity, J.W. Polylactic Acid Microspheres containing Quinidine Base and Quinidine Sulfate prepared by the solvent evaporation technique. 2. Some process parameters influencing the preparation and properties of microspheres. *Journal of Microencapsulation* **1987**, *4*: 289-297.
- [6] Hildebrandt, J.H.; Scott, R.L. *The solubility of non-electrolytes*, Dover Publications **1964**, New York.
- [7] Moldenhauer, M.G.; Nairn, J.G. The control of ethylcellulose microencapsulation using solubility parameters. *Journal of Controlled Release* **1992**, *22*: 205-218. [8] Bordes,C.; Freville,V.; Ruffin,E.; Marote,P.; Gauvrit,J.Y.; Briancon,S.; Lanteri,P. Determination of poly(epsilon-caprolactone) solubility parameters: Application to solvent substitution in a microencapsulation process. *International Journal of Pharmaceutics* **2010**, *383* (1-2), 236-243.
- [9] De,S.J.; Robinson,D.H. Particle size and temperature effect on the physical stability of PLGA nanospheres and microspheres containing Bodipy. *Aaps Pharmscitech*, **2004**, *5* (4).
- [10] Panyam,J.; Williams,D.; Dash,A.; Leslie-Pelecky,D.; Labhasetwar,V. Solid-state solubility influences encapsulation and release of hydrophobic drugs from PLGA/PLA nanoparticles. *Journal of Pharmaceutical Science* **2004**, *93* (7), 1804-1814.
- [11] Reuteler-Faoro, D.; Ruelle, P.; Nam-Tran, H.; de Reyff, C.; Buchmann, M.; Negre, J.C.; Kesselring, U. A new equation for calculating partial cohesion parameters of solid substances from solubilities. *The Journal of Physical Chemistry* **1988**, *92*: 6144-6148.

- [12] Martin, A.; Wu, P.L.; Adjei, A.; Beerbower, A.; Prausnitz, J.M. Extended Hansen Solubility Approach - Naphthalene in Individual Solvents. *Journal of Pharmaceutical Sciences* **1981**, *70* (11):1260-1264.
- [13] Beerbower, A.; Wu, P.L.; Martin, A. Expanded Solubility Parameter Approach .1. Naphthalene and Benzoic-Acid in Individual Solvents. *Journal of Pharmaceutical Sciences*, **1984**, *73* (2), 179-188.
- [14] Bustamante, P.; Escalera, B.; Martin, A.; Selles, E. A Modification of the Extended Hildebrand Approach to Predict the Solubility of Structurally Related Drugs in Solvent Mixtures. *Journal of Pharmacy and Pharmacology* **1993**, *45* (4), 253-257.
- [15] Van Krevelen, D.W.; Cohesive Properties and Solubility. *Properties of polymers*, **2009**, p. 189-224. Elsevier, Amsterdam, Netherlands.
- [16] Scifinder version 7.2 Chemical Abstracts Service, OH, USA. Accessed 2010-11-04, calculated using ACD/Labs software V 8.14 (©1994-2010 ACD/Labs, Toronto, Canada)
- [17] Koleske, J.V. *Paint and Coating Testing Manual: Fourteenth Edition of the Gardner-Sward Handbook*, **1995**. ASTM International, West Conshohocken, PA, USA.
- [18] Dwan`lsa, J.L.; Dinguizli, M.; Preat, V.; Arien, A.; Brewster, M. Qualitative prediction of solubilization of highly hydrophobic drugs in block copolymer micelles. *Journal of Controlled Release* **2005**, *101*: 366-368.
- [19] Schenderlein, S.; Lück, M.; Müller, B.W. Partial solubility parameters of poly(D,L-lactide-co-glycolide). *International Journal of Pharmaceutics* **2004**, *286*: 19-26.
- [20] Hansen, C. *Hansen solubility parameters : A user's handbook*, CRC Press **2000**, Boca Raton/Florida.
- [21] Tse, G.; Blankschtein, D.; Shefer, A.; Shefer, S. Thermodynamic prediction of active ingredient loading in polymeric microparticles. *Journal of Controlled Release* **1999**, *60*: 77-100.
- [22] Chiou, W.L.; Riegelman, H.A. Pharmaceutical Applications of solid dispersion systems. *Journal of Pharmaceutical Sciences* **1971**, *60*: 1281-1282.
- [23] Vippagunta, S.R.; Maul, K.A.; Tallavajhala, S.; Grant, D.J.W.. Solid-state characterization of nifedipine solid dispersions. *International Journal of Pharmaceutics* **2002**, *236*: 111-123.
- [24] Minghetti, P.; Cilurzo, F.; Casiraghi, A.; Montanari, L. Application of viscosimetry and solubility in miconazole patches development. *International Journal of Pharmaceutics* **1999**, *190*: 91-101.

- [25] Rawat, A.; Burgess, .D.J.;Effect of ethanol as a processing co-solvent on the PLGA characteristics. *International Journal of Pharmaceutics* **2010**, 394: 99-105.
- [26] Yu, L.X.; Furness, M.S.; Raw, A.; Outlaw, K.P.W.; Nashed, N.E.; Ramos, E.; Miller, S.P.F.; Adams, R.C.; Fang, F.; Patel, R.M.; Holcombe, F.O.; Chiu, Y.Y.; Hussain, A.S. Scientific considerations of pharmaceutical solid polymorphism in abbreviated new drug applications. *Pharmaceutical Research* **2003**, 20: 531-536.

CHAPTER 3

Control of the droplet size of the primary emulsion in a solvent removal process

Abstract

In an emulsion solvent removal process for the preparation of PLGA microspheres the particle size can be affected at various stages in the process. First of all the particle size depends on the droplet size of the primary emulsion injected into the preparation vessel and can subsequently change during extraction of the solvent from the droplets and transformation into solid particles.

The primary emulsion was prepared using a static mixer. Thereby the effects of three factors on the droplet formation were studied: the pump rate of organic and aqueous phases as well as the application of different numbers of flow obstacles (mixing elements) in the static mixer. The test series was set up by a factorial design as this is an efficient way to study the influence of several process parameters in parallel. By illustrating the relationship between process parameters and obtained droplet size the optimum process parameters to obtain a desired droplet size could be easily determined.

1 Introduction

The particle size is of vital importance for various attributes of microparticulate carrier systems. In case of biodegradable microparticles for injection the particle size is primarily important for their suspensibility and syringeability [1]. Furthermore it influences the in vivo degradation, the drug release kinetics and phenomena like the particle uptake by phagocytic cells. Thus, the control and monitoring of the particle size is necessary to ensure the production of microparticles with desired properties.

In case of a solvent removal process the particle size can be influenced at different stages of the process. The first step in this process is the preparation of a primary emulsion from an organic solution of drug and polymer and an aqueous phase. At this stage of the process the original droplet size is defined. The emulsion can be prepared by a variety of methods, including stirring, static mixing, homogenization, sonication and microfluidization [2-4]. Depending on the applied emulsification method the droplet size can be affected by a variety of formulation parameters like mixer/stirrer geometry, ratio of organic and aqueous phase volume, temperature or polymer concentration among others, which may cause problems in process scale up. In this context, the utilization of a static mixer is advantageous as for scale up several mixers can be used in parallel flow [5, 6] and mathematical extrapolation of the flow rates to larger mixer dimensions is possible [7]. Furthermore, a kinetically stable primary emulsion will only be obtained in the presence of a stabilizer, commonly polyvinyl alcohol. The type and concentration of the stabilizer affects the particle size, shape and the drug encapsulation efficiency [8-10]. This primary emulsion is subsequently added to a large surplus of aqueous phase and stirred to allow extraction and, in case of volatile organic solvents, evaporation of the organic solvent. Throughout this extraction phase and hardening of the droplets to solid particles, size changes can occur. Moreover the emulsion droplets in one single process will show different hardening and result in microparticles with varying characteristics. Whereas the emulsion droplets from the beginning of the process are fed into fresh extraction medium, the droplets from the end come in contact with extraction medium already containing a certain amount of organic solvent.

In this work the size control during droplet formation using a static mixer was studied. The effects of three factors on the droplet size in the primary emulsion were

studied: the pump rate of organic and aqueous phase as well as the application of different numbers of flow obstacles in the static mixer.

2 Materials and methods

2.1 Materials

Poly(D,L-lactide-co-glycolide) 75:25 (Resomer 755 S, Mw = 64710 Da) was purchased from Boehringer Ingelheim (Ingelheim, Germany). Methylene chloride analytical grade was obtained from Merck (Darmstadt, Germany), and TRIS (Tris(hydroxymethyl)-aminomethan) from AppliChem (Darmstadt, Germany). 3-{2-[4-(6-fluor-1,2-benzisoxazol-3-yl)piperidono]ethyl}-2-methyl-6,7,8,9-tetrahydro-4H-pyrido[1,2-a]pyrimidin-4-on was purchased from Jubilant Organosys (Mysore, India) and polyvinylalcohol PVA 18-88 (PVA) from Kuraray Europe GmbH (Frankfurt, Germany).

2.2 Determination of the droplet size – single particle optical sizing (SPOS)

The droplet size distribution was determined by single particle optical sizing (SPOS) with an Accusizer 780 particle sizing system, Sensor: LE400-05SE (Particle Sizing Systems, Santa Barbara, CA). This instrument uses the principle of light obscuration to count and size particles from 0.5 to 400 μm . The data are collected in 512 logarithmically spaced channels with a minimum and maximum fraction width of 1 to 5.54 μm . The primary emulsion was measured without further treatment or dilution promptly after emulsion preparation to prevent hardening of the droplets by evaporation of methylene chloride. To ensure a uniform emulsion, the sample was stirred with a magnetic stirrer. 50 ml of the suspension were analyzed per measurement.

2.3 Formation of the primary emulsion

The primary emulsion was formed from an organic phase, consisting of a solution of 2.8 g 3-{2-[4-(6-fluor-1,2-benzisoxazol-3-yl)piperidono]ethyl}-2-methyl-6,7,8,9-tetrahydro-4H-pyrido[1,2-a]pyrimidin-4-on and 3.2 g PLGA 75:25 in 40 mL

methylene chloride and 500 mL of an aqueous solution of 0.5% (w/v) PVA and 0.1 M Tris buffer (pH 9.0). Both phases were pumped (with a gear pump MCP-Z Process, Ismatec IDEX Health & Science GmbH, Wertheim-Mondfeld equipped with Coriolis-massflowmeters, Sitrans FC Massflo, Siemens AG, Wien, Austria) through a static mixer (Sulzer mixer with SMXE mixing elements, Sulzer Chemtech AG, Winterthur, Switzerland) containing a variable number of mixing elements. The pump rate of the organic phase was varied between 10 and 14 g/min, the flow rate of the aqueous phase between 60 and 80 g/min, and the number of mixing elements from 0 to 4. The utilized mixing elements have a size of 6x6 mm and are arranged end-to-end in a pipe of 60 mm length. The primary emulsion was taken directly from the outlet of the mixer and analyzed by SPOS.

The set-up of the test series was made by Design of Experiments using the software MODDE (Version 9.0.0.0 from Umetrics AB, Umeå, Sweden) [11].

3 Results and discussion

Design of Experiments is a time and cost saving way for screening, optimization and robustness testing of preparation processes. Especially in a microparticle preparation process where many variables have an influence on the resulting product, a statistical experimental design is beneficial [12-14]. It can also be applied on the preparation of the emulsion in a microparticle preparation process [15]. In order to simplify up scaling, the organic phase was dispersed in the continuous phase by the application of a static mixer (Fig. 1). The static mixer consists of a tube with integrated flow obstacles (mixing elements), which, in the laminar operation mode, cause splitting up and recombining of the fluid streams. Thus the average droplet size is achieved when the equilibrium between droplet break up and coalescence is reached [16]. If the geometry of the mixing elements and the composition of the organic and continuous phase are not changed and the experiments are performed at room temperature, there are mainly 3 factors influencing the resulting droplet size: flow rate of the aqueous phase, flow rate of the organic phase and the number of mixing elements.

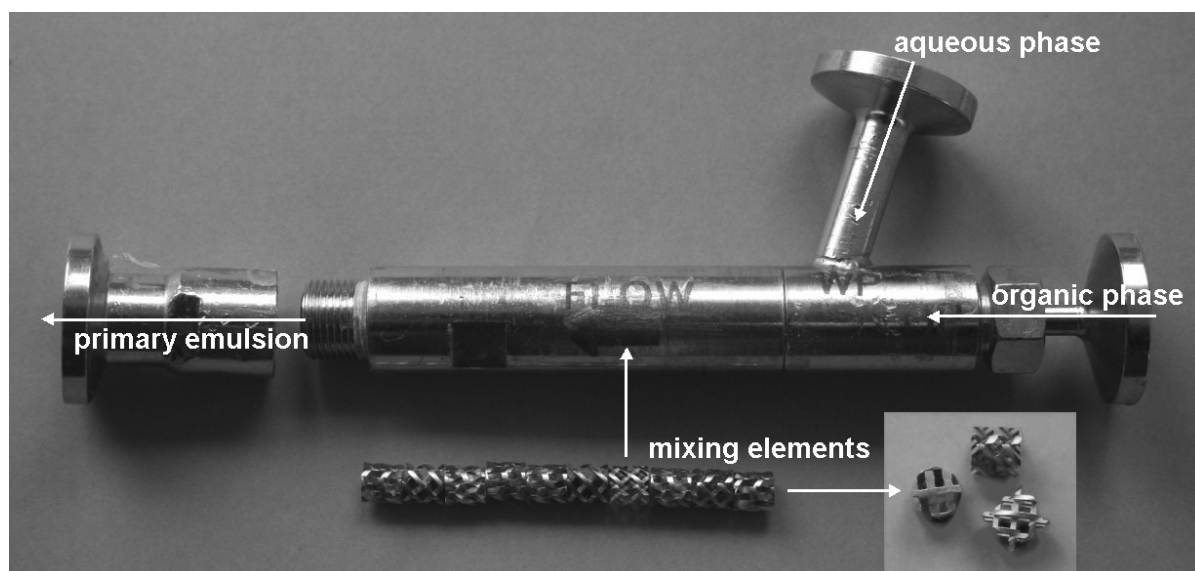


Figure 1: Static mixer with SMXE mixing elements

With a central composite face-centered (CCF) design the three factors and their interactions were investigated. In the CCF design the experimental region is a cube, with the axial points centered on the faces of the cube (Fig. 2). The CCF design with 3 variable factors is based on 14 experiments and three replicated center-points, which are performed in randomized order (Tab. 1).

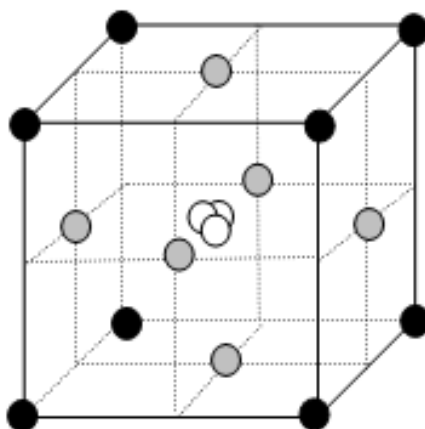


Figure 2: The CCF design in three factors

The resulting droplet size of the primary emulsion as determined by SPOS ranged between approx. 50 and 130 μm and is provided in Table 1.

Table 1: Experimental set up of the CCF design study

	Factor 1	Factor 2	Factor 3	Response
Run order	Flow rate aqueous phase [g/min]	Flow rate organic phase [g/min]	Number of mixing elements	Droplet size * [µm]
8	60	10	0	132.1
9	80	10	0	110.9
10	60	14	0	105.8
11	80	14	0	85.3
23	60	10	4	78.0
24	80	10	4	93.3
15	60	14	4	59.6
16	80	14	4	56.2
3	60	12	2	55.1
4	80	12	2	73.8
5	70	10	2	97.2
6	70	14	2	52.6
12	70	12	0	103.7
17	70	12	4	59.0
1	70	12	2	85.0
2	70	12	2	80.1
7	70	12	2	63.1

* volume weighted median

The experimental data were investigated using regression analysis with a quadratic model. The coefficient plot was obtained by correlating the changes in the factors to the changes in the response (Fig. 3). The error bars of only two factors, the flow rate of the organic phase and the number of mixing elements, do not cross the x-axis indicating a significant impact. The flow rate of the aqueous phase has no significant influence in the examined range of 60 to 80 g/min. Furthermore, there is no significant interaction between the individual factors influencing the particle size.

The not significant interactions of the factors were therefore eliminated from the model and the regression analysis was re-calculated.

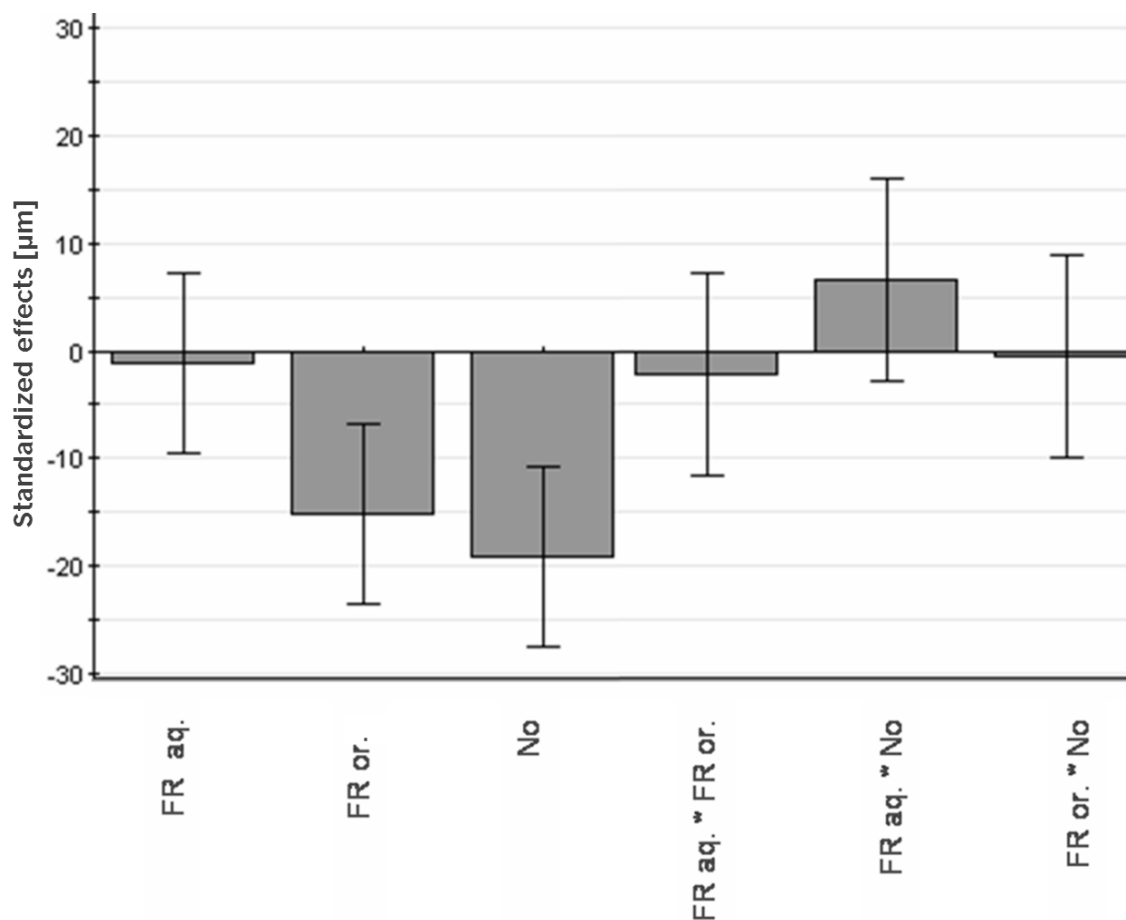


Figure 3: Effects of the flow rates of aqueous phase (FRaq), and organic phase (FRor) and number of mixing elements (No) as well as their interactions on the resulting droplet size

Additionally, the results were converted into response contour plots (Fig. 4). The models show, that the droplet size decreases with an increasing number of mixing elements. At constant flow rates of 70 g/min for the aqueous phase and 12 g/min for the organic phase the droplet size decreases from 103.7 μm without mixing elements to 80.1 μm for 2 and finally 59.0 μm for 4 mixing elements. Such an inverse correlation was also found by Theron et al. [16].

Without the utilization of mixing elements the droplet size is determined only by the flow rates of the phases. By increasing the overall flow rates of both phases at a constant ratio smaller droplet sizes are obtained. This effect is diminished by an increasing number of mixing elements. Whereas the flow rate of the aqueous phase itself has no significant impact on the droplet size, the resulting droplet size is significantly influenced by the flow rate of the organic phase. Increasing flow rate of

the latter reduces the resulting droplet size. Without utilization of mixing elements and at a constant flow rate of 60 g/min for the aqueous phase the resulting droplet size decreases from 132.1 μm at 10 g/min to 105.8 μm at 14 g/min. This effect is less pronounced the higher the number of mixing elements. With 4 mixing elements the droplet size varies only from 78 μm to 59.6 μm . First of all a higher number of mixing elements increases the efficiency of splitting and recombining the fluid streams leading to smaller emulsion droplets at lower flow rates. However, when using 4 mixing elements instead of 2 the droplet size reduction becomes less pronounced.

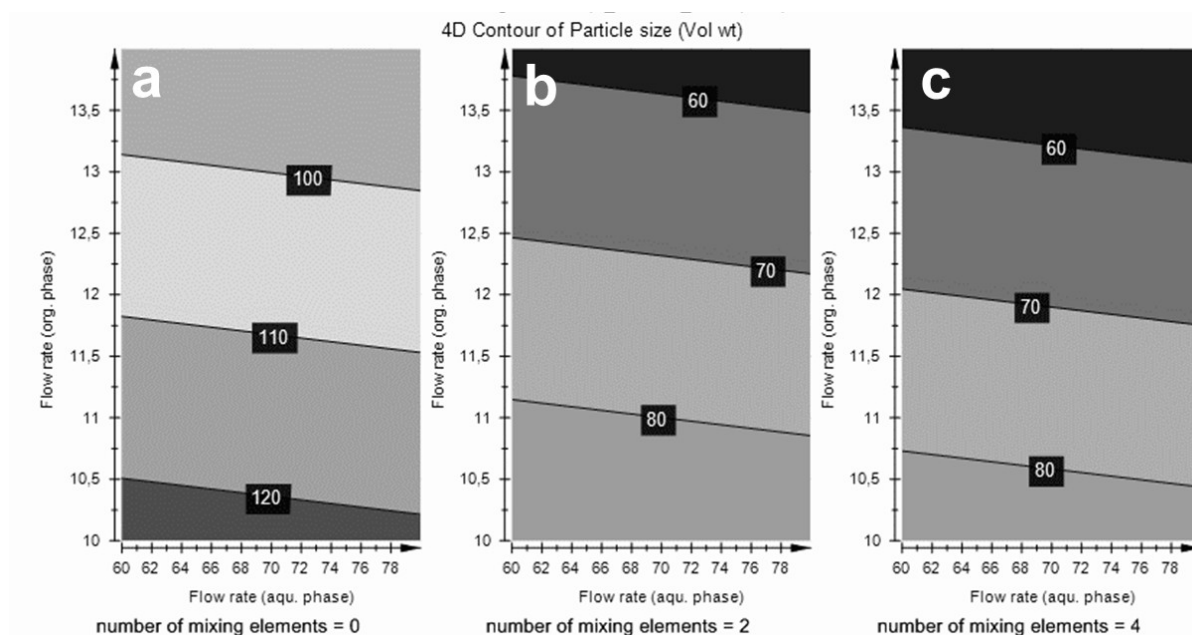


Figure 4: Response contour plot of the flow rates of organic and aqueous phase: (a) without mixing elements, (b) with 2 mixing elements and (c) with 4 mixing elements

The data can also be used to define the parameters necessary to achieve a certain droplet size as illustrated in Figure 5. In this study the target droplet size was between 50 to 60 μm . In fast particle forming processes the particles will show a log normal distribution, which can therefore also be expected for the emulsion solvent removal process. Thus a particle size distribution with a median diameter of 60 μm will range approximately from 30 to 150 μm , which allows a good injectability and syringeability with a standard injection needle [17].

The grey region in the Sweet spot plot indicates the process parameters for the desired droplet size between 50 and 60 μm . This target droplet size cannot be achieved without using mixing elements with the applied flow rates. Only with 2 or 4

mixing elements droplets smaller than 60 μm can be achieved. By using only 2 mixing elements high flow rates have to be applied to obtain a fine dispersion with the desired droplet size. By applying 4 mixing elements this small droplet size can also be obtained at lower velocities of the phases. Over the whole range of 60 to 80 g/min for the aqueous phase and in a range of 11.5 to 14 g/min for the organic phase a droplet size between 50 and 60 μm should be achieved.

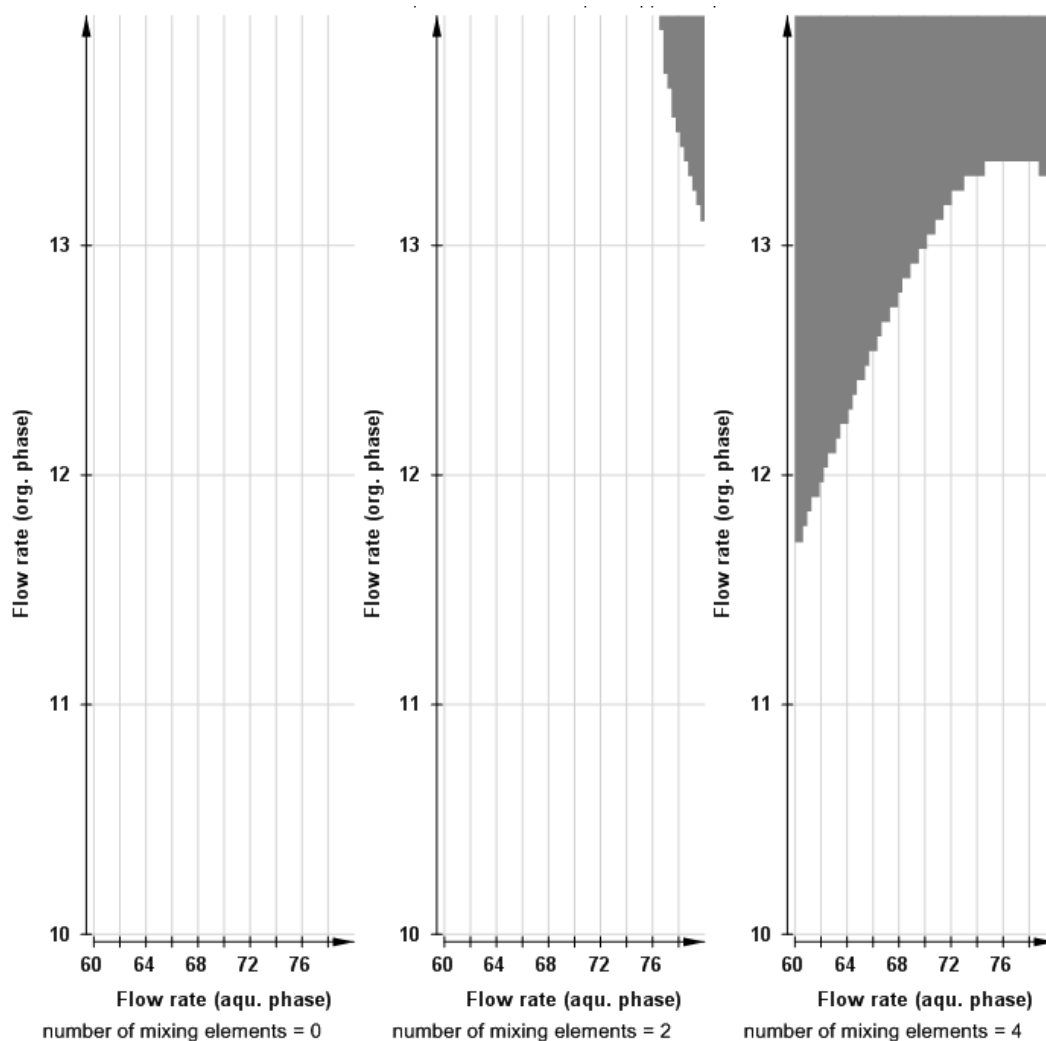


Figure 5: „Sweet spot plot“ for a desired droplet size between 50 to 60 μm

4 Conclusion

With regard to the commercial production of a microparticulate dosage form by the emulsion solvent evaporation technique one critical step especially for the up-scale of the process is the preparation of the primary emulsion droplets. The droplet size is an important factor for the particle size of the resulting microspheres. To investigate, which droplet size will be achieved under certain process parameters, “Design of Experiments” is a versatile tool. With a minimum number of experiments the flow rates and number of static mixing elements can be determined, which are necessary to obtain an appropriate droplet size.

5 References

- [1] Freitas,S.; Merkle,H.P.; Gander,B. Microencapsulation by solvent extraction/evaporation: reviewing the state of the art of microsphere preparation process technology. *Journal of Controlled Release* **2005**, *102* (2), 313-332.
- [2] Berkland, C.; Kim, K.K.; Pack, D.W. Fabrication of PLG microspheres with precisely controlled and monodisperse size distributions. *Journal of Controlled Release* **2001**, *73* (1), 59-74.
- [3] Berkland, C.; King, M.; Cox, A.; Kim, K.; Pack, D.W. Precise control of PLG microsphere size provides enhanced control of drug release rate. *Journal of Controlled Release* **2002**, *82* (1), 137-147.
- [4] Schalper, K.; Harnisch, S.; Muller, R.H.; Hildebrand, G.E. Preparation of microparticles by micromixers: Characterization of oil/water process and prediction of particle size. *Pharmaceutical Research* **2005**, *22* (2), 276-284.
- [5] Wischke, C.; Lorenzen, D.; Zimmermann, J.; Borchert, H.H. Preparation of protein loaded poly(D,L-lactide-co-glycolide) microparticles for the antigen delivery to dendritic cells using a static micromixer. *European Journal of Pharmaceutics and Biopharmaceutics* **2006**, *62* (3), 247-253.
- [6] Siepmann, J.; Siepmann, F. Microparticles Used as Drug Delivery Systems. *Progress in Colloid and Polymer Science* **2006**, *133*, 15-21.
- [7] Kiss, N., Brenn, G., Pucher, H., Wieser J., Scheler, S., Jennewein, H., Suzzi, D. , Khinast, J., Formation of O/W emulsions by static mixers for pharmaceutical applications, *Chemical Engineering Science*, article in press
- [8] Bodmeier, R.; McGinity, J.W. Solvent Selection in the Preparation of Poly(DI-Lactide) Microspheres Prepared by the Solvent Evaporation Method. *International Journal of Pharmaceutics* **1988**, *43* (1-2), 179-186.
- [9] Cavalier, M.; Benoit, J.P.; Thies, C. The Formation and Characterization of Hydrocortisone-Loaded Poly((+/-)-Lactide) Microspheres. *Journal of Pharmacy and Pharmacology* **1986**, *38* (4), 249-253.
- [10] Sansdrap, P.; Moes, A.J. Influence of Manufacturing Parameters on the Size Characteristics and the Release Profiles of Nifedipine from Poly(DI-Lactide-Co-Glycolide) Microspheres. *International Journal of Pharmaceutics* **1993**, *98* (1-3), 157-164.
- [11] Eriksson, L.; Johansson, N.; Kettaneh-Wold, N.; Wikström, C.; Wold, S. *Design of Experiments - Principles and Applications*; Umetrics Academy: Umea, **2008**.

- [12] Kincl, M.; Turk, S.; Vrečer, F. Application of experimental design methodology in development and optimization of drug release method. *International Journal of Pharmaceutics* **2005**, *291* (1-2), 39-49.
- [13] McCarron, P.A.; Woolfson, A.D.; Keating, S.M. Response surface methodology as a predictive tool for determining the effects of preparation conditions on the physicochemical properties of poly(isobutylcyanoacrylate) nanoparticles. *International Journal of Pharmaceutics* **1999**, *193* (1), 37-47.
- [14] Aubert-Pouessel, A.; Venier-Julienne, M.C.; Clavreul, A.; Sergent, M.; Jollivet, C.; Montero-Menei, C.N.; Garcion, E.; Bibby, D.C.; Menei, P.; Benoit, J.P. In vitro study of GDNF release from biodegradable PLGA microspheres. *Journal of Controlled Release* **2004**, *95* (3), 463-475.
- [15] Prinderre, P.; Piccerelle, P.; Cauture, E.; Kalantzis, G.; Reynier, J.P.; Joachim, J. Formulation and evaluation of o/w emulsions using experimental design. *International Journal of Pharmaceutics* **1998**, *163* (1-2), 73-79.
- [16] Theron, F.; Le Sauze, N.; Ricard, A. Turbulent Liquid-Liquid Dispersion in Sulzer SMX Mixer. *Industrial & Engineering Chemistry Research* **2010**, *49* (2), 623-632.
- [17] Whitaker, M.A.; Langston, P.; Naylor, A.; Azzopardi, B.J.; Howdle, S.M. Particle size and shape effects in medical syringe needles: experiments and simulations for polymer microparticle injection. *Journal of Materials Science-Materials in Medicine* **2011**, *22* (8), 1975-1983.

CHAPTER 4

Understanding reflection behavior as a key for interpreting complex signals in FBRM monitoring of microparticle preparation processes ‡

Abstract

The application of focused beam reflectance measurement (FBRM) was studied in a larger scale PLGA microparticle preparation process for monitoring changes of the particle size and the particles' surface properties. Further understanding how these parameters determine the chord length distribution (CLD) was gained by means of single object measurements and data of monodisperse microparticles. It was evaluated how the FBRM signal is influenced by the surface characteristics of the tested materials and the measuring conditions. Particles with good scattering properties provided comparable values for the CLD and the particle size distribution. Translucent particles caused an overestimation of the particle size by FBRM, whereas the values for transparent emulsion droplets were too low. Despite a strong dependence of FBRM results on the optical properties of the samples, it is a beneficial technique for online monitoring of microparticle preparation processes. The study demonstrated how changing reflection properties can be used to monitor structural changes during the solidification of emulsion droplets and to detect process instabilities by FBRM.

‡ Published in International Journal of Pharmaceutics, 2012, 437 (1-2), p. 1-10: Vay,K.; Friess,W.; Scheler,S. Understanding reflection behavior as a key for interpreting complex signals in FBRM monitoring of microparticle preparation processes.

1 Introduction

Since the launch of the PAT initiative by the American Food and Drug Administration (FDA) in 2002 in-process measuring methods have become more and more important for manufacturers of pharmaceuticals. The PAT strategy relies on a thorough understanding of the whole manufacturing process and requires predictive relationships between product properties during intermediate process steps and the final product quality. Thus online monitoring methods have become increasingly interesting.

In case of the preparation of biodegradable polymeric microspheres for sustained drug release, the particle size is a decisive factor for their release behaviour [1, 2]. If such particles are prepared by an emulsion/solvent removal process the size of the resulting microspheres is determined by the droplet diameter of the primary emulsion. In the course of further processing the droplet size undergoes secondary changes which depend, via various mechanisms, on the process parameters of the solvent extraction/evaporation step, for example the stirring rate [3-5]. At-line measurements of the microsphere or droplet size are usually accomplished with laser-based particle size analyzers [6, 7] or the coulter principle [8, 9].

An ideal technique for in-process monitoring of manufacturing process should be non-destructive and fast enough to allow real-time tracking of the particle or droplet size, respectively. There are several particle sizing methods for in- and online applications based, for example, on laser diffraction [10], ultrasonic attenuation spectroscopy or phase Doppler anemometry [13]. A preferably used technique for process monitoring is the focused beam reflectance measurement (FBRM) [14]. An advantage of this measuring principle is the large particle size range from 1 to approximately 4000 μm depending on the rotating speed of the laser beam. Core piece is a probe, emitting a rotating laser beam, which is mounted in a pipe or dipped into a stirred medium. The laser beam with a wavelength of 780 nm revolves with high velocity of 2 m/sec to 8 m/sec depending on the chosen mode, so that the particles' own motion is negligible. When the focus of the laser beam passes a particle, the light is scattered back to the probe window, where the detector is located. The signal is processed by a discrimination circuit with a selectable threshold level. A chord length is calculated from the period during which the light is

backscattered to the detector and the speed of the revolving laser beam. Because the radius of the beam's revolution is much larger than the particle diameter, the chord length can be approximated by the length of a straight line between the two points at which the laser beam randomly intersects the boundary line of the particle's projected area. The FBRM is applicable within a wide concentration or viscosity range and, as up to 100000 chord lengths are measured per second, statistically robust chord length distributions (CLD) are obtained. However such CLDs are difficult to compare with results of common particle sizing methods because they represent a superimposition of the size distribution of all measured particles and the lengths distribution of all possible chord lengths of each single particle. For example, from monodisperse spheres a chord length distribution can be obtained for which the probability $P_k(x)$ of a chord to lie within an interval from $x-w$ to $x+w$ is

$$P_k(x) = \frac{\sqrt{D_k^2 - (x-w)^2} - \sqrt{D_k^2 - (x+w)^2}}{D_k}$$

with D_k being the sphere diameter. In a polydisperse particle distribution D_k is the middle of the k^{th} diameter band and w is half the width of the diameter band. The total number of chord size detections at a certain size x ($n(x)$) is the sum of the probability-weighted number of particles in the k^{th} diameter band (n_k):

$$n(x) = \sum_{k=1}^K n_k P_k(x)$$

k is the number of bands into which the size range is divided. In order to restore the particle size distribution (PSD) from the CLD the equation has to be solved for n_k . Several methods are available to accomplish this. Calculation is easiest in case of spherical particles. However, if the particle geometry is known it is often possible to convert also CLDs from non-spherical particles into PSDs. This transformation has been subject of several studies [15-17].

Typical applications of FBRM are process optimization, control of crystallization processes [18, 19], polymorphic transformations [20, 21] or the characterization of plant suspension cultures [22]. Furthermore several studies using the FBRM for investigation of emulsion systems [23, 24] were published.

In many of these applications the signal pattern measured by FBRM does not only reflect the geometric characteristics of a CLD as explained above but is strongly biased by additional factors. Especially in case of emulsion droplets and other smooth or transparent particles a marked effect of reflection phenomena becomes apparent. In many cases FBRM data are more dependent on the particles' optical properties than those of other particle sizing methods [25]. However most of the previous studies failed to consider these effects. This is also true for the so far only study which describes the use of FBRM in order to monitor a solvent extraction process for microparticle preparation [14]. Our work also addresses the application of FBRM in a solvent removal process but puts special emphasis on reflection phenomena affecting the measurement. Deeper knowledge of this issue could broaden the field of possible applications and help to avoid misinterpretations. The study also investigates how this technique can be used in order to monitor alterations of the particles' surface and the interior of transparent particles even if they do not involve any changes of size or shape.

2 Materials and methods

2.1 Materials

Transparent polystyrene research particles ($98.7 \pm 1 \mu\text{m}$) and black polystyrene microspheres ($103.9 \mu\text{m}$) were obtained from Microparticles GmbH (Berlin, Germany).

Poly (D,L-lactide-co-glycolide) 75:25 (Resomer 755 S): $M_w = 64710 \text{ Da}$ was purchased from Boehringer Ingelheim, (Ingelheim, Germany). Methylene chloride analytical grade was obtained from Merck (Darmstadt, Germany), and TRIS (Tris(hydroxymethyl)-aminomethan) from AppliChem (Darmstadt, Germany). 3-{2-[4-(6-fluor-1,2-benzisoxazol-3-yl)piperidono]ethyl}-2-methyl-6,7,8,9-tetrahydro-4H-pyrido[1,2-a]pyrimidin-4-on was purchased from Jubilant Organosys (Mysore, India) and PVA 18-88 from Kuraray Europe GmbH (Frankfurt, Germany).

2.2 Microparticle preparation

Plain microparticles were prepared by an emulsification solvent extraction/evaporation technique. 4.8 g PLGA were dissolved in 46.1 g of methylene

chloride and the solution was emulsified in 500 ml of the extraction medium consisting of an aqueous solution of 0.5% (w/v) povidon and 0.1 M Tris buffer (pH 9.0). For the purpose of the droplet size measurements this emulsion was pumped through a flow through cell.

Microparticle preparation started with feeding the emulsion into a 5 L jacketed glass reactor containing 3.5 L of the aqueous phase. By stirring for 5 hours the droplets were hardened by solvent extraction and evaporation with an air flow through the headspace of the reactor, which was exactly controlled by a mass flow meter (Vögtlin instruments AG, Aesch, Switzerland). The obtained particles were separated by filtration and dried under vacuum in a desiccator. Different particle batches were produced by varying the extraction temperature between 10 and 35 °C, the air flow through the reactor from 5 to 20 L/min, the stirring speed from 120 to 260 rpm and by adding 0.6% solvent to the aqueous extraction phase. In the same way microparticles containing API were prepared by dissolving 2.8 g 3-{2-[4-(6-fluor-1,2-benzisoxazol-3-yl)piperidono]ethyl}-2-methyl-6,7,8,9-tetrahydro-4H-pyrido[1,2-a]pyrimidin-4-on and 3.2 g PLGA in 46.1 g of methylene chloride.

2.3 Methods

2.3.1 Focused beam reflectance measurement

The FBRM measurements were performed using a Lasentec[®] D600 FBRM system with a probe for laboratory use (Mettler-Toledo AutoChem, Inc., Redmond, USA). At-line measurements were made at a stirring speed of 400 rpm in a glass beaker using the fixed beaker stand which is an accessory part of the Lasentec[®] instrument. For this purpose the microparticles were suspended in an aqueous solution of polysorbate 80 (approximately 150 ml) and measured over 5 minutes. For process monitoring purposes the probe was inserted through the top of the reactor into the stirred suspension (stirring speed 260 rpm), so that the angle of incidence was between 30 to 60°, and the flow was directed obliquely towards the window surface. All measurements were performed using the fine discrimination mode and the default focus position was -20 µm. The FBRM system counts the number of detected chords per second in each size fraction.

2.3.2 Single particle optical sizing (SPOS)

The particle size distributions of polystyrene and PLGA microparticles were additionally measured with an AccuSizer 780 particle size analyzer (Sensor: LE400-05SE; Particle Sizing Systems, Santa Barbara, CA). This instrument uses the principle of light obscuration to count and size particles from 0.5 to 400 μm (single particle optical sensing, SPOS). The data are collected in 512 logarithmically spaced channels with a minimum and maximum fraction width of 1 to 5.54 μm . Approximately 20 mg of particles were weighed in a sample vessel and suspended in 100 ml of an aqueous solution of polysorbate 80. To ensure a uniform suspension, the sample was stirred with a magnetic stirrer and per measurement 50 ml of the suspension was analyzed.

2.3.3 Microscopical image analysis

Microscopical size measurements were performed by the analysis of about 1000 particles per sample using a Nikon eclipse 50i microscope (Nikon Instruments Europe B.V., Kingston, England). The sized particles are classified in size ranges of 2 μm . For every particle size fraction the average volume of a single particle was calculated from the average diameter d_i of each fraction range assuming an ideal spherical shape. By multiplication of the particle count in each fraction with the respective single sphere volume the total volume of each fraction was obtained and a volume weighted particle size distribution was calculated.

3 Results and discussion

3.1 Single object measurements

Techniques, which are based on reflection measurement, can be assumed to be not accurate for particles with strongly convex contours like microspheres. Furthermore as this method is strongly depending on the optical properties, the validity of FBRM should be critically questioned if it is intended to be used for the analysis of reflecting or translucent material. In order to check the quality of the cord length analysis and its suitability for particles with convex surfaces, a simple 2-dimensional system was chosen to investigate the influence of reflecting and curved surfaces on the measured signals. For this purpose thin copper strands with diameters ranging

from 80 to 510 μm were attached radially to the sapphire window of the probe. Thus, the laser beam should sweep the copper strand only in the transverse direction. As the strand has the same diameter at each point not a CLD but a single narrow signal peak is obtained. The true diameter of the wires can be easily measured with a caliper or micrometer screw. In contrast to particulate objects, which have shorter chord length at the flanks, the strands have clearly defined diameters. Nevertheless by FBRM values smaller than the true dimensions were obtained.

The median of the chord length differed between 13 and 28% from the true diameters due to the optical surface properties (Tab. 1). As the surface of the copper strands is smooth and glossy, the laser light is poorly scattered. Because their cross section is not flat, but convex, the intensity of the light which is reflected back to the detector from strongly inclined parts of the surface is below the threshold of detection.

Table 1: Median of the square weighted CLD and chord- tangent- angle

Diameter [μm] (micrometer screw)	Median chord length (Sqr Wt) [μm]	Deviation [%]	Angle α [$^\circ$]
510	443.8	13.0	60.48
260	204.7	21.3	41.93
240	174.1	27.5	46.50
235	203.0	13.6	59.74
80	66.2	17.3	55.84

On the basis of these measurements a critical chord-tangent angle α was calculated by computing the arcsine of the quotient of the median chord length (sqr.wt.) and the diameter determined by the micrometer screw. α ranged from 44 to 60 $^\circ$, beyond which the laser beam is no longer reflected towards the probe head (Fig. 1). The copper strands are an appropriate simplified model to study the FBRM signals obtained from particles with mainly specular or quasi-specular reflection characteristics and convex surfaces. They help to understand the sole influence of reflection phenomena on the FBRM signal, unbiased by chord length effects.

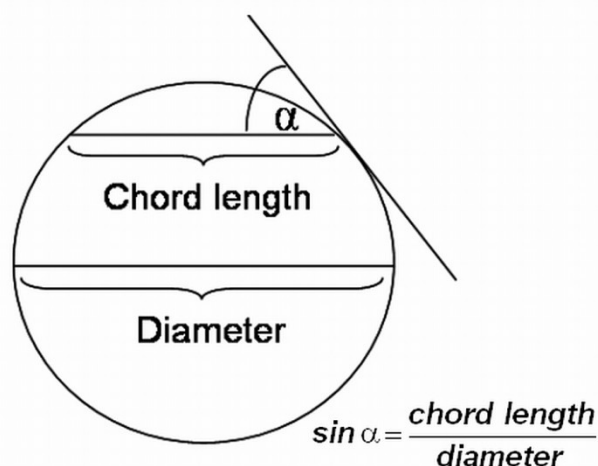


Figure 1: Cross sectional view of a copper strand: Calculation of the chord tangent angle

3.2 Measurements of monodisperse particle collectives

As a second model, which considers also the fact that from particulate objects chord length distributions rather than uniform values are obtained, monodisperse, spherical polystyrene particles of known size were investigated. The shape of a size distribution is always determined by the weighting method which is employed. Number weighted (called “unweighted” by the Lasentec® software) and square weighted CLDs are chosen below according to the issue being addressed. It is often stated that the square weighted median of the chord length distribution meets best the volume weighted median of the diameter distribution obtained by other particle sizing techniques [26, 27]. Also the manufacturer of the Lasentec® device prefers the square weighted median for many applications to be used by default. In order to check this information, the CLD of monodisperse black polystyrene microspheres ($\varnothing = 103.9 \mu\text{m}$) was measured by FBRM and compared with the PSD obtained by SPOS. First monodisperse samples of black polystyrene microspheres with a diameter of $103.9 \mu\text{m}$ (microscopically sized) were suspended in water (concentration $< 1\%$) and measured in a stirred glass beaker. These results were compared to values obtained by SPOS measurements. The square weighted median of the chord length distribution met best the volume weighted median of the diameter distribution obtained by other particle sizing techniques (Fig. 2). This is in agreement with Heath et al. and consequently in the further course of the work the

square weighted CLD or its median is mainly used for comparison with volume weighted PSDs derived from other methods [27].

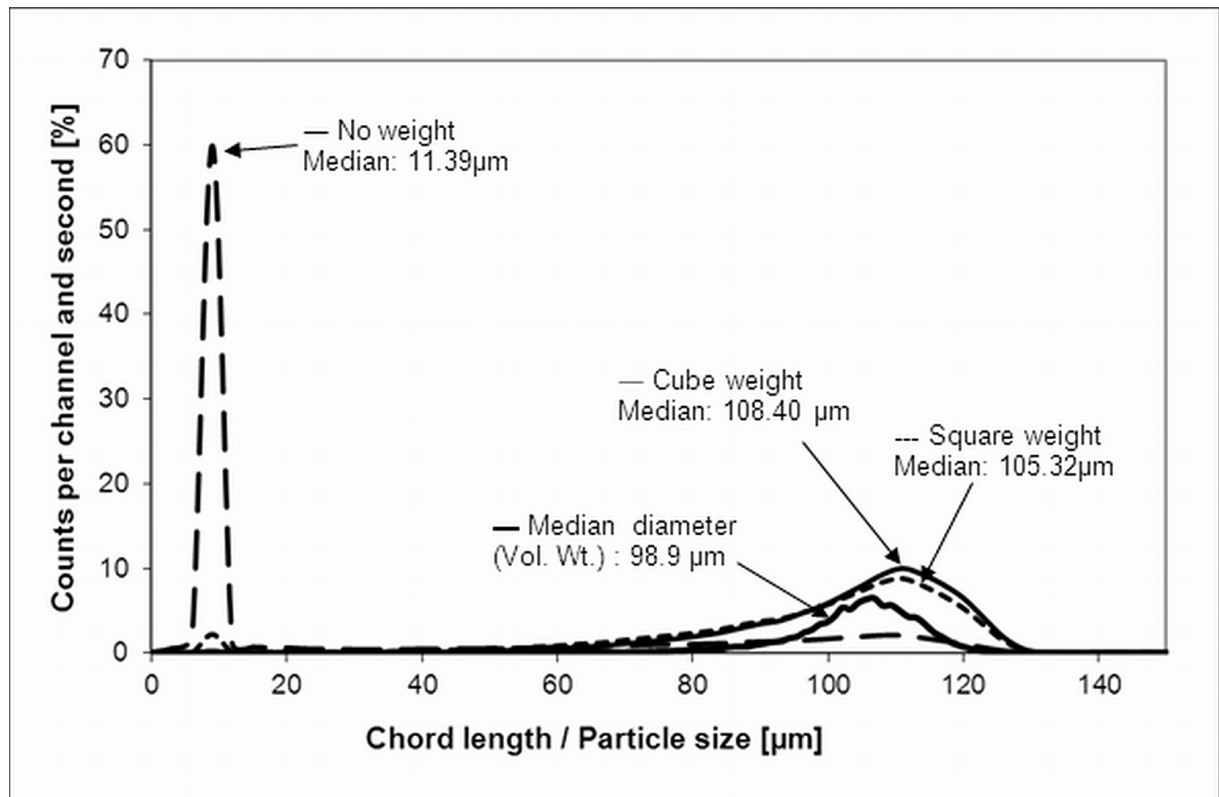


Figure 2: Effect of various weightings on the median of the chord length distribution of monodisperse black polystyrene microspheres ($\varnothing = 103.9 \mu\text{m}$, microscopically sized): unweighted median (dashed line): $11.39 \mu\text{m}$, square weighted median (dotted line): $105.32 \mu\text{m}$ and cube weighted median (solid line): $108.40 \mu\text{m}$.

An explanation for this relationship can be found considering the unweighted ($[1,0]$) and the square weighted ($[3,2]$) mean chord lengths x_{mean} and x_{mean}^2 .

$$x_{\text{mean}} = \frac{\sum_{k=1}^K f(k) x_k}{\sum_{k=1}^K f(k)}$$

$$x_{\text{mean}}^2 = \frac{\sum_{k=1}^K f(k) x_k^3}{\sum_{k=1}^K f(k) x_k^2}$$

K is the number of intervals, x_k is the center of the k^{th} interval and $f(k)$ is the probability of measuring a chord included in the k^{th} interval, The terms in the numerators and denominators are the moments of the CLD. As shown by Wynn, E.J.W., the i^{th} moment of the CLD (μ_i) is proportional to the $(i + 1)^{\text{th}}$ moment of the PSD (m_{i+1}) [28].

$$\mu_i = UTS_i m_{i+1}$$

where U is the speed with which the revolving laser beam progresses, T is the scanning depth, and S_i is a constant dependent on the particle shape. Thus, square weighting of the (unweighted) [1,0] average of the CLD leads to the [3,2] CLD average which, according to the above mentioned equation, is proportional to the [4,3] average of the PSD. Because this volume weighted mean diameter ($d[4,3]$) is also obtained by laser diffraction, square weighting of the CLD provides a good approximation to those volume-based PSDs.

Surprisingly, in the unweighted distribution shown in Fig. 2 a first peak occurs at a small size of only about 10 μm . This signal can be explained by chord splitting which means that low-amplitude signals are superimposed by the baseline noise thus triggering the analyzer to detect multiple small peaks instead of one large signal [25]. Such an artificial chord splitting peak can also be found in case of transparent monodisperse polystyrene microspheres (Fig. 3).

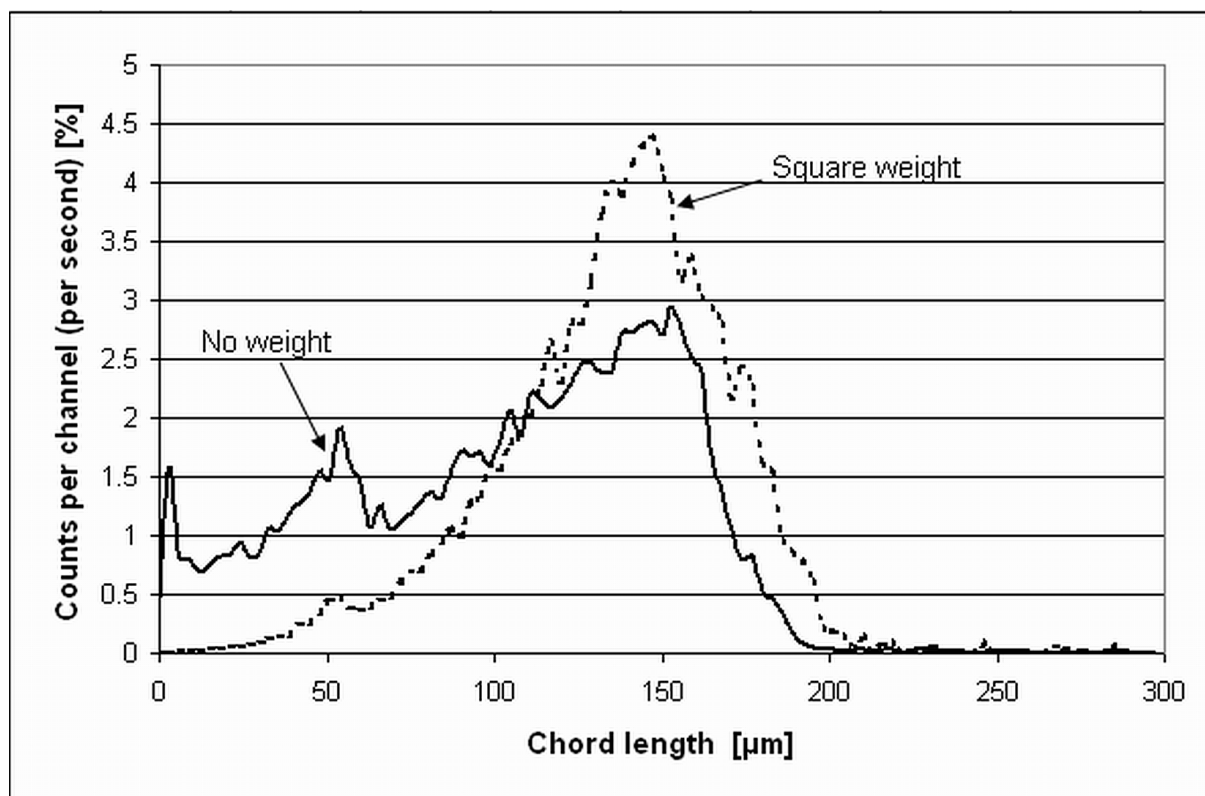


Figure 3: Optical pathways in case of objects with subsurface scattering (polystyrene microspheres), mixed specular and lambertian (copper strands, emulsion droplets), and lambertian (e.g. PLGA microspheres) scattering properties

The CLD of the transparent particles shows also another signal without any obvious reference to the particle diameter. This peak at 54 μm can be attributed to specular reflection phenomena. As the particles do not have a flat but a convex shape, their margins are disinclined to the incident laser beam. In case of a smooth particle surface a large proportion of the light is specularly reflected. At a certain surface inclination the reflected ray, which makes the same angle as the incident ray with respect to the surface normal, does no longer pass the probe's aperture. A signal is detected as long as the light cone hits the particle surface in a position which allows at least partial reflection back to the detector. This depends on the beam's divergence angle, the aperture diameter, the distance between aperture and particle surface, the particle size, and its distance to the focus point. It can be shown that these conditions are fulfilled within a 54 μm -section of the focus path in case of 98.7 μm microspheres [29].

The main peak at 153 μm indicates a chord length which is much larger than the diameter of the spheres. Such large chord lengths can only be caused by divergent rays of the light cone which hit a particle even before the optical axis reaches the particle's outline. However, during this time frame of oblique illumination no

substantial reflection towards the detector can be expected if the surfaces have only specular reflecting or Lambertian scattering properties because in these cases angular incident beams are reflected in the opposite direction of the detector (at least if the particles are not in far distance to the probe window). Only in case of internal reflection or subsurface scattering, which occurs if the particles are transparent or translucent, a substantial part of the light flux is reflected or scattered towards the detector for a longer period than the focus point needs to cross the particles projection plane.

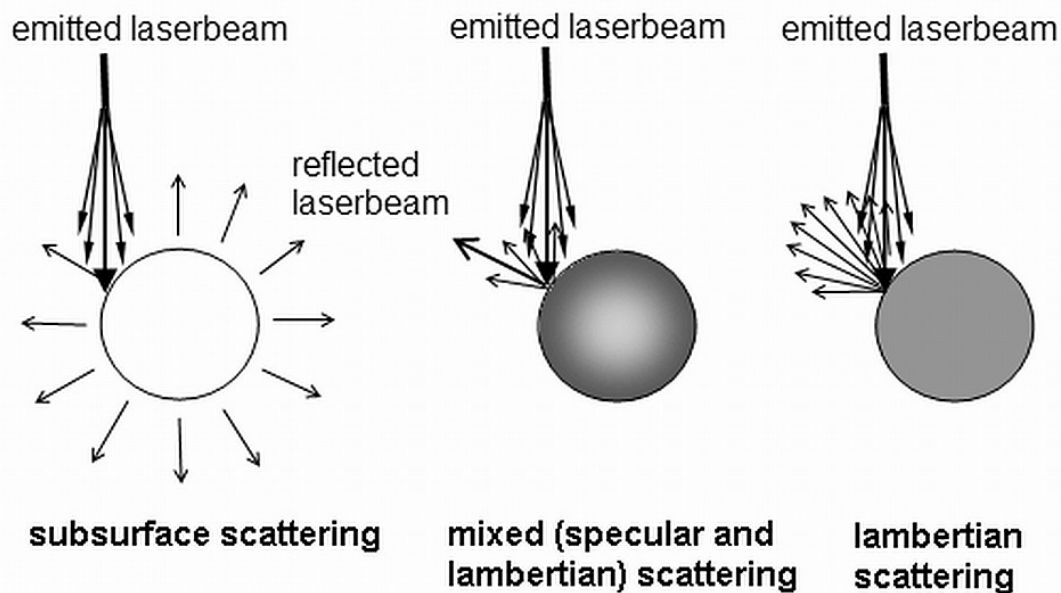


Figure 4: Unweighted and square weighted chord length distribution of monodisperse transparent polystyrene particles ($\varnothing 98.7 \pm 1 \mu\text{m}$ according to manufacturer's data)

If the laser beam hits a translucent particle multiple reflections within the particle occur and the whole sphere lights up (Fig. 4). This effect lasts from the first contact of the light cone with the edge of the particle until the light spot has moved completely off the particle. Thus the duration of the signal is longer than the time span which the focus point itself would need to pass from the one edge to the other and chord lengths larger than the particle diameter are obtained (Fig. 5). Such reflection phenomena can explain the third maximum at $153 \mu\text{m}$ of the unweighted CLD curve in Figure 3.

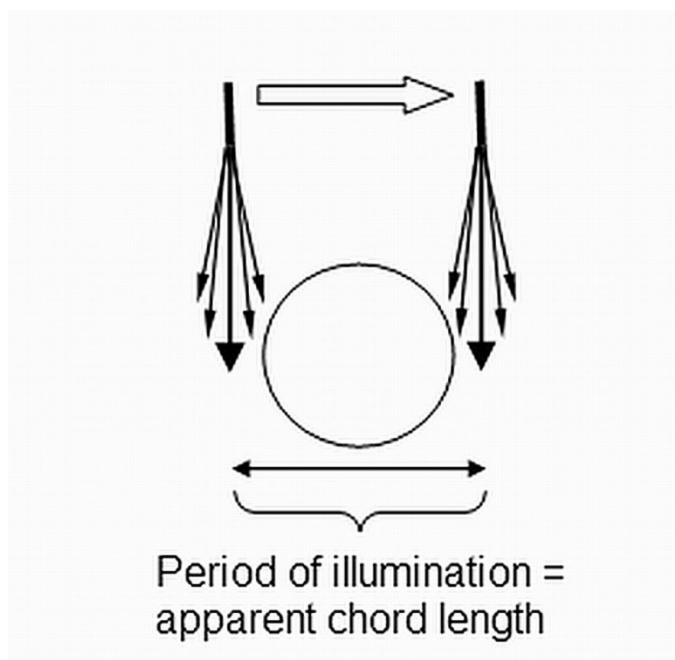


Figure 5: Illumination time for subsurface scattering and resulting apparent chord length

The square weighting of the chord length distribution masks the trimodal distribution pattern resulting in only one broad peak with a median (square weighted) of 141.1 μm and a square weighted mean of 137.2 μm . By contrast the volume weighted diameter measured by SPOS shows a very narrow distribution with a much smaller mean value of only 98.3 μm . It correlates well with the microscopically obtained mean particle size provided by the manufacturer (98.7 μm) and with measurements from own photomicrographs (98.9 μm) (Fig. 6a). As the data show, there is a considerable deviation between the particle diameter and the chord length values measured by FBRM with the latter being about 40% larger than the true particle size.

In order to prove the assumption that this mismatch is caused by internal reflections, as discussed above, the measurements were compared with non-transparent, black microspheres. The volume weighted median diameter of the black microspheres (Fig. 6b) was measured as 103.9 μm with SPOS and exactly the same value was also found by microscopy. In this case, however, the square weighted median measured with FBRM was found to be 105.0 μm (mean = 98.8 μm), which meets the mean particle diameter much better than observed with transparent particles (Fig. 2). Due to the high absorbance of the black particles, the backscattered signal is only very weak, which results in a high degree of chord splitting recognizable by a huge peak at 10 μm in the unweighted distribution. However, the chord splitting

peak becomes nearly insignificant if square weighted data are plotted. This effect is also reflected by the median of the CLD which rises from 11.39 μm to 105.32 μm (unweighted mean: 36.4, square weighted mean: 98.8 μm) when applying the square weighted instead of the unweighted distribution.

Summarizing the aforementioned results, the square weighted mean or median of a chord length distribution is a much better estimate for the mean or median particle diameter than the unweighted statistics. However, it was also shown that FBRM data, regardless by which type of weighting they are obtained, might not represent the true size if transparent or translucent particles are measured.

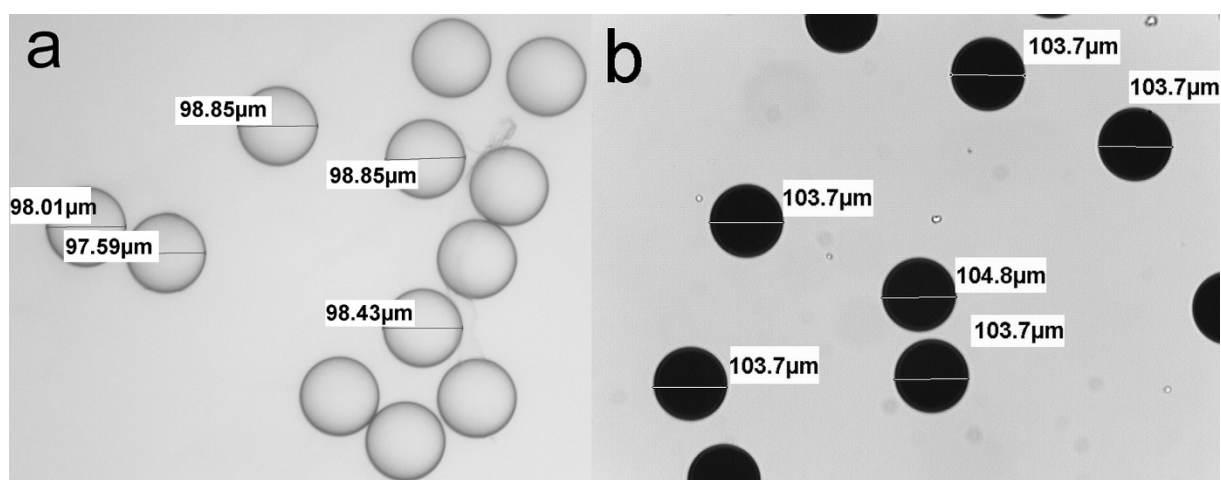


Figure 6: Photomicrographs of transparent ($\varnothing = 98.7 \pm 1 \mu\text{m}$) (a) and black ($\varnothing = 103.9 \mu\text{m}$) (b) monodisperse polystyrene microparticles

In contrast to copper strands which are singular objects positioned in a fixed distance (i.e. directly at the probe window) particle suspensions contain a large number of reflecting objects located at varying distances which are hit randomly by the laser beam. Both factors, the particle concentration and their distance from the focus point, affect the detector signal. Depending on their distance to the probe a more or less broadened light spot is projected onto the particles by the divergent beam. As the focus position is displaceable, the cross sectional size of the beam in front of the probe window can be varied, which, in turn, changes the reflection signal. These complex interactions make it very difficult to pre-estimate the effect of these parameters. For this purpose a series of tests was performed to study the influence of these factors.

3.2.1 Influence of the position of the focal point

There are different variables which can affect the optimum focus position like the particle size range, the solid concentration of the suspension or the optical properties like the refractive index of the dispersant. For very fine particles best results are usually obtained if the focus is positioned inside the probe window, for larger particles the optimum is found by moving the focus position into the suspension [17]. A generally recommended default setting given by the manufacturer of the Lasentec® instrument is $-20\ \mu\text{m}$, which means, that the focus of the laser beam lies slightly inside the sapphire window. The more the focal point is moved inside the probe window, the more the laser beam is broadened and weakened in front of the window [30]. Thus the intensity of the laser beam hitting the particle surface decreases and in turn the backscattered light flux is reduced. This causes a change in the measured particle size because reflection from the tilted peripheral areas of the spheres falls below the detection threshold.

To determine whether a more accurate particle size can be obtained with an optimized focal position, transparent polystyrene particles were measured with varying positions of the focus ranging from -80 to $+200\ \mu\text{m}$. A focus position between -40 and $100\ \mu\text{m}$ showed no significant influence on the unweighted and only a slight influence on the square weighted median chord length (Fig. 7). Only a position of the focal point more than $40\ \mu\text{m}$ inside the probe window produced a sudden and significant drop of the measured particle size. However, neither the unweighted nor the square weighted median of the CLD reached the true particle diameter even at the $-80\ \mu\text{m}$ focus position. The focus position seems to be a parameter which has only limited influence on the measured particle size. For this reason the default setting of $-20\ \mu\text{m}$ was maintained for all further measurements.

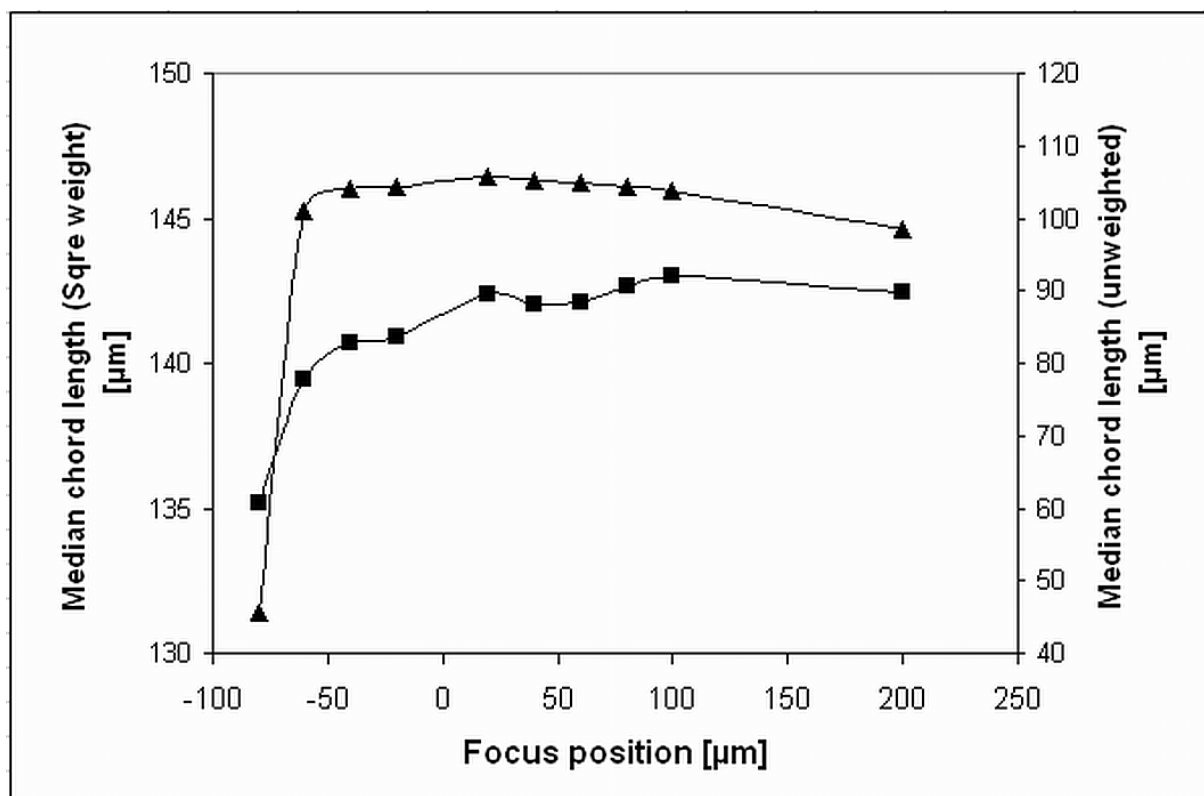


Figure 7: Influence of the focus position on the unweighted (- \blacktriangle -) and square weighted (- \blacksquare -) median of the CLD of transparent monodisperse polystyrene microparticles ($\varnothing = 98.7 \pm 1\mu\text{m}$)

3.2.2 Influence of the particle concentration

FBRM is a particle sizing method, which is well suited for analysis in suspensions with a high solid concentration. In typical solvent extraction evaporation processes for the preparation of PLGA microparticles the concentration is about 0.2% and thus it is rather low with respect to the range covered by this measuring method. To ascertain whether the method can be used for such applications, low concentrated suspensions with 0.2 to 3% (m/v) solids were investigated using slightly translucent PLGA microspheres. Despite a volume weighted median of the PSD of 103.2 μm , determined with SPOS, the square weighted median of the CLD (FBRM measurement) ranged between 79.5 and 82.5 μm depending on the particle concentration. The maximum value was found at a solid concentration of 1% (Fig. 8). Above this concentration it decreases marginally, which is in accordance with the findings of Yu et al., who reported, that the square weighted median of the CLD decreases with rising solid concentration of PVC particles [26]. By analyzing single ceramic beads Ruf et al. constituted that the laser penetration depth is reduced with an increase of the solid concentration and is thus limiting the diameter

of the light spot by which the furthestmost particles are scanned [25]. At a high solid concentration only those particles are detected, which are passing the laser beam in short distance to the probe window, and thus very close to the focal point.

If the particle concentration is low also particles, which are not directly at the probe window are detected. The deeper the laser beam penetrates into the suspension, the more it is widened and the measuring signal is prolonged. For this reason the median of the CLD increases slightly when the solid concentration decreases. In case of very low solid concentrations weak reflections from distant particles cause noisy fluctuations of the detected signal, resulting in chord splitting as described above. This leads to a sharp decline of the square weighted mean at particle concentrations below 1%. Yu et al. could find this behavior only for the unweighted mean but with no effect on the square weighted mean [26].

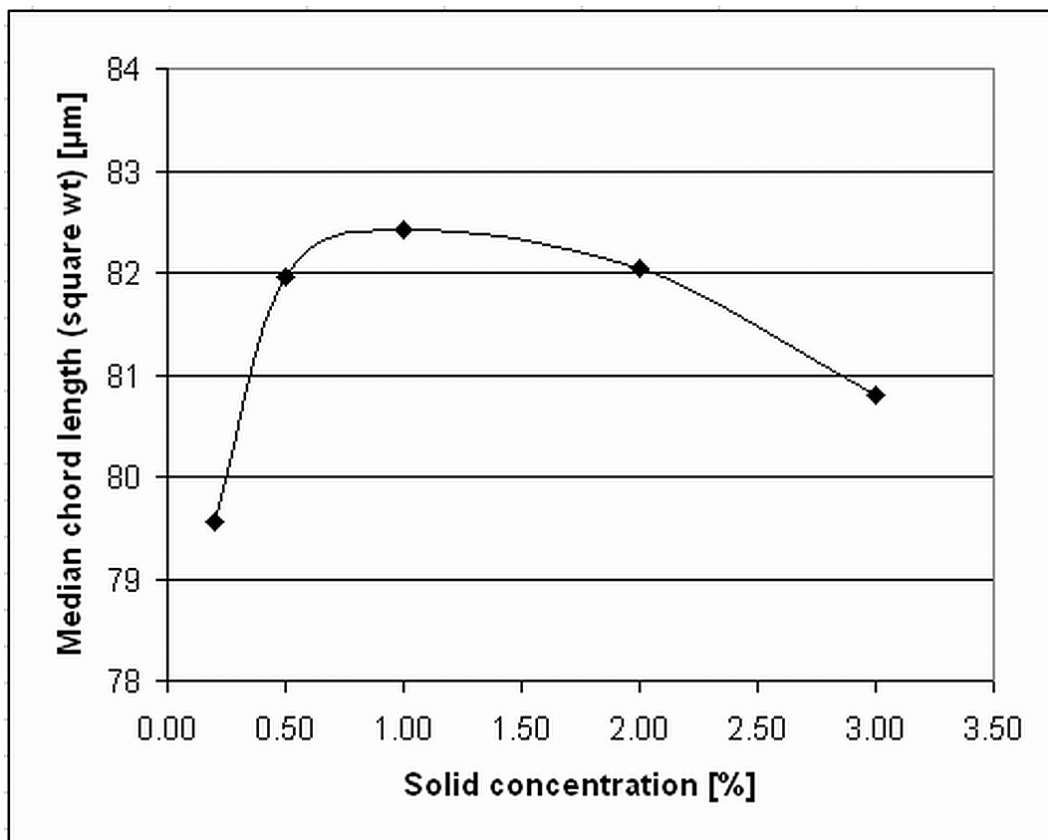


Figure 8: Correlation between square weighted CLD and solid concentration (% m/v) in suspensions of PLGA microparticles

Although the FBRM is applicable for a wide concentration range, its main field of application is the measurement of dispersions with high solid concentrations. As the experiments show, a variation of the concentration from 0.2 to 3.0% does not change the square weighted median chord length by more than 3 μm which is acceptable for the intended application of the method. Considering this low sensitivity to the solids concentration within the range of interest, the method was shown to be also suitable for processes with highly diluted suspensions, e.g. for monitoring of microparticle preparation by emulsion/solvent removal techniques.

3.2.3 CLDs of heterodisperse particle collectives and emulsion droplets

As mentioned above, microparticles consisting of PLGA are usually slightly translucent depending on type, amount and dispersity of incorporated drug substances. Before using FBRM for in-process monitoring in PLGA-microparticle preparation, it has to be clarified whether the kind of reflectiveness allows for accurate measurements or whether a high degree of internal scattering distorts the results.

A series of batches of plain and drug loaded PLGA microspheres was produced under different process conditions by varying the stirrer speed and the rate of the head space ventilation. As can be seen by microscopy, all tested PLGA particles have a rougher surface and are much less translucent than PS particles, which leads to the expectation that superficial scattering might be more pronounced than internal scattering or reflection (Fig. 9).

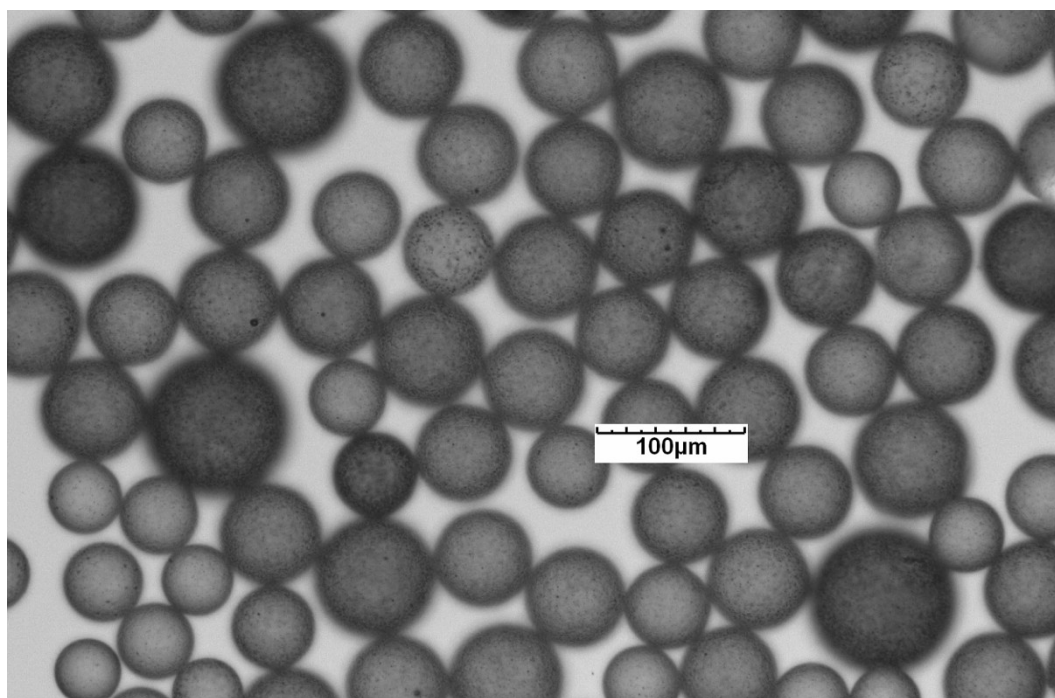


Figure 9: PLGA placebo microspheres (batch no. 4 (Tab.2))

The particle size of the samples was analyzed by FBRM and SPOS. For all types of particles the two methods produced diverging results, with the square weighted median of the CLD (measured by FBRM) being consistently lower than the volume weighted median of the PSD (obtained by SPOS) (Tab. 2, batches 1-5).

Table 2: Process parameters of PLGA microspheres and CLD, resp. PSD measured by FBRM and SPOS

Batch No.	API	Air flow [l/min]	Stirring speed [rpm]	FBRM - Median Sqr Wt [μm]	Accusizer - Median Vol Wt [μm]
1	—	10	260	39.28	61.43
2	+	10	260	71.8	83.7
3	—	5	220	48.47	58.11
4	—	5	120	36.14	55.04
5	+	5	120	38.25	50.37
6	—	1	220	39.49	56.31

Due to the particles' poor transparency, this deviation is mainly caused by non-Lambertian reflection phenomena, most probably by those of a specular type, which were shown above to decrease the measured chord lengths.

Figure 10 shows, as an example, the cumulative volume weighted PSD and the square weighted CLD of particle batch 2. As indicated by about the same slope of both curves, square weighting is able to transform a CLD into an equally shaped distribution as the PSD. The missing congruence in form of a parallel offset is due to the difference of the medians which is caused by the fact that the particles show also other types of reflection than solely diffuse (Lambertian) surface scattering.

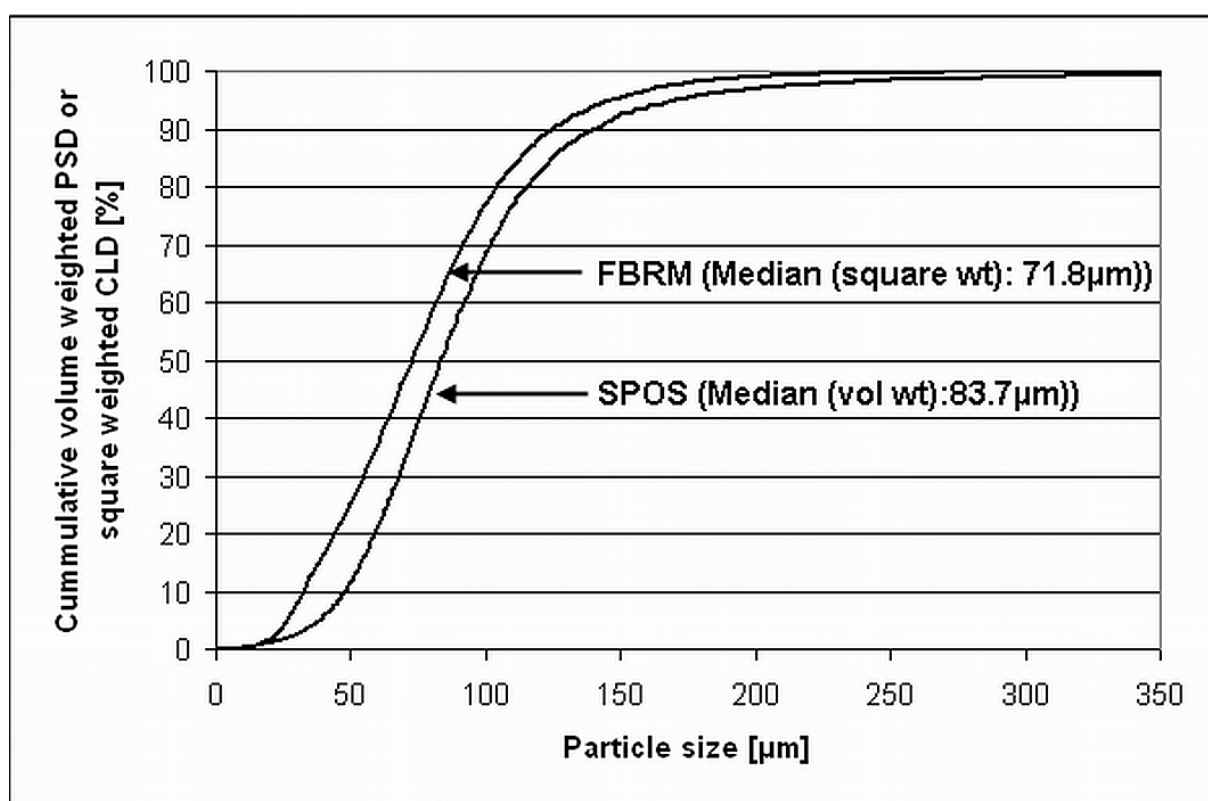


Figure 10: Cumulative size distributions of PLGA microspheres (batch 2) measured with FBRM and SPOS

In microparticle manufacturing by a solvent extraction/evaporation process, which is based on the preparation and further processing of a primary emulsion, monitoring of the initial droplet size and its change in the course of the process can be a valuable tool for development and process control. The determination of the primary emulsion's initial droplet size is a demanding problem as the droplets are transparent and thus FBRM might not provide accurate values. On the other hand

the emulsion is too concentrated for undiluted measurement with SPOS. Dilution however causes solvent extraction and in turn changes of the droplet size.

To clarify these problems the emulsion was measured on the one hand with the FBRM probe mounted in a flow through cell at the outlet of the mixer and on the other hand with microscopic image analysis. As expected, due to their transparency the droplets caused only low backscatter to the detector. The square weighted median of the chord length measured with FBRM was $41.8\ \mu\text{m}$ which is only half of the mean droplet size obtained by image analysis (Fig. 11). This demonstrates that FBRM is strongly dependent on the optical properties of the measured specimens and is not an appropriate method to determine the size of transparent emulsion droplets. This is in agreement with Greaves et al. and was also found by Sparks and Dobbs, who concluded that only droplets which are opaque and highly reflective (with microstructure on the surface) give reproducible and accurate results [31, 17].

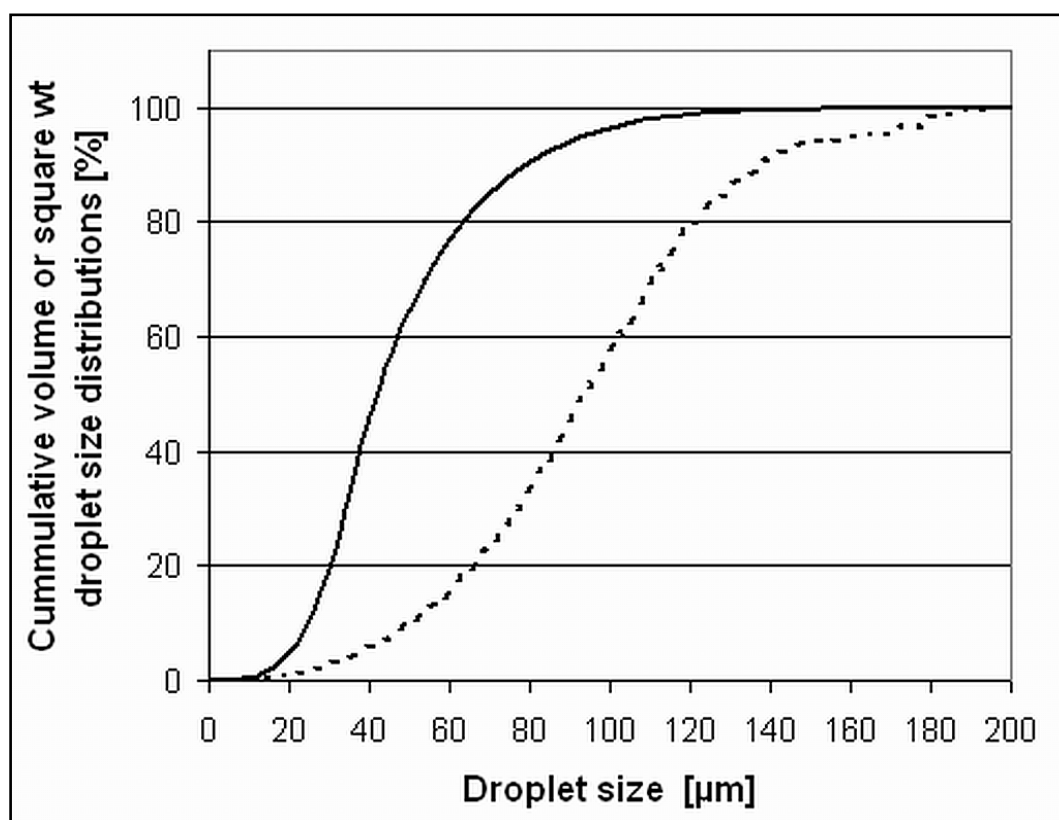


Figure 11: Comparison of the droplet size distribution measured with FBRM (—) (median (square wt): $41.8\ \mu\text{m}$) and with image analysis by microscopy (---) (median (vol wt): $94.7\ \mu\text{m}$)

The unweighted CLD of the emulsion (data not shown) shows again a very high number of small chord lengths, as in the case of the transparent polystyrene microparticles. This indicates again the phenomenon of chord splitting which

appears if reflection is weak. Thus, the at-line measurement of the primary emulsion and the finished particles demonstrates that FBRM does not provide reliable values for emulsion droplets. The finished microspheres, however, can be measured in many cases with only small and acceptable deviations.

3.3 Online-monitoring of a microparticle preparation process by FBRM

While FBRM is only of limited use for measuring absolute droplet or particle size distributions, it can nevertheless be an appropriate tool for process monitoring. This was studied with different batches of microspheres which were prepared under conditions with modified solvent extraction from the emulsion droplets, resulting in “rapid” or “slow” hardening of the microspheres. The rate of solvent evaporation has a strong influence on the encapsulation efficiency and on the morphology of the resulting microspheres, which is an important factor controlling the drug release [32, 33].

Two batches prepared at 35 °C with different stirring speed and air flow were compared to each other. Fast solvent extraction was obtained at a high stirring speed of 260 rpm and an intensive air flush of 10 l/min through the head of the reactor (batch no. 1). The process parameters for slow extraction were 120 rpm and 5 l/min (batch no. 4) (Tab. 2). As described above, the FBRM is strongly dependent on the surface properties and the transparency of the measured samples. For this reason different values are obtained from emulsion droplets and equally sized solidified particles. Thus the transition of liquid emulsion droplets into solid microparticles should be accompanied by a significant change of the FBRM signal. As Figure 12a shows, in case of fast solvent removal the first measurable (artificial) value for the square weighted median is about 28 µm. Within a minute it increases to 40.8 µm (sqr. wt median). By contrast, slow solvent extraction produces particles with initial FBRM signals of more than 160 µm. However, within the first 4-6 minutes of the process the signal drops down to a value of 45 µm, which corresponds to the apparent size of the rapidly extracted particles.

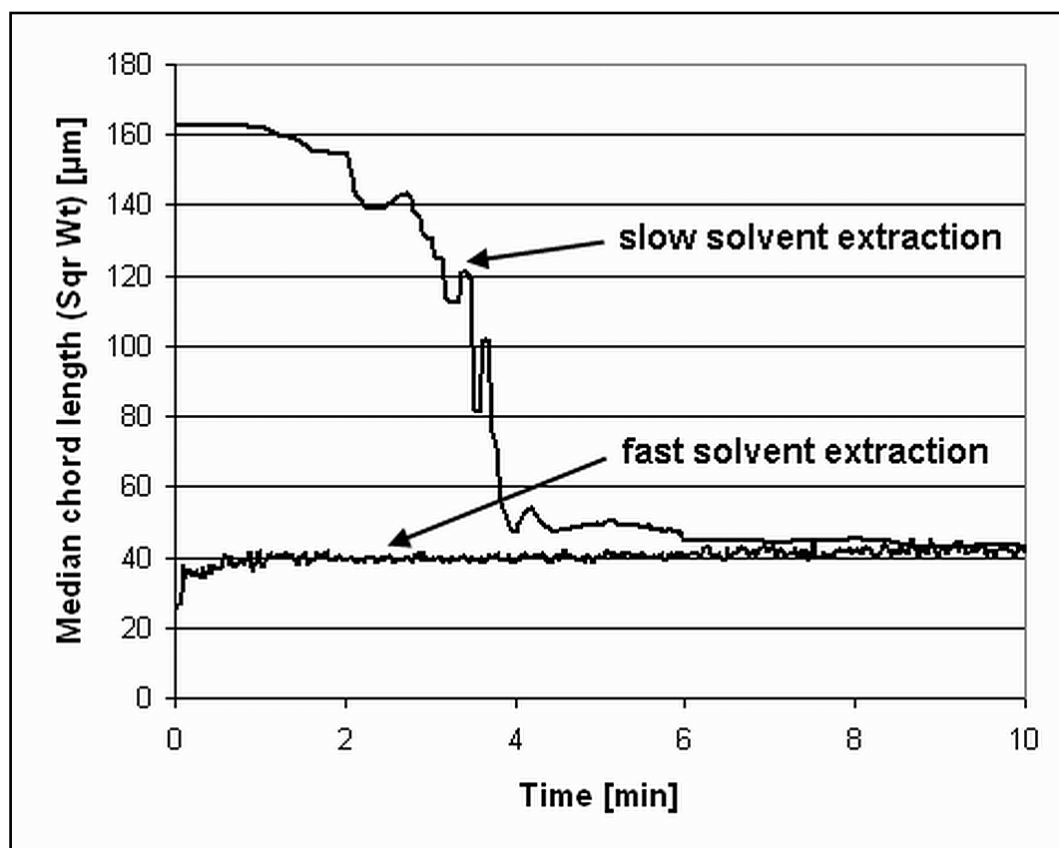


Figure 12a: Droplet, resp. particle size during processing of placebo microparticles with fast (10 l/min, 260 rpm; batch no. 1) and slow (5 l/min, 120 rpm; batch no. 4) solvent extraction

There are also other ways to slow down the solvent extraction rate and thus to affect the product properties, e.g. to apply a low process temperature of only 10 °C. Under these conditions of fast stirring and fast air flush (260 rpm, 20 L/min) but low extraction temperature (10 °C) a significantly higher initial particle size (about 100 µm) than in case of 35 °C and otherwise equal parameters was measured. Again it dropped down to about 45 µm after 1-2 minutes. Feeding the emulsion droplets into an aqueous phase already containing methylene chloride was tested as an option to decelerate the extraction process. However, the addition of 0.6% of methylene chloride to the aqueous phase did not render a markedly delayed particle formation (Fig. 12b).

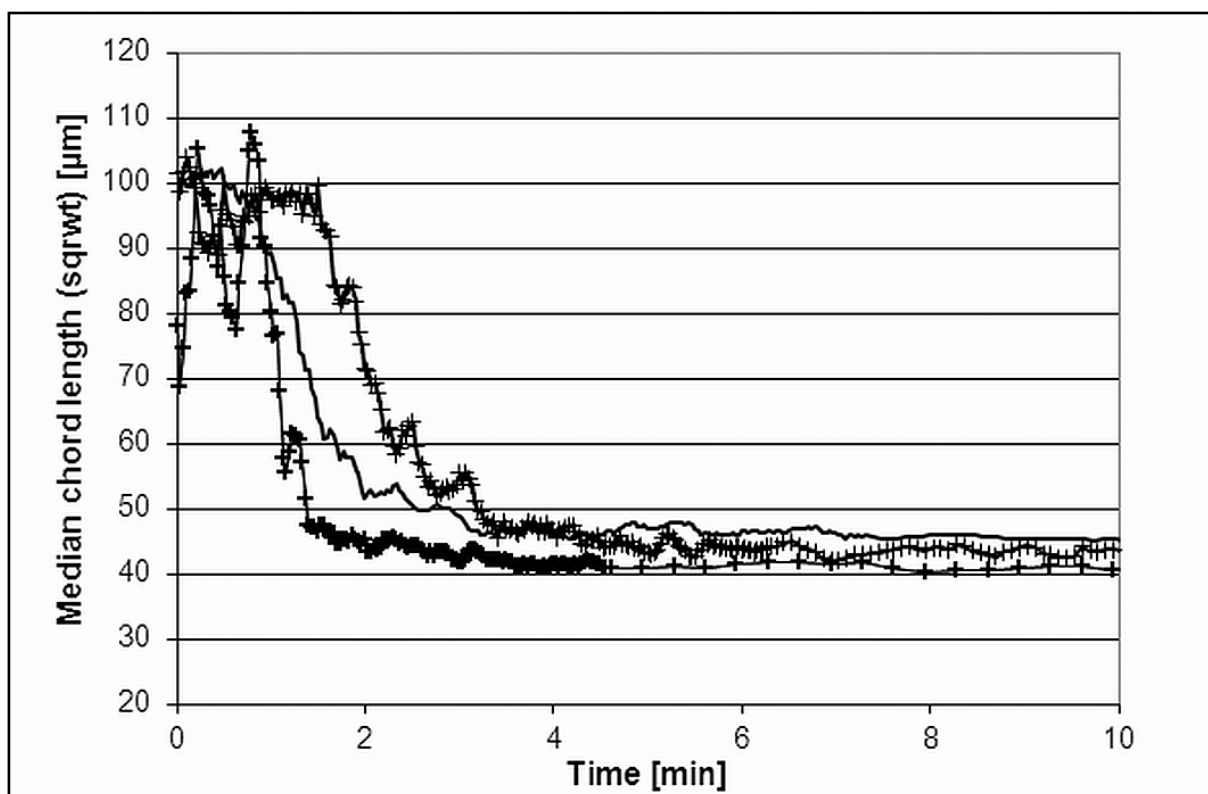


Figure 12b: Droplet, resp. particle size of placebo microparticles during processing with solvent extraction at 10 °C (air flow: 20 L/min, stirring speed: 260 rpm) with methylene chloride addition to aqueous phase (---) and without solvent in the extraction phase (-+ -)

It has to be pointed out that the measured size values must not be considered as true particle sizes rather than as FBRM signals which are strongly determined by the optical properties of the particles and thus need a thorough interpretation regarding the information derivable from these data.

The first process, which starts even in the mixer and continues after the emulsion is fed into the extraction tank, is a very fast redistribution of methylene chloride from the droplets into the continuous phase and into the extraction medium. As long as the polymer solution in the droplets is rather diluted solvent removal does not cause any, not even any locally limited phase transition. The droplets remain liquid but lose solvent within seconds and shrink abruptly in size. This step is too fast for monitoring it by FBRM. After the polymer concentration has reached a certain limit the further course of the process is determined by the rate of solvent removal.

In case of fast solvent extraction, the polymer solidifies rapidly on the droplet surface [34], which, as a result, becomes to a certain degree diffusely scattering. This change from solely specular reflecting to partly Lambertian scattering properties is most probably the reason for the apparent increase of the median chord length from about 28 to 40 µm, which can be seen in Figure 12a. During

further processing, water molecules penetrate into the initially solvated polymer matrix and replace the molecules of the organic solvent. The subsequently hydrated, as well as the initially solvated microparticles show a smooth surface with partly diffuse but dominating specular characteristics like in case of the copper strands described above. Thus the value obtained by FBRM is distinctly smaller than the true particle size which was found to be characteristic for specular objects. The square weighted median of about 40 μm remains constant all over the extraction period which indicates, that the optical properties do not change for the entire duration of the process.

In case of slow extraction, during the first 2 to 4 minutes the square weighted median is considerably higher than the value which is measured for the primary emulsion. Subsequently, it drops down to a value between 40 and 50 μm which remains nearly constant until the end of the extraction process. This phenomenon could be observed for all batches with decelerated solvent removal irrespectively of the method by which the extraction rate was decreased. As shown by the preliminary experiments subsurface scattering was identified as the main reason for a significant overestimation of the particle size. Most likely it causes also the apparent droplet expansion immediately after feeding the emulsion into the extraction medium. In case of slow solvent extraction no instantaneous formation of a skin layer on the particle surface is to be expected. Instead segregation processes inside the droplets or embryonic particles are recorded. Due to phase separation the optical properties of the previously transparent emulsion droplets change to opaque. Under the microscope the formation of a granular structure inside the particles can be observed in this phase. After this transitional stage, solidification progresses with a further opacification of the internal particle structure and the formation of a smooth and largely specular surface which both impede the penetration of the laser beam into subsurface regions. The specular reflection behavior causes an underestimation of the particle size as discussed before. Thus the decrease of the FBRM signal has to be assumed not to reflect a size change but rather marks the point where particle solidification occurs.

In all cases the conversion of liquid droplets into solid particles was exceptionally fast. At the latest about 4-6 minutes after feeding the emulsion into the reactor the square weighted median had reached its final value. This period of the process has therefore the greatest impact on the resulting particle morphology and should be the main target for measures to control the particle properties.

In the preparation of drug loaded PLGA particles another additional phenomenon could be observed by FBRM. In some cases about 40 minutes after starting the process a high signal peak occurred at a chord length of 185 μm (Fig. 13a).

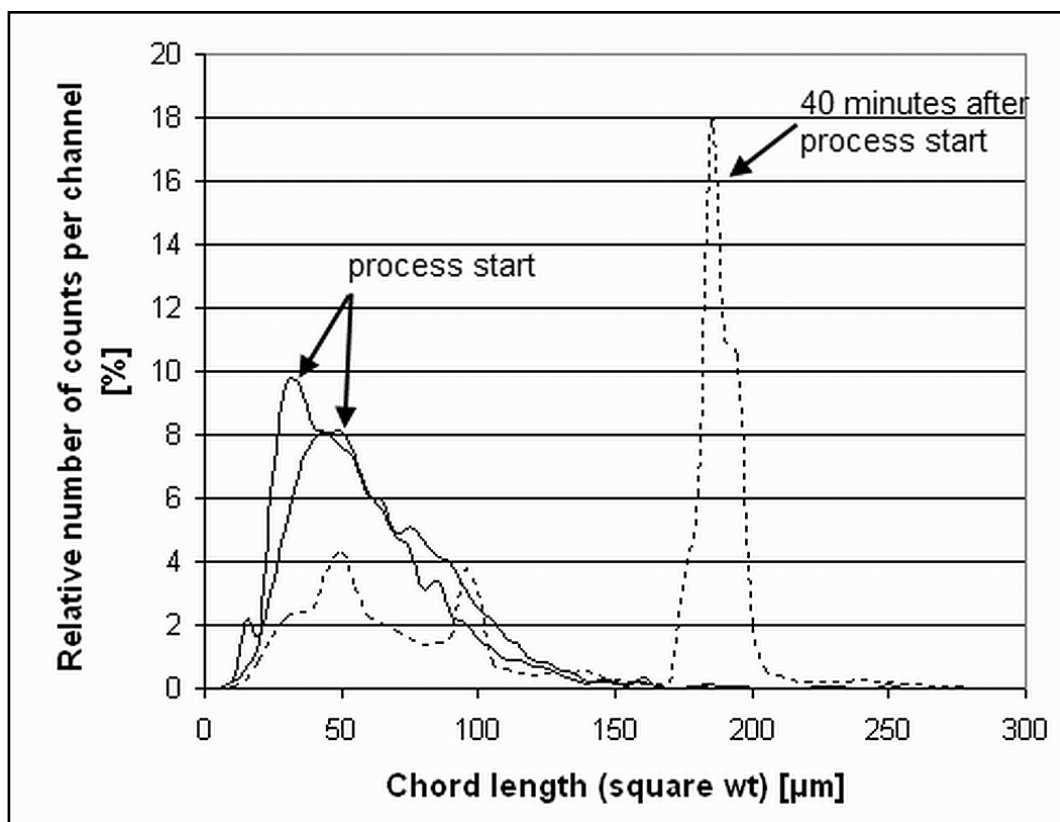


Figure 13a: CLD pattern during processing. CLD at the beginning of the process (—) after delivering the emulsion into the reactor and after 40 minutes of process duration (--) of batch no. 5

Subsequently this main peak shifted from 185 μm to 90 μm and then a third peak appeared at 35 μm . After another 50 min the peaks disappeared completely (Fig. 13b). After occurrence of the first signal peak a sample was taken and examined microscopically, revealing thin drug crystal needles with a length up to approximately 200 μm .

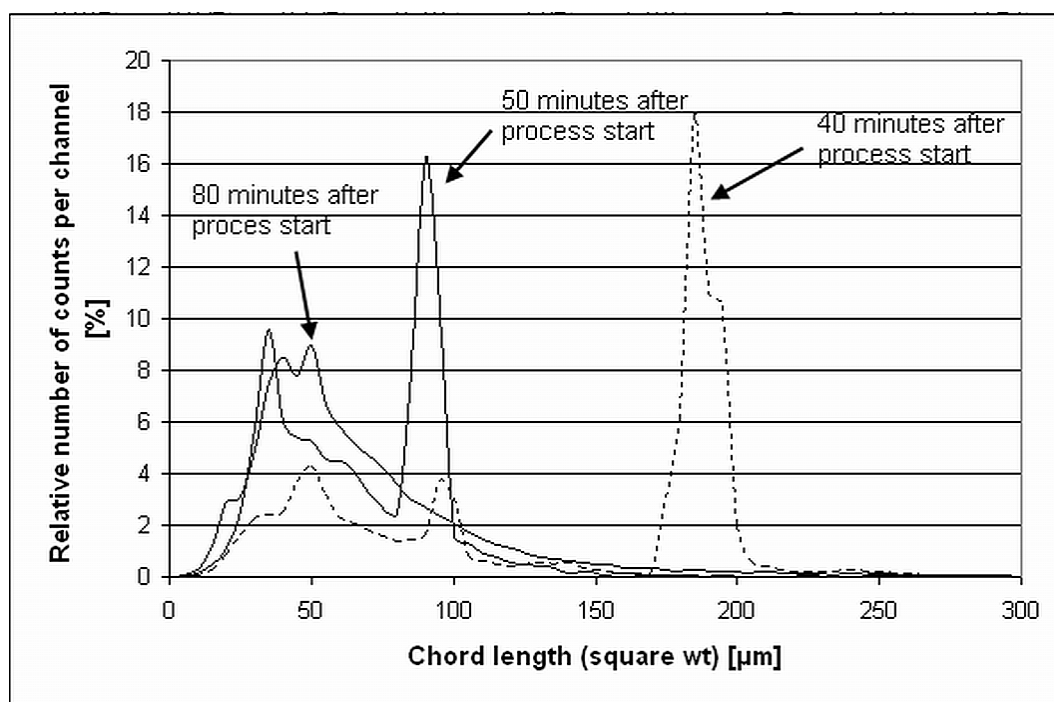


Figure 13b: Occurrence of crystal needles and shift of the signal peaks during processing (batch 5)

By encapsulating a high amount of the poorly water soluble active ingredient into polymer particles, the process can get unstable under unfavorable process conditions.

If hardening of the microspheres occurs too slowly (batch no. 5, Tab. 2), the drug substance is not tightly enclosed inside the polymer matrix and can diffuse out of the nascent particles and precipitate in the aqueous phase (Fig. 14). These needle shaped crystals are detected by FBRM and sharp peaks occur representing their longitudinal dimension. In the course of stirring the fragile crystal needles break to pieces and the signal shifts to smaller values. It seems that each fracture results in needles with about half the size of the initial crystals ($185 \mu\text{m} \rightarrow 90 \mu\text{m} \rightarrow 35 \mu\text{m}$). At a certain time point, the needles are so small, that their signals cannot be distinguished from those of the microspheres.

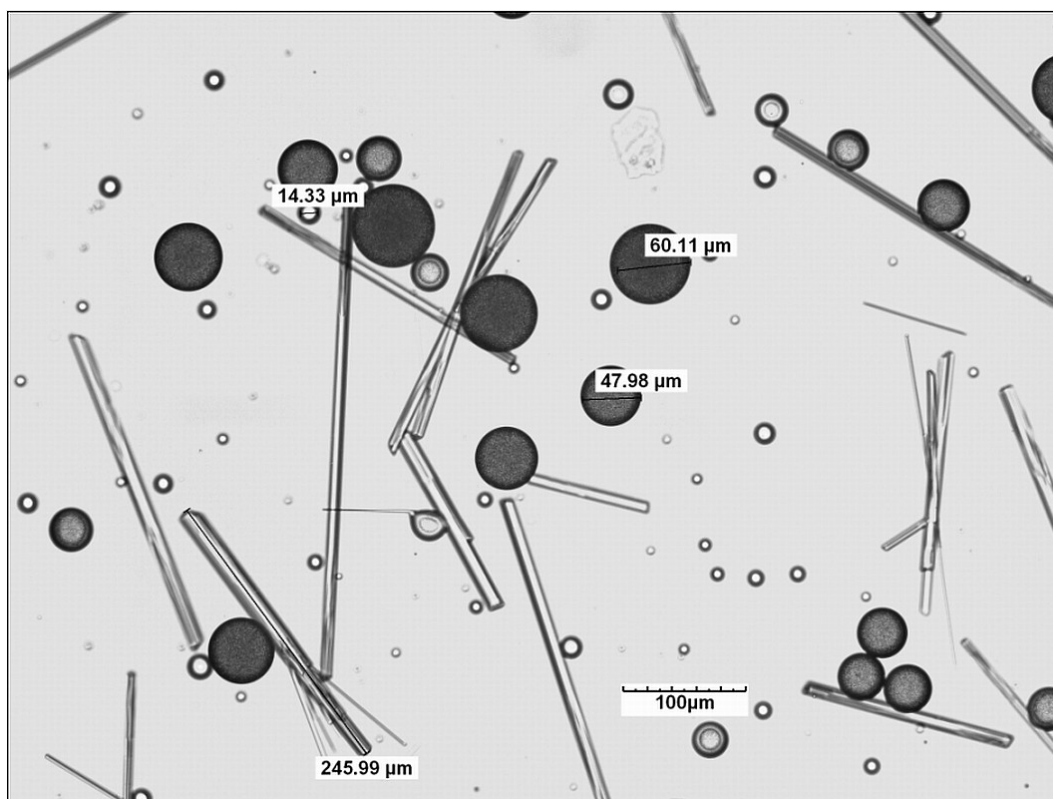


Figure 14: Crystal needles and microparticles in aqueous phase during processing (batch 5)

4 Conclusions

In this work the use of focused beam reflectance measurement for the determination of chord length distributions of spherical microparticles and emulsion droplets and its applicability for monitoring of microparticle preparation processes has been studied.

FBRM data are highly dependent on the material properties of the analysed samples and were influenced by measuring parameters like the solid concentration in the suspension or the focal point position. Materials with reflective properties due to smooth surfaces are not suitable to be accurately analysed by FBRM. They tend to provide signals much smaller than their true particle size. By contrast, translucent emulsion droplets usually originate signals mimicking too large particles. However, the size of particles with a rough surface and thus good backscattering properties, like PLGA microspheres, could be well estimated.

In spite of these limitations, FBRM is a strong tool to provide new insights into the microparticle formation in a solvent removal process. The transformation of the emulsion droplets into solidifying particles can be detected by a change in the

FBRM signal. In a solvent extraction/evaporation process based on methylene chloride, solidification of the emulsion droplets and particle size changes occur within the first seconds to minutes after feeding the emulsion into the reactor. These changes cannot be monitored by any at-line particle size measurements. As the FBRM signal is strongly depending on the surface properties of the measured sample, it provides an effective solution to track this process. It is a great advantage of the FBRM, that it requires no sampling and separate analysis. With regard to controlling such a microparticle preparation process the determination of the rate and time point of conversion from liquid droplets to solid particles is of great interest. The solidification rate is an important parameter influencing the encapsulation efficiency and the initial burst in microparticulate systems. A very slow hardening of the emulsion droplets leads to the diffusion of the drug substance out of the droplets and precipitation in the external phase. This event could be monitored by FBRM. For these reasons FBRM is a useful tool to investigate the effect of different process variables, like stirring speed or air flow, on the solidification rate and to assess its influence on the resulting particles and thus can help support a subsequent scale up process. However, unlike conventional applications of FBRM, monitoring of such processes which are accompanied by changes of optical properties requires a thorough understanding of the measuring principle and a deep knowledge of signal generation and processing by the instrument. Basically, FBRM is not a trivial method. In every application the possibility of artefacts due to changes of reflective properties should be considered and results should always be critically questioned.

5 References

- [1] Qi S, Marchaud D, Craig DQM. An Investigation into the Mechanism of Dissolution Rate Enhancement of Poorly Water-Soluble Drugs from Spray Chilled Gelucire 50/13 Microspheres. *Journal of Pharmaceutical Sciences* **2010**, *99*, 262-274.
- [2] Nilkumhang S, Basit AW. The robustness and flexibility of an emulsion solvent evaporation method to prepare pH-responsive microparticles. *International Journal of Pharmaceutics* **2009**, *377*, 135-141.
- [3] Conti B, Genta I, Modena T, Pavanetto F 1995. Investigation on Process Parameters Involved in Polylactide-Co-Glycolide Microspheres Preparation. *Drug Development and Industrial Pharmacy* *21*:615-622.
- [4] Barkai A, Pathak YV, Benita S. Polyacrylate (Eudragit Retard) Microspheres for Oral Controlled Release of Nifedipine .1. Formulation Design and Process Optimization. *Drug Development and Industrial Pharmacy* **1990**, *16*, 2057-2075.
- [5] Tamilvanan S, Sa B. Effect of production variables on the physical characteristics of ibuprofen-loaded polystyrene microparticles. *Journal of Microencapsulation* **1999**, *16*, 411-418.
- [6] Jeyanthi R, Thanoo BC, Metha RC, Deluca PP. Effect of solvent removal technique on the matrix characteristics of polylactide/glycolide microspheres for peptide delivery. *Journal of Controlled Release*, **1996**, *38*, 235-244.
- [7] Maa YF, Hsu CC. Effect of primary emulsions on microsphere size and protein-loading in the double emulsion process. *Journal of Microencapsulation*, **1997**, *14*, 225-241.
- [8] Sansdrap P, Moes AJ. Influence of Manufacturing Parameters on the Size Characteristics and the Release Profiles of Nifedipine from Poly(DI-Lactide-Co-Glycolide) Microspheres. *International Journal of Pharmaceutics*, **1993**, *98*, 157-164.
- [9] Berkland C, Kim K, Pack DW. Fabrication of PLG microspheres with precisely controlled and monodisperse size distributions. *Journal of Controlled Release*, **2001**, *73*. 59-74.
- [10] Harvill TL, Hoog JH, Holve DJ. In-process particle size distribution measurements and control. *Particle & Particle Systems Characterization* **1995**, *12*, 309-313.
- [11] Babick F, Ripperger S. Characterization of concentrated emulsions by means of ultrasonic spectroscopy. *Chemie Ingenieur Technik*, **2004**, *76*, 30-40.
- [12] Richter A, Voigt T, Ripperger S. Ultrasonic attenuation spectroscopy of emulsions with droplet sizes greater than 10 µm. *Journal of Colloid and Interface Science*, **2007**, *315*, 482-492.

- [13] Black DL, Mcquay MQ, Bonin MP. Laser-based techniques for particle-size measurement: A review of sizing methods and their industrial applications. *Progress in Energy and Combustion Science*, **1996**, 22, 267-306.
- [14] Zidan AS, Ziyaur R, Mansoor AK. Online monitoring of PLGA microparticles formation using Lasentec Focused Beam Reflectance (FBRM) and Particle Videa Microscope (PVM). *AAPS* **2010**.
- [15] Simmons MJH, Langston PA, Burbidge AS. Particle and droplet size analysis from chord distributions. *Powder Technology*, **1999**, 102, 75-83.
- [16] Monnier O, Klein JP, Hoff C, Ratsimba B. Particle size determination by laser reflection: Methodology and problems. *Particle & Particle Systems Characterization*, **1996**, 13, 10-17.
- [17] Sparks RG, Dobbs CL. The Use of Laser Backscatter Instrumentation for the Online Measurement of the Particle-Size Distribution of Emulsions. *Particle & Particle Systems Characterization*, **1993**, 10, 279-289.
- [18] bu Bakar MR, Nagy ZK, Rielly CD. Seeded Batch Cooling Crystallization with Temperature Cycling for the Control of Size Uniformity and Polymorphic Purity of Sulfathiazole Crystals. *Organic Process Research & Development*, **2009**, 13, 1343-1356.
- [19] Chen JX, Yuan JS, Ulrich JC, Wang JK. Online Measurement of Hydrocortisone Particles and Improvement of the Crystallization Process. *Chemical Engineering & Technology*, **2009**, 32, 1073-1077.
- [20] Howard KS, Nagy ZK, Saha B, Robertson AL, Steele G, Martin D. A Process Analytical Technology Based Investigation of the Polymorphic Transformations during the Antisolvent Crystallization of Sodium Benzoate from IPA/Water Mixture. *Crystal Growth & Design*, **2009**, 9, 3964-3975.
- [21] Jia CY, Yin QX, Zhang MJ, Wang JK, Shen ZH. Polymorphic Transformation of Pravastatin Sodium Monitored Using Combined Online FBRM and PVM. *Organic Process Research & Development*, **2008**, 12, 1223-1228.
- [22] McDonald KA, Jackman AP, Hurst S. Characterization of plant suspension cultures using the focused beam reflectance technique. *Biotechnology Letters*, **2001**, 23, 317-324.
- [23] Turner DJ, Miller KT, Sloan ED. Direct conversion of water droplets to methane hydrate in crude oil. *Chemical Engineering Science*, **2009**, 64, 5066-5072.
- [24] Dowding PJ, Goodwin JW, Vincent B. Factors governing emulsion droplet and solid particle size measurements performed using the focused beam reflectance technique. *Colloids and Surfaces A-Physicochemical and Engineering Aspects*, **2001**, 192, 5-13.

- [25] Ruf A, Worlitschek J, Mazzotti M. Modeling and experimental analysis of PSD measurements through FBRM. *Particle & Particle Systems Characterization*, **2000**, *17*, 167-179.
- [26] Yu W, Erickson K. Chord length characterization using focused beam reflectance measurement probe - methodologies and pitfalls. *Powder Technology*, **2008**, *185*, 24-30.
- [27] Heath AR, Fawell PD, Bahri PA, Swift JD. Estimating average particle size by focused beam reflectance measurement (FBRM). *Particle & Particle Systems Characterization*, **2002**, *19*, 84-95.
- [28] Wynn EJW. Relationship between particle-size and chord-length distributions in focused beam reflectance measurement: stability of direct inversion and weighting, *Powder Technology*, **2003**, *133*, 125-133.
- [29] Scheler, S., Interpretation of FBRM signals by ray tracing, Joint Meeting of the Austrian and German Pharmaceutical Societies, September 20-23, **2011**, Innsbruck, Austria, <http://www.uibk.ac.at/news/oephg-dphg2011/program/final-program-and-book-of-abstracts---joint-meeting-oephg-dphg-2011b.pdf>
- [30] Worlitschek J. Monitoring, modeling and optimization of batch cooling crystallization. **2003**, Dissertation, ETH Zürich.
- [31] Greaves D, Boxall J, Mulligan J, Montesi A, Creek J, Sloan ED, Koh CA. Measuring the particle size of a known distribution using the focused beam reflectance measurement technique. *Chemical Engineering Science*, **2008**, *63*, 5410-5419.
- [32] Li WI, Anderson KW, Mehta RC, Deluca PP. Prediction of solvent removal profile and effect on properties for peptide-loaded PLGA microspheres prepared by solvent extraction/evaporation method. *Journal of Controlled Release*, **1995**, *37*, 199-214.
- [33] Yeo Y, Park KN. Control of encapsulation efficiency and initial burst in polymeric microparticle systems. *Archives of Pharmaceutical Research*, **2004** *27*, 1-12.
- [34] Freitas S, Merkle HP, Gander B. Microencapsulation by solvent extraction/evaporation: reviewing the state of the art of microsphere preparation process technology. *Journal of Controlled Release*, **2005**, *102*, 313-332.

CHAPTER 5

A detailed view of microparticle formation by in-process monitoring of the glass transition temperature ‡

Abstract

Biodegradable poly(D,L-lactide-co-glycolide) microspheres were prepared by a well-controlled emulsion solvent extraction/evaporation process. The objective of this study was to investigate how drug release can be modified by changing the morphology of the polymer matrix. The matrix structure was controlled by the preparation temperature which was varied between 10 and 35 °C, thus changing the four weeks release pattern from almost linear kinetics to a sigmoidal profile with a distinct lag phase and furthermore decreasing the encapsulation efficiency. By monitoring the glass transition temperature during the extraction process it was shown that the preparation temperature determines the particle morphology by influencing the time span in which the polymer chains were mobile and flexible during the extraction process.

Further factors determining drug release were found to be the molecular weight of the polymer and the rate of solvent removal. The latter, however, has also influence on the encapsulation efficiency with slow removal causing a higher drug loss. A secondary modification of the outer particle structure could be achieved by ethanolic post-treatment of the particles, which caused an extension of the lag phase and subsequently an accelerated drug release.

‡ Published in European Journal of Pharmaceutics and Biopharmaceutics 2012, 81 (2), 399-408. Vay,K.; Friess,W; Scheler,S., A detailed view of microparticle formation by in-process monitoring of the glass transition temperature.

1 Introduction

By now a variety of biodegradable poly(lactide-co-glycolide) microspheres for the sustained release of several drug substances are commercially available. As many new drugs are peptides, proteins or small molecules with low solubility and permeability and thus poor oral bioavailability research on these dosage forms is still of growing interest [1]. Biodegradable depot formulations offer numerous benefits. For example they can help to reduce side effects and to enhance the therapeutic compliance and efficiency.

There is a variety of different preparation techniques to encapsulate an active ingredient into a PLGA matrix including coacervation, spray drying, melting techniques, methods using supercritical fluids and emulsion solvent removal techniques. The latter is the oldest and most popular technique, especially for active ingredients with poor water solubility [2-4]. The influences of numerous process parameters on the characteristics and the drug release profile of the resulting microspheres have been extensively studied [5-8]. It was shown that drug release from these dosage forms depends strongly on the molecular order, the amorphous or crystalline state of the active ingredient and how it is embedded in the polymer matrix. Furthermore the morphology of the surrounding polymer matrix is crucial for the resulting drug release rates.

Most of these studies concerned drug substances with good aqueous solubility and thus the results are not valid for drugs with poor water solubility. Furthermore the majority of the experiments were performed on a laboratory batch scale without exact determination of the solvent removal rate and temperature of the external phase. We examined the structure formation mechanism of PLGA microspheres in a well-controlled emulsion solvent extraction/evaporation process on a 5 L batch scale by monitoring the glass transition temperature during solvent removal. The encapsulated drug was 4-[2-[4-(6-fluorobenzo[d]isoxazol-3-yl)-1-piperidyl]ethyl]-3-methyl-2,6-diazabicyclo[4.4.0]deca-1,3-dien-5-one, a substance with poor aqueous solubility.

The glass transition temperature (T_g) of the polymer, which marks the change between the rigid, glassy and the more flexible, rubbery state, is closely correlated to the amount of solvent in the polymer matrix. As the latter decreases in the course

of the extraction step, the T_g should rise during the microsphere preparation process. It can be assumed that the morphology of the particle structure is only formed in the rubbery state, as long as T_g is below the process temperature. As the extraction rate is also controlled by the process temperature, it can be expected that the mobility of the polymer chains and the duration of the rubbery phase is determined by the extraction temperature in a complex way [9]. We investigated the change of T_g during processing in relation to the applied extraction temperature and its influence on the particle morphology and functional characteristics.

As the T_g of the forming microparticles is strongly dependent on the solvent content in the polymer matrix we assumed that the modification of the solvent removal rate should result in a change of the particle properties. These factors are supposed to be in close interaction with the molecular weight of the polymer, which was also varied in this study. Similarly and as a third factor investigated subsequent suspension of the resulting microspheres in a second solvent or solvent-water-mixture should also change the particle morphology and thus alter the drug release profile.

Firstly, however, for a better understanding of the process data, we examined the influence of the solvent concentration on the glass transition temperature of the polymer in the presence and absence of the drug substance and correlated the experimentally derived T_g values with the theoretical ones predicted by the Gorgon-Taylor-Equation.

2 Materials and Methods

2.1 Materials

Poly(D,L-lactide-co-glycolide) 75:25 with different molecular weight were purchased from Boehringer Ingelheim, (Ingelheim, Germany): Resomer 753S (36510 Da), Resomer 755S (57670 Da), and Resomer 756S (107200 Da) (Tab. 1). Methylene chloride analytical grade was obtained from Merck (Darmstadt, Germany), and TRIS (Tris(hydroxymethyl)aminomethan) from AppliChem (Darmstadt, Germany). 4-[2-[4-(6-fluorobenzo[d]isoxazol-3-yl)-1-piperidyl]ethyl]-3-methyl-2,6-diazabicyclo[4.4.0]deca-1,3-dien-5-one was purchased from Jubilant Organosys (Mysore, India) and PVA 18-88 from Kuraray Europe GmbH (Frankfurt, Germany).

Table 1: Characteristics of the different types of PLGA (75:25) used

PLGA 75:25	Weight average molecular weight (Mw in Da)	Polydispersity (Mw/Mn)	End group	Inherent viscosity [mL/g]
RG 753 S	36510	1.6	Alkyl	0.39
RG 755 S	56020	1.6	Alkyl	0.56
RG 756 S	109200	1.6	Alkyl	0.98

2.2 Microparticle preparation

An emulsification solvent extraction/evaporation technique was employed to prepare PLGA microparticles. For plain particles (free of drug) 4.8 g PLGA, for all other particle batches 3.8 g active agent and 5.1 g PLGA were dissolved in 46.1 g of methylene chloride and the solution was emulsified with 500 ml of 0.5% (w/v) povidone in 0.1 M Tris buffer (pH 9.0) (aqueous phase). The emulsion was fed into a 5 L jacketed glass reactor containing additional 3.5 L of the aqueous phase. By stirring for 5 hours the droplets were hardened by solvent extraction and evaporation with an air flow of 10 L/min (exactly regulated by a mass flow controller (red-y smart meter, Vögtlin instruments AG, Aesch, Switzerland)) and a stirring speed of 260 rpm (curved blade paddle-type stirrer). The obtained particles were separated by filtration and dried under vacuum in a desiccator. Different particle batches were produced by varying the extraction temperature between 10 and 35 °C. For further modifications the air flow was reduced to 1.5 L/min and the stirring speed to 180 and 220 rpm. In another experiment, after collection on a filter, the particles were re-suspended in 25% ethanol at 25 or 40 °C for 1 or 2 hours, collected and dried as described above.

2.3 Analytical methods

2.3.1 Thermal analysis – Differential scanning calorimetry (DSC)

The glass transition temperature (T_g) was determined by differential scanning calorimetry (DSC) using a DSC (823e/500) (Mettler Toledo (Greifensee, Switzerland)). For in-process measurements about 50 ml of the suspension were sampled (after 10, 30, 60, 120, 180, 240 minutes of processing and at the end of the

process) and centrifuged at 4000 rpm for 2 minutes. Approximately 10 mg were weighed into 40 μ l aluminium pans and hermetically sealed. As a reference an empty aluminium pan was used. Samples were cooled down to -40 °C and then heated up to 80 °C at 10 °C/minute to eliminate any sample history, cooled to -10 °C and then heated again up to 200 °C at 10 °C/minute. For T_g determination the data were analyzed using the STAR software (Mettler Toledo, Switzerland) and the midpoint of the corresponding glass transition was evaluated. The T_g was determined in duplicate at every time point of sampling.

2.3.2 Particle size – Single Particle Optical Sizing (SPOS)

The particle size distribution was determined by single particle optical sizing (SPOS) with an Accusizer 780 particle sizing system (Anasysta, Santa Barbara, CA). Approximately 20 mg of microspheres were suspended in an aqueous solution of polysorbate 80 and deagglomerated by sonication. Per measurement a minimum of 10000 particles were sized.

2.3.3 Particle morphology characterization - Scanning electron microscopy (SEM)

The morphological structure of the particles was examined by scanning electron microscopy (JEOL JSM – 5310LV; JEOL Ltd., Tokyo, Japan). To study the internal structure, the particles were frozen in liquid nitrogen and cut with a razor blade. The specimens were sputtered with gold.

2.3.4 Drug distribution – Chemical Imaging

The drug distribution inside the microspheres was analyzed by IR-Imaging of cross-sections of the microspheres. To produce even cross sections, the microspheres were as first step embedded in an epoxy resin, afterwards cooled in liquid nitrogen and cut with a high precision milling cutter (Leica EM Rapid, Leica Microsystems GmbH, Wetzlar, Germany).

From this cross section, an IR image of 150×150 μ m area with a pixel size of 1.56 μ m was subsequently obtained with a Perkin Elmer Spectrum&Spotlight 400 IR-NIR (PerkinElmer LAS, Rodgau-Jügesheim, Germany) imaging system. The IR spectra were obtained between $4000 - 750$ cm^{-1} with a spectral resolution of 4 cm^{-1} and 2 spectra averaged per pixel. To display the distribution of PLGA and the drug

substance within the obtained image, the adsorption intensity images at 1643 cm⁻¹ (characteristic for the drug substance) and 1747 cm⁻¹ (characteristic for PLGA) were selected.

2.3.5 Drug loading and in-vitro dissolution studies –RP-HPLC

The drug load of the microspheres was determined by dissolving 20 mg microspheres in 25 ml acetonitrile using sonication and filling up to 200 ml with 0.1 M HCl. The drug concentration was determined by HPLC with a DAD detector at 235 nm and evaluated with the Chromeleon 6.7 software (Dionex, USA). A RP 18 column (20 x 2.1 mm) column was used with a flow rate of 1 ml/min and an injected volume of 50 µl. The mobile phase consisted of a 75:25 (v/v) mixture of 0.25 M phosphate buffer (pH 8.5) and acetonitrile. A membrane filtered (0.45 µm hydrophilic cellulose filter) clear test solution was analyzed.

For the in-vitro release studies the microspheres (17 mg) were placed in 100 ml of a 10 mmol phosphate buffer solution (pH 7.4) in a screw cap bottle and incubated in electrically heated aluminum blocks with drill holes on an orbital shaker (rotating speed 200 ± 10 rpm) at 37 °C. At predefined time points 0.2 ml samples were taken and analyzed by HPLC as described above.

2.3.6 Molecular weight of PLGA – SE-HPLC

30 mg microparticles were dissolved in 5 ml tetrahydrofuran. The molecular weight was determined by gel permeation chromatography with refractive index detection. Three columns (30 x 8 mm) filled with a stationary phase of styrene-divinylbenzene copolymers with different pore sizes (0.1, 10, 100 µm) were connected in series for the size separation. THF was used as mobile phase, stabilized with 0.025% of butylhydroxytoluene.

3 Results and discussion

3.1 Effects on the glass transition temperature of the polymer

In microparticle formation the structure of the polymer matrix is a result of the arrangement of the polymer chains and is thus strongly determined by the mobility of the chains before they become fixed in their final positions. This stage is achieved

when the T_g falls below the process temperature and the polymer changes from a rubbery to a glassy state. During the preparation of PLGA microspheres a variety of formulation and process parameters affect the T_g of the polymer and thus influence the microparticle formation [10]. One of them is the type of organic solvent utilized and its concentration profile during extraction. We investigated this effect by monitoring both, the concentration of methylene chloride and the T_g of the hardening microspheres.

A significant decrease of the methylene chloride concentration in the microspheres took place in the first hour of processing (Fig. 1). During this period most of the solvent is extracted. The further removal of the remaining solvent from the particles occurs slowly. Depending on the extraction temperature a fraction between 1 and 3.5% of methylene chloride remains in the particles. The most effective removal of the solvent is achieved with a process temperature of 35 °C. The lower the process temperature the higher is the amount of residual solvent in the microspheres.

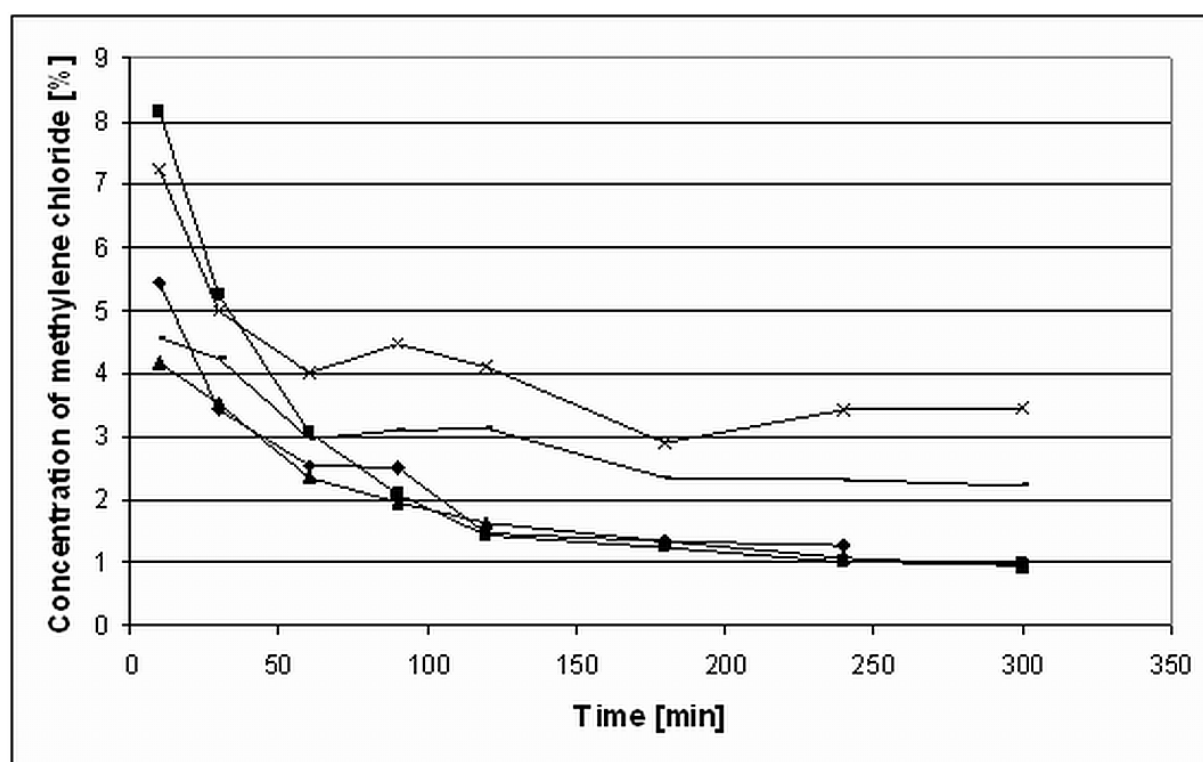


Figure 1: Concentration of methylene chloride in PLGA microspheres during solvent extraction (referring to solvated and hydrated particles) at 10 °C (-x-), 20 °C (---), 27.5 °C (-▲-), 30 °C (-■-) and 35 °C (-◆-)

In order to analyze whether the plasticizing effect of the solvent is the only factor determining the T_g and, otherwise, to detect additional parameters of influence, the

solvent concentrations were plotted against the measured T_g and regressed using the Gordon-Taylor-equation (Eq. (1)).

$$T_{gm} = \frac{w_p T_{gp} + k w_s T_{gs}}{w_p + k w_s} \quad (1)$$

The Gordon Taylor equation, which has been developed to calculate the glass transition temperature of polymer blends, has proved to be also applicable to predict of the T_g of polymers which are plasticized by solvents, i.e. to predict the glass transition temperature of polymer/solvent mixtures (T_{gm}). In equation 1 T_{gp} and T_{gs} are the glass transition temperatures of the polymer and the solvent while w_p and w_s are the weight fractions of the two components. k is a constant. In a first step the relationship between solvent concentration and T_{gm} was investigated with placebo PLGA microspheres (Fig. 2). As expected, the T_{gm} decreases with increasing amount of residual solvent. The T_{gm} values range between 22.5 and 32.5 °C for amounts from 4.2% to 0.9% of methylene chloride (the amount of methylene chloride was calculated referring to the undried sample weight). Regressing the glass transition temperature on the amount of residual methylene chloride, a value of 36.0 °C was calculated for T_{gp} (T_g of the polymer with 0% methylene chloride in a fully hydrated state), which is consistent with the literature [11]. For T_{gs} a value of -173.0 °C was obtained (corresponding to 100% methylene chloride) which also meets the literature values for the T_g of methylene chloride ranging between -170 and -174 °C [12]. Identical results are also obtained by using the Kelley-Bueche equation (Eq. (2)) instead of the Gordon-Taylor equation.

$$T_{gm} = \frac{\alpha_p V_p T_{gp} + \alpha_s (1 - V_p) T_{gs}}{\alpha_p V_p + \alpha_s (1 - V_p)} \quad (2)$$

where V_p is the volume fraction of the polymer, α_p and α_s are the volumetric expansion coefficients of the polymer and the solvent, respectively. The other symbols have the same meaning as before. In this case also the expansion coefficients are close to values given in literature: $\alpha_p = 5.3 \cdot 10^{-4} \text{ } ^\circ\text{C}^{-1}$ (Lit.: thermal expansion coefficient for polylactic acid (PLA) = $7.4 \cdot 10^{-4} \text{ } ^\circ\text{C}^{-1}$ [13], α_p for PLGA is assumed to be close to α_p for PLA) and $\alpha_s = 8.6 \cdot 10^{-4} \text{ } ^\circ\text{C}^{-1}$ (Lit.: $1.4 \cdot 10^{-3} \text{ } ^\circ\text{C}^{-1}$) [14].

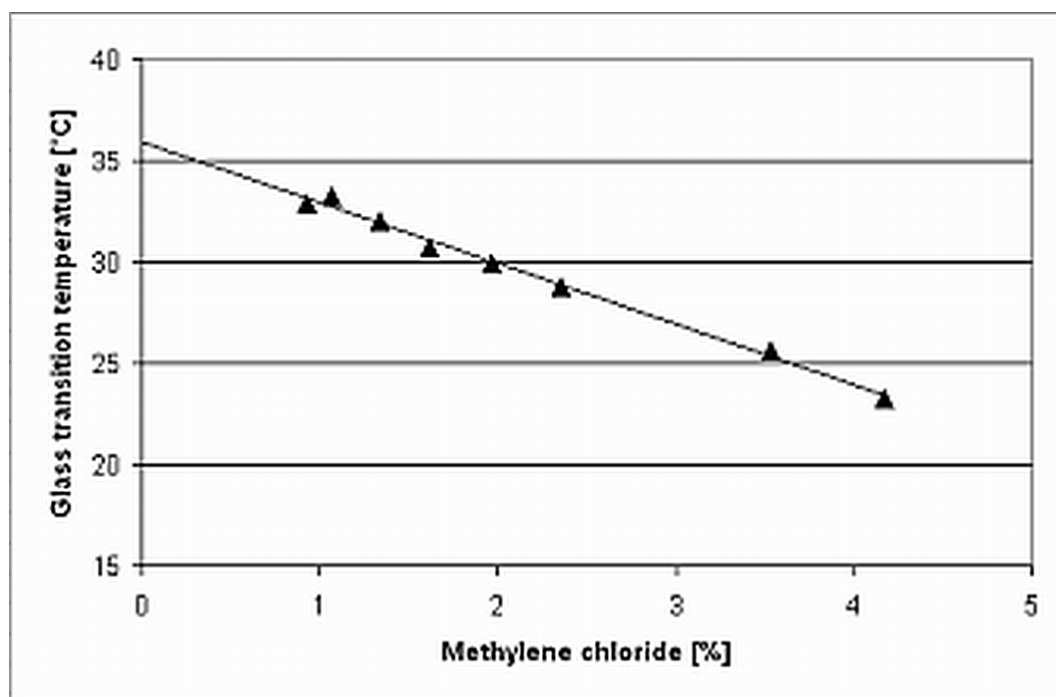


Figure 2: Correlation between concentration of methylene chloride and T_g for plain microparticles: measured values (\blacktriangle) and regression line calculated by the Gordon-Taylor-equation

The samples were taken from the aqueous suspension and the polymer matrix was therefore fully hydrated, reducing the T_g of the polymer from 54 °C in the dry state to 36 °C. Methylene chloride has a much stronger impact on the glass transition temperature than the water molecules, reflected by a decreasing T_g with rising methylene chloride concentrations. Overall, for the placebo microparticles the experimentally determined glass transition temperatures at different methylene chloride concentrations are in good agreement with the calculated values and hence other factors co-influencing the T_g can be excluded.

At the beginning of the process, the polymer is fully solvated by methylene chloride. During processing the methylene chloride is extracted from the hardening particles and in return water diffuses into the particles. Both, methylene chloride and water have a plasticizing effect on the T_g of the PLGA. If poly(lactide-co-glycolide) copolymers undergo the transition between their glassy and rubbery state, the molecular relaxation time changes. The polymer chains get more mobile and molecular deformation occurs [15-17]. The small solvent molecules embed themselves between the molecules of the amorphous solid and increase the spacing and free volume of the sample, resulting in an increased degree of molecular mobility. An increase of the T_g , called antiplasticization, can for example occur by the addition of a drug substance to the polymer matrix [18].

In case of drug loaded PLGA microspheres a similar correlation was found. However, for these particles experimentally determined T_g values deviated stronger from the theoretical T_g values (Fig. 3). Starting with about the same T_1 value for the fully hydrated microparticles as in case of placebo microparticles, the T_g decrease is steeper with rising methylene chloride concentration. As can be seen in SEM, the active ingredient is deposited in the polymer matrix mainly in crystalline form and only a very small portion is molecularly dispersed [19]. The crystalline fraction is not active with respect to the T_g depression. When the methylene chloride in the particles increases, more drug becomes dissolved, which obviously causes a substantial additional plasticizing effect.

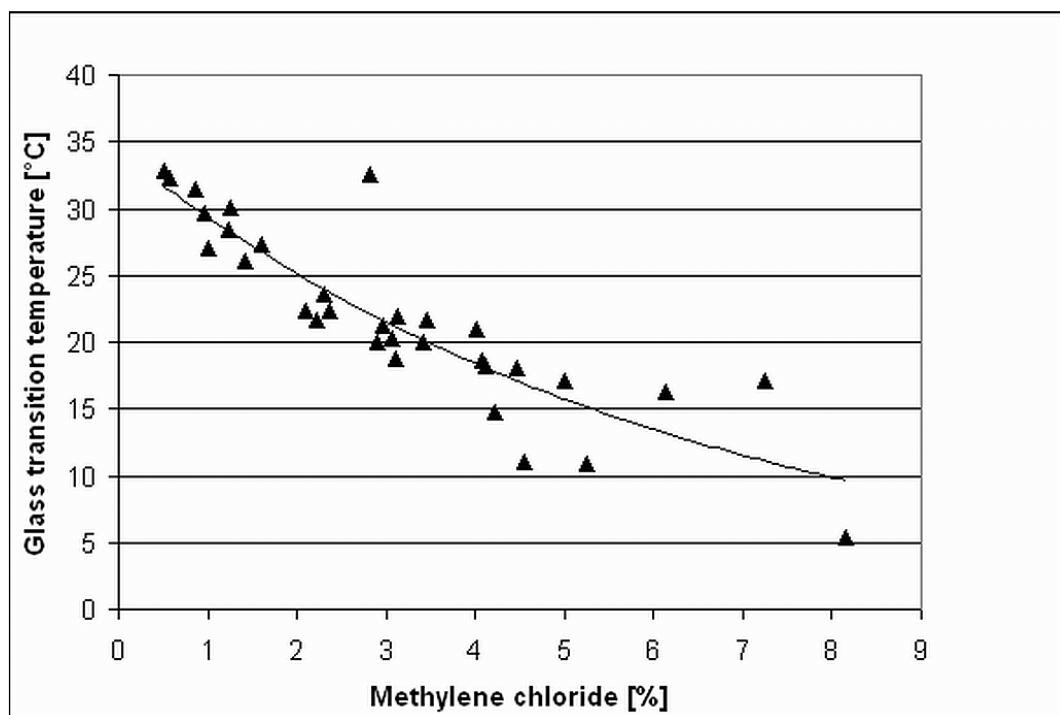


Figure 3: Correlation between concentration of methylene chloride and T_g depression for drug loaded particles: measured values (▲) and regression line calculated by the Gordon-Taylor-equation

3.2 Effect of the process temperature on the particle properties

3.2.1 Influence on the particle morphology

Previous experiments showed that particles with different drug release and morphology, specifically pore size distribution, can be obtained when the extraction temperature was varied between 10 and 35 °C [16]. In order to understand the role

of the process temperature on the structure formation the extraction process was monitored. In a series of microparticle preparation processes at 10, 20, 27.5, 30, 32.5, and 35 °C both the glass transition temperature of the polymer and the amount of residual methylene chloride within the particles were measured in intervals between 10 and 60 minutes. All other process variables like stirring speed or air flush through the reactor were kept constant. Fig. 4 shows the T_g changes during solvent extraction. In all experiments the first sample, which was withdrawn 10 min after the emulsion was fed into the reactor, had a T_g between 8 and 17 °C. In the further course of the preparation process the samples showed an increase of the T_g . In all cases the T_g did not increase at a constant rate. After an initial fast phase, the increase slowed down and in some cases came to a hold. The substantial change in T_g during the first 90 minutes of processing corresponds to the loss of methylene chloride from the microspheres (Fig. 1). Depending on the applied process temperature the final T_g value ranged from 22 °C for 10°C (Fig. 4a) to 34 °C (Fig. 4f) for 35 °C process temperatures. Except for the experiment at 10 °C the T_g tended to approach the process temperature.

At the beginning of the process the T_g of the microspheres is below 17 °C due to the high concentration of methylene chloride in the polymer matrix and rises with decreasing solvent concentration. Usually mass transfer processes start with a high rate when the concentration gradient is high and decelerate when the reservoir depletes. This should be reflected in the T_g vs. time profiles. During the first 60 min (30 minutes in case of the 27.5 °C experiment) of the studied solvent evaporation process a slight acceleration of the T_g increase could be observed. We assume that the solvent transfer from the particles into the extraction medium may be superimposed by another mass transfer within the particles which is caused by phase separation.

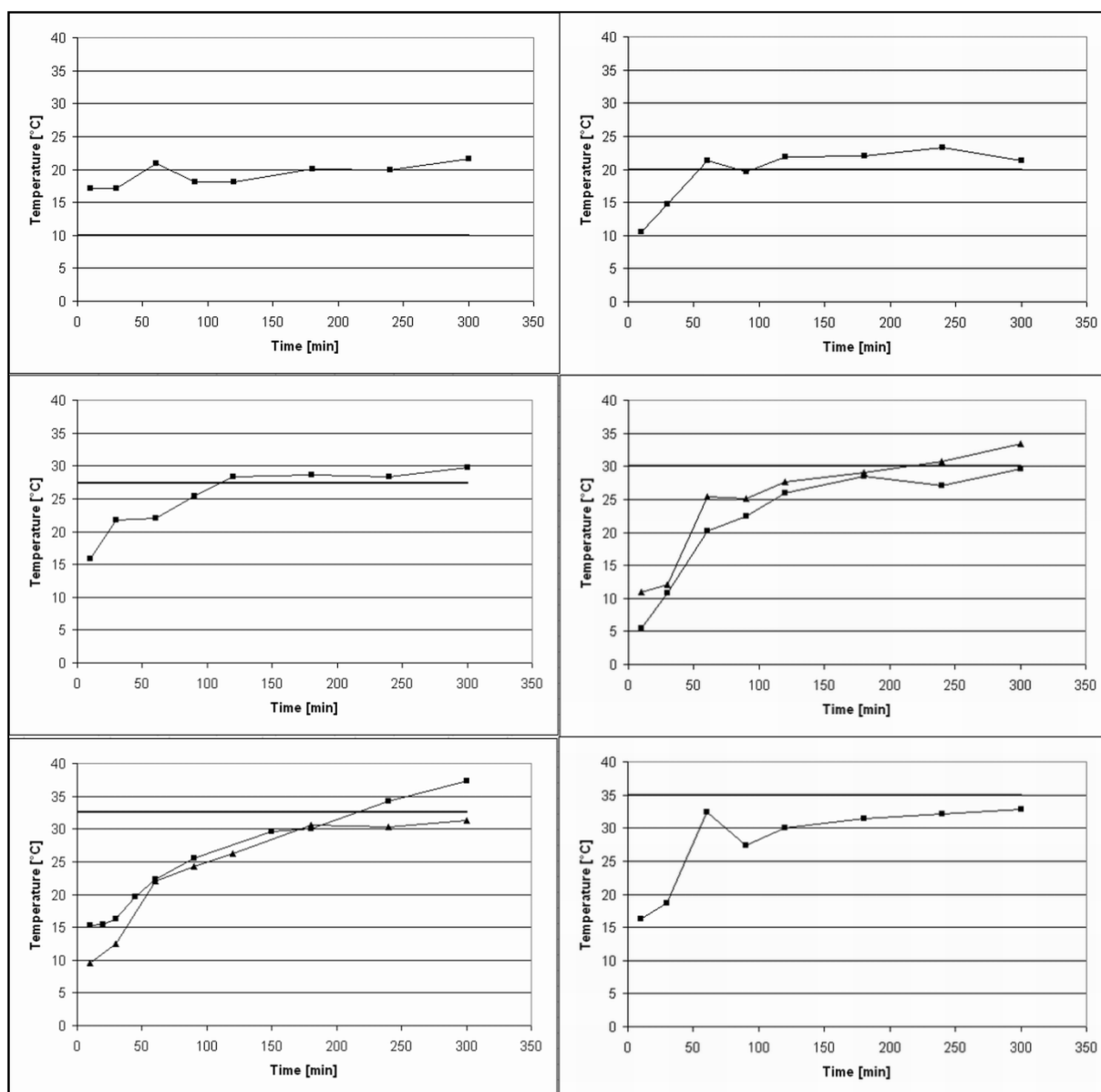


Figure 4: Change of the T_g (-■-) depending on the applied preparation temperature (—) of 10 °C (a), 20 °C (b), 27.5 °C (c), 30 °C (d), 32.5 °C (e) and 35 °C (f)

Phase separation occurs when a solved polymer precipitates and a polymer rich phase separates from a solvent-rich phase. This process accelerates the desolvation of the polymer. Because of its poor solubility in PLGA the drug will partition mainly into the solvent phase. However, if the volume of the solvent phase shrinks due to a proceeding solvent extraction, the drug is forced to redistribute into the polymer matrix where it intensifies the plasticizing effect of the remaining methylene chloride. This process could explain the temporary drop of the T_g at about 90 minutes which occurs only in drug loaded but not in plain microparticles (data not shown).

Overall, a higher variance at the first sampling time point may be due to the fact that the T_g is more difficult to analyze with high amounts of residual solvents, because the change of the DSC signal is small and prolonged. With decreasing amount of methylene chloride the transition becomes more distinct.

The process temperature also influences the amount of residual solvent in the microspheres at the end of the process (Fig. 1). For this reason there is no uniform final T_g value. The particles prepared at 10 °C with the highest amount of residual solvent (3.46%) show the lowest T_g (21.6 °C) at the end of the process and the particles prepared at 35 °C with only 0.93% residual solvent exhibit the highest T_g of 34 °C after 5 hours.

The variation of the process temperature strongly determines the properties of the resulting microsphere. This is attributed to the flexibility of the polymer chains during processing. After 10 minutes the T_g of the particles prepared at 10 °C is already above the process temperature. Thus the polymer matrix becomes rigid and immobile and its structure is fixed within the first minutes of the process, resulting in a sponge-like morphology of the microspheres and a porous surface (Fig. 5a). A higher preparation temperature prolongs the time span, in which the process proceeds above the glass transition temperature. By applying a preparation temperature of 20 °C the polymer is in a rubbery state for the first 50 minutes of the process and this time span becomes more and more extended for the batches prepared at higher process temperatures. At 35 °C the T_g does not exceed the preparation temperature at all during the total 5 hours of processing, leading to microspheres with a dense outer layer, a smooth surface and a fine porous structure inside (Fig. 5b). This does not agree with the findings of Fu et al, who observed the opposite effect, i.e. a highly porous structure at high temperatures and a smooth surface at low temperatures [17]. In case of other ingredients, like a low molecular PLGA as used by Fu et al. these conditions might lead to other morphological properties.

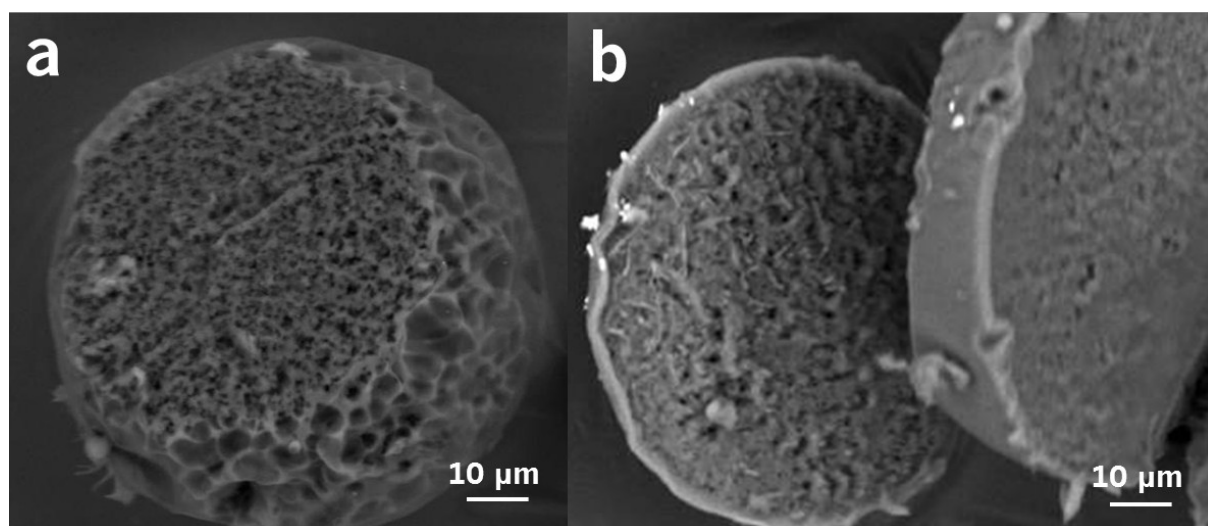


Figure 5: SEM micrographs of microspheres prepared at 10 °C (a) and 35 °C (b)

3.2.2 Influence on the encapsulation efficiency and molecular weight

In this investigation the highest drug encapsulation efficiency was found at low process temperatures of 10 and 20 °C and decreased with rising temperature of the external phase (Fig. 6b). Graves et al found that the encapsulation efficiency is significantly influenced by the rate of polymer precipitation [18] and thus also by the applied preparation temperature. A fast solidification rate is considered to be beneficial for a high entrapment of drug substance. Whereas Yang et al. found the best encapsulation efficiency for the lowest and highest formation temperatures [19] we obtained the best encapsulation efficiency between 93 and 96% of the introduced drug substance only at low process temperatures. At higher process temperatures of 27.5 °C and above we obtained a sharp decrease in the encapsulation efficiency with a minimum of 80% for 30 °C.

Not only the temperature of the external phase but also the phase ratio of dispersed and continuous phase is an important parameter for the fast precipitation of the polymer. As the amount of the dispersed phase is very low (1:100), the solidification rate is very fast even for low preparation temperatures. Soon after mixing both phases the T_g of the polymer exceeds the process temperature leading to a slower diffusion rate of the dissolved drug substance in the polymer matrix and thus favouring the drug entrapment. By applying a higher temperature the polymer molecules stay flexible and the drug molecules can diffuse through this soft matrix into the external phase resulting in reduced encapsulation efficiency.

Besides the encapsulation efficiency the polymer molecular weight of the resulting microspheres is influenced by the applied process temperature. As expected, it decreased with increasing process temperature, as the hydrolysis of PLGA is accelerated by rising temperature [20]. No significant temperature dependence of the degradation rate could be detected between 10 and 27.5 °C. Within this temperature range the molecular weight drops during the process from the initial value of 56.0 kDa by an average of approximately 2.0 kDa. A sharp further decline occurs between 30 and 35 °C with a decrease by up to 5.5 kDa which is about 10% of the initial value. The degree of polymer degradation correlates with the time span during which the process temperature exceeds T_g . In other studies even more dramatic weight losses during the time of process temperature above the T_g of the polymer have been reported [21]. Thus the process temperature not only affects the glass transition temperature and structure formation but also clearly leads to differences in the molecular weight. For all these factors the process temperature and the process time below and above the T_g appear to be crucial.

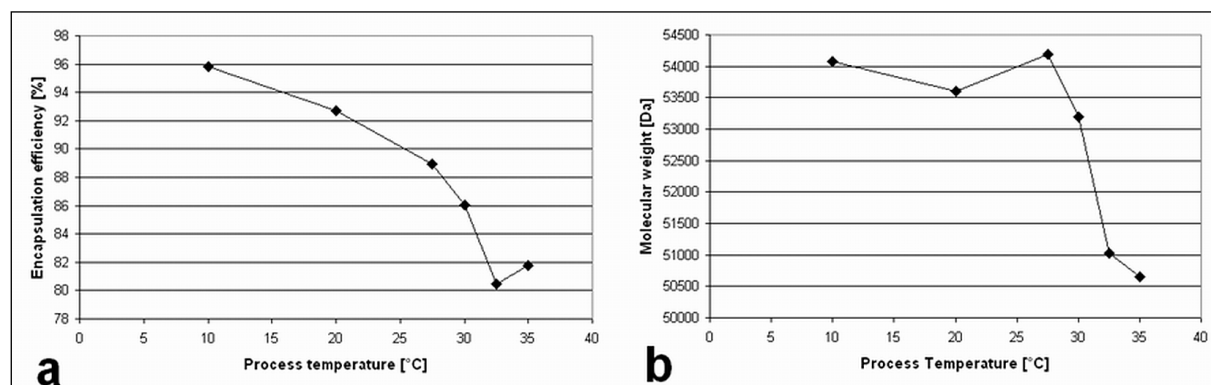


Figure 6: Influence of the preparation temperature on the encapsulation efficiency (a) and the molecular weight (b) of the resulting microspheres

3.2.3 Influence on the drug release rate

The drug release from PLGA microspheres is influenced by a variety of process parameters in an emulsion solvent removal process [22, 23] and by the resulting morphology of the microspheres [24]. Su et al. studied the influence of the homogenization speed, the molecular weight of PLGA and PVA and the PLGA concentration on the drug release profiles of microspheres at room temperature [25]. Among all the process parameters in an emulsion solvent extraction process,

the temperature during formation and hardening of the microspheres must have a crucial impact on the resulting drug release profile.

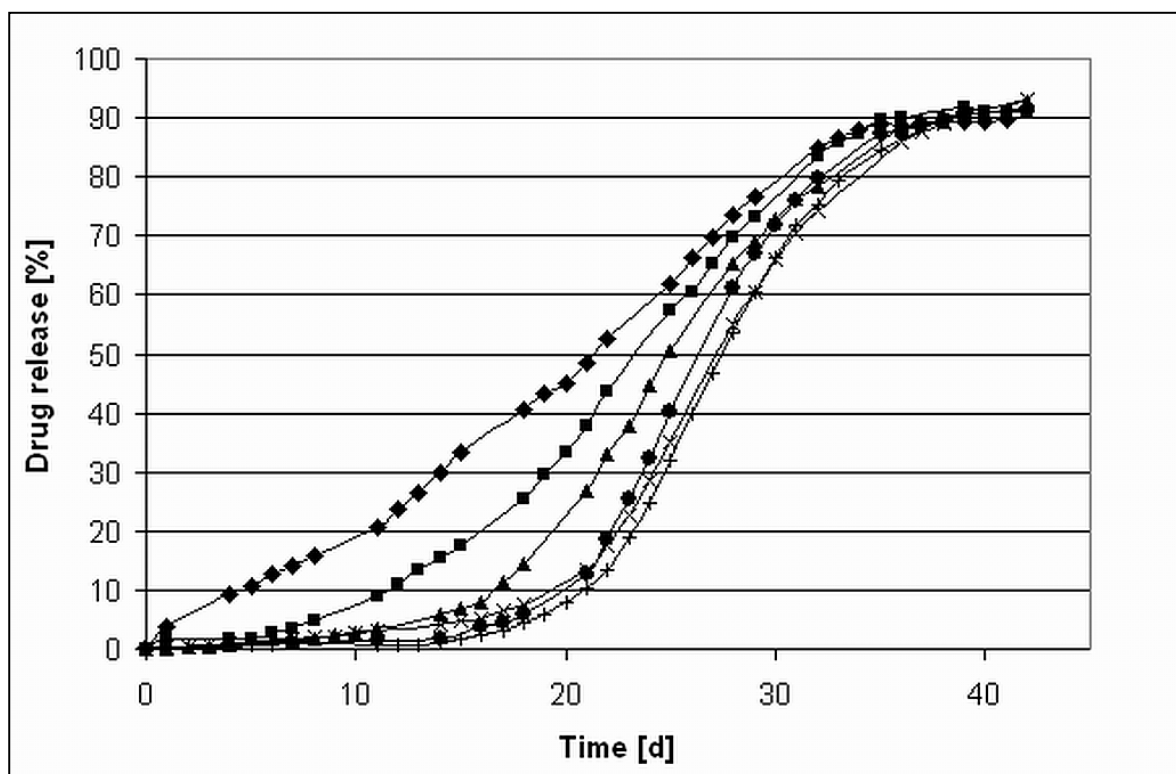


Figure 7: Drug release profiles of the microspheres prepared at 10 °C (-◆-), 20 °C (-■-), 27.5 °C (-▲-), 30 °C (-×-), 32.5 °C (-+-) and 35 °C (-●-) (37 °C and pH 7.4)

The particles prepared at 10 °C showed an almost linear release of the drug substance (Fig. 7). Process temperatures of 20 °C and above caused more and more sigmoidal profiles. They start with a lag phase without any significant drug release, followed by a second phase with an accelerated release rate. The higher the applied process temperature the more pronounced is the lag phase and the sigmoidal drug release profile. At a process temperature of 30 °C the lag-phase reached a maximum of 15 days which was prolonged by applying higher temperatures.

As discussed before, at a preparation temperature of 10 °C the polymer matrix is not exposed to a temperature above its T_g resulting in microspheres with a sponge-like porous structure without any visible shell (Fig. 5a). As a result, water can rapidly penetrate into the microspheres and dissolve the drug substance out of the polymer matrix. Simultaneously degradation of the polymer matrix starts throughout the whole particle. This causes a bulk erosion of the microspheres as described by Burkersroda et al. [26]. From a certain point in time the drug release is a result of

both, drug diffusion and erosion of the polymer matrix. Because of the open-porous structure the degradation products of the polymer hydrolysis diffuse out of the particles into the surrounding medium. This impedes the accumulation of these acidic hydrolysis products inside the microspheres which otherwise would cause an autocatalytic acceleration of the degradation process [27]. For this reason the drug release does not achieve the rate of the particles with a denser structure.

When the solvent extraction is performed at 20 °C the process temperature exceeds the T_g of the microspheres for about 50 minutes. Thus a more compact structure is formed and the drug release does not start before day 5. The higher the applied preparation temperature, the longer the polymer matrix is exposed to a temperature above its T_g . In case of the batch prepared at 35 °C the T_g does not reach the preparation temperature for the entire process. The polymer chains are flexible and mobile and the polymer matrix remains in a rubbery state. A dense structure is formed during processing, which has a crucial impact on the lag-phase and the release characteristic of the resulting microspheres (Fig. 5b). The small water molecules can diffuse through the dense matrix into the microspheres and hydrolysis of the polymer chains starts. As the resulting fragments of the polymer chains cannot diffuse out of the particles, their accumulation leads to a significant drop of the pH in the interior of the spheres [27]. This drop of the pH accelerates the polymer degradation and at a certain molecular weight, mostly between 10000 and 15000 Da the drug release rate strongly increases [28]. Furthermore the pH drop leads to a better solubility of the drug substance. 4-[2-[4-(6-fluorobenzo[d]isoxazol-3-yl)-1-piperidyl]ethyl]-3-methyl-2,6-diazabicyclo[4.4.0]deca-1,3-dien-5-one is only poorly soluble at neutral pH (0.06 mg/ml), but its solubility increases considerably with decreasing pH to 10.91 mg/ml at pH 3. Thus not only the diffusion coefficient within the polymer is increased by acidic degradation but also the concentration of the saturated drug solution in the core of the particles rises as a result of the acidification. According to Fick's first law of diffusion both factors increase the diffusion flux of drug out of the particles. For these reasons a dense structure is essential for a sigmoidal drug release profile with a lag-phase and subsequent fast drug release, whereas a porous outer surface of the microspheres leads to an almost linear drug release profile from the beginning of the dissolution testing. Plotting the lag time against the time interval in which the process takes place above the T_g ($tT_p > T_g$) suggests, that a distinct change in microparticle morphology, which

is caused by treatment at temperatures above T_g , determines the length of the lag phase (Fig.8).

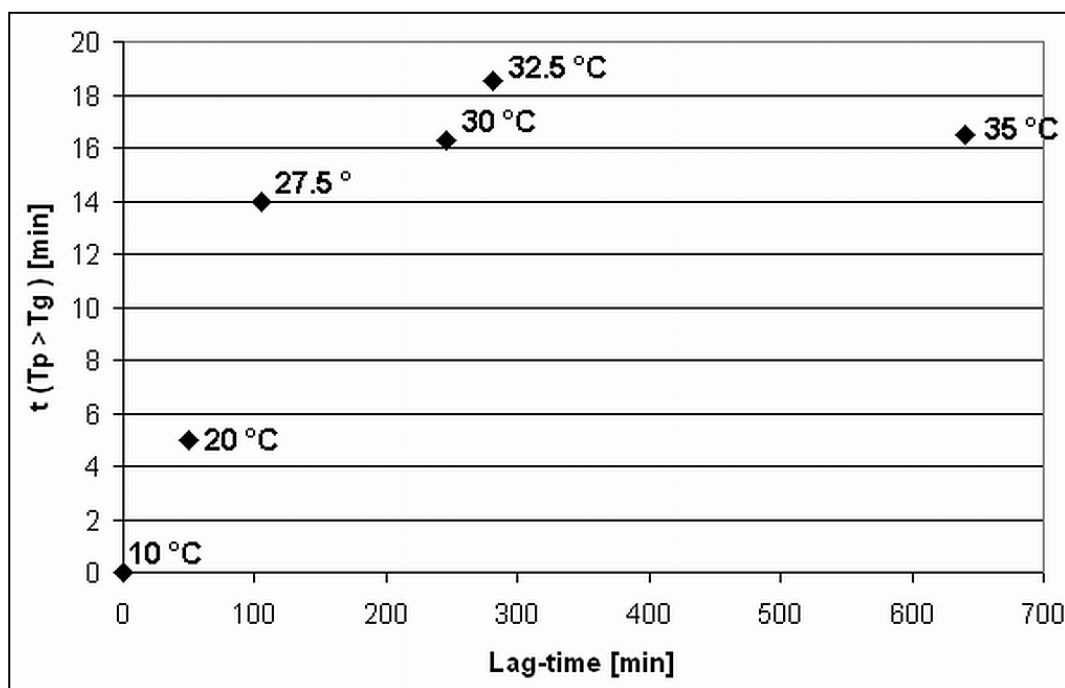


Figure 8: Lag-time of drug release vs. period of time during which processing takes place above the T_g of the polymer ($t_{T_p > T_g}$)

In addition to the time span, the process takes place above the T_g of the polymer also the difference between the applied process temperature and the T_g at a certain point in time might influence the resulting morphology of the particles. For this reason the area between the curves for the process temperature and the T_g was calculated by integration. The larger this area, the more pronounced is the difference between the applied process temperature and T_g of the microspheres. Figure 9 shows the correlation between the integral of the temperature by which T_p exceeds T_g and the lag-time before drug release. The diagram reveals a positive correlation between the integrated temperature difference and the lag-time.

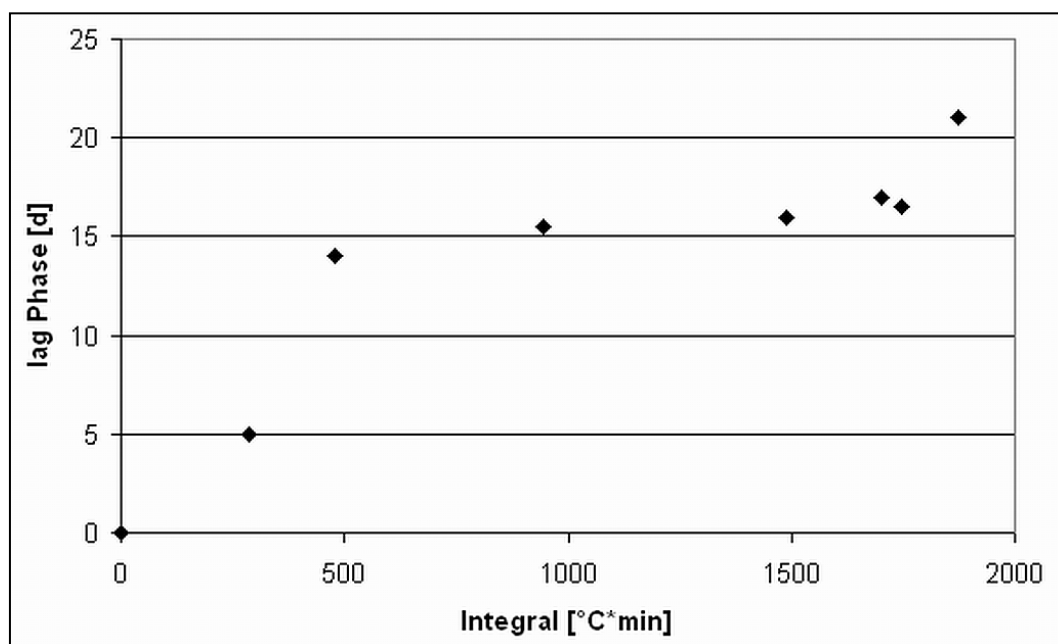


Figure 9: Lag-time depending on the integral of T_p and T_g

3.2.4 Influence of the polymer chain length

The molecular weight of the employed PLGA has a strong influence on the encapsulation efficiency and the drug release rate of microspheres [29]. Su et al found, that the encapsulation efficiency increased with higher molecular weight of the polymer [25]. In other cases, depending on the drug to be encapsulated, a low molecular weight polymer could be more appropriate for a high drug load [17]. As the length of the polymer chains has an impact on the resulting morphology of the polymer matrix, the molecular weight has also an influence on the drug distribution and release rate from the microspheres. Fu et al. found, that a high molecular weight leads to a high initial burst and a subsequent slow release, whereas the use of a low molecular weight PLGA resulted in a fast drug release. This effect occurs in addition to the impact that the polymer degradation itself has on drug release.

We investigated the influence of the molecular weight on the solidification rate of the polymer matrix measured by the change of the glass transition temperature during particle formation.

Although the molecular weight of the applied polymers ranged from 36.5 to 109.2 kDa no differences in the T_g vs. time profiles at a manufacturing temperature of 35 °C could be observed (Fig. 10).

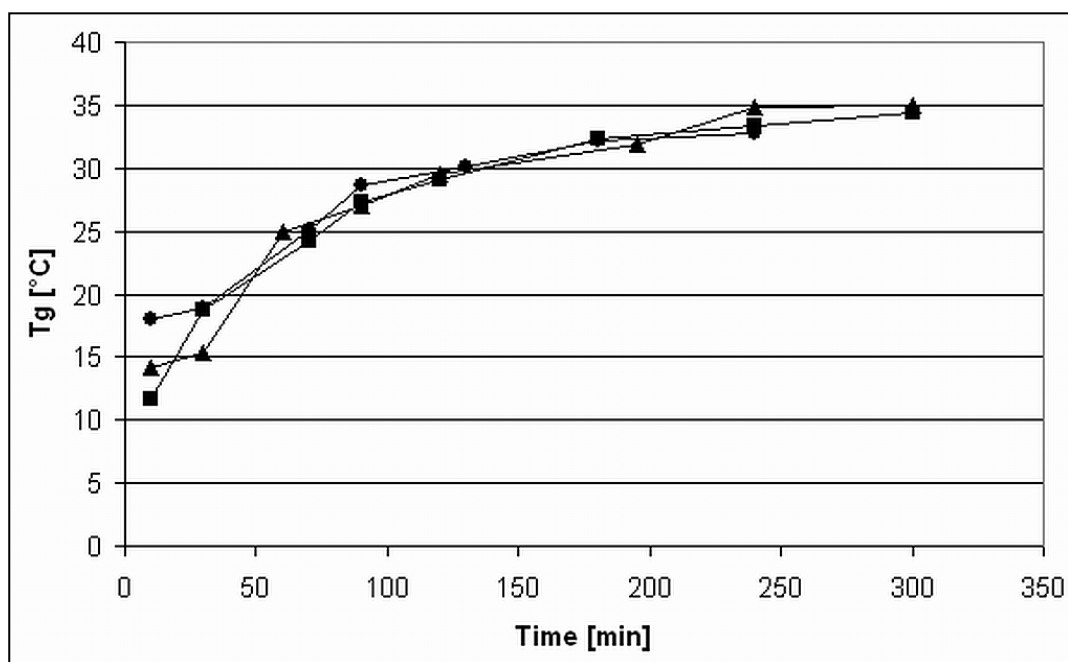


Figure 10: T_g vs. time profiles from particle preparations using PLGA types of different molecular weight (36510 Da (-▲-), 58300 Da, (-■-), 109200 Da(-●-)) at a process temperature of 35 °C.

However there is a significant influence of the molecular weight on drug release. The fastest release was obtained for the polymer with the lowest molecular weight (Fig. 11).

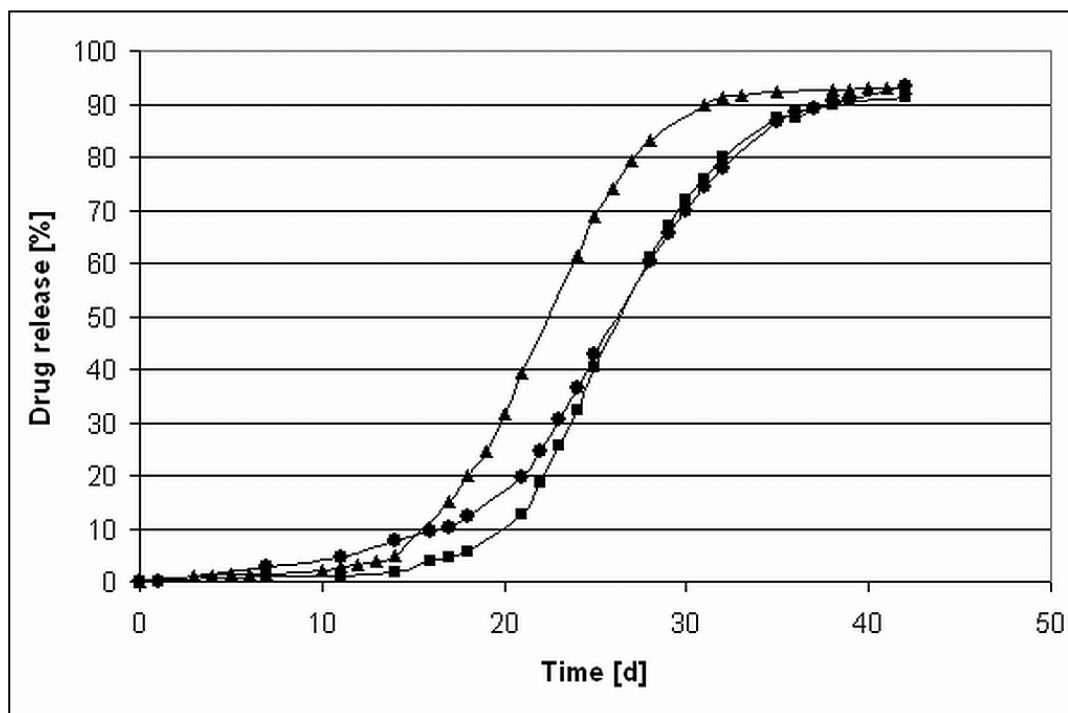


Figure 11: Drug release profiles of the microspheres prepared at 35 °C with PLGA types of different molecular weights (36510 Da (-▲-), 58300 Da (-■-), 109200 Da (-●-))

The drug release starts after 13 days for the 36510 Da PLGA and thus about 4 days earlier compared to the batch prepared with 58.3 kDa PLGA. This is due to the fact, that the low molecular weight PLGA exhibits enhanced water permeation and accelerated erosion of the polymer matrix. The lag-time is followed by a steep incline of the curve during the erosive phase of the drug release. The microspheres prepared with 109.2 kDa PLGA showed an only marginally changed drug release profile compared to the batch prepared with 58.3 kDa PLGA. The only small difference in lag-phase of the particles prepared with 109.2 kDa PLGA and those of 58.3 kDa PLGA can be referred to the fact, that the degradation of the high molecular weight polymer during processing is much more pronounced, resulting in particles 70.5 kDa compared to 54.7 kDa after manufacturing.

3.2.5 Influence of solvent removal rate

As mentioned above, the flexibility of the polymer chains during processing has a strong influence on the resulting particle morphology and it depends, inter alia, on the solvent content of the polymer phase. The higher the amount of solvent in the polymer matrix, the lower its T_g . A decelerated solvent evaporation can be achieved by reducing the stirring speed and the air flow through the reactor (Tab. 2).

Table 2: Process parameters and properties of microspheres prepared at 35 and 32.5 °C with fast and slow solvent evaporation

Process temperature [°C]	Stirring speed [rpm]	Air flow [l/min]	Encapsulation efficiency [%]	Molecular weight end of process [kDa]
35	260	10	81.8	50.7
35	180	1.5	79.3	44.9
32.5	260	10	80.4	51.0
32.5	200	1.5	44.7	51.5

At a process temperature above 30 °C such conditions lead to a prolonged interval, during which the process proceeds above the T_g of the particles (Fig. 12). The change of the glass transition temperature in case of slow solvent removal was significantly decelerated compared to fast evaporation. The particles prepared at

32.5 °C and slow solvent evaporation showed an almost linear increase of the T_g from 8 °C at the beginning to 32 °C after 5 hours of processing.

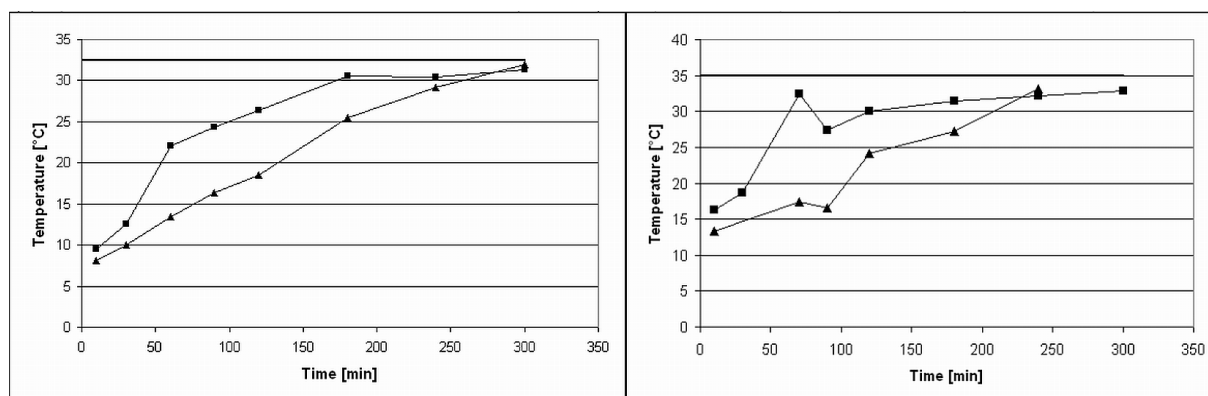


Figure 12: T_g vs. time profiles during processing at 32.5 °C (left) and 35 °C (right) with fast (-■-) and slow (-▲-) solvent extraction according to Tab. 2

At 35 °C the slow solvent extraction leads to a marked amplification of the polymer degradation during processing (Tab. 2). The encapsulation efficiency was hardly affected in case of the batch prepared at 35 °C, whereas in the case of the batch prepared at 32.5 °C only half of the drug substance was encapsulated, if the evaporation was slowed down. The microscopic pictures revealed that no spherical but irregular shaped and broken particles were obtained under these process conditions. With a very slow removal of the organic solvent and thus a delayed skin formation on the particle surface the preparation process can become unstable. During processing the organic solvent diffuses from the liquid emulsion droplets or hardening particles into the surrounding extraction medium. Consequently solidification starts from the surface of the particles and at the beginning of the process a highly viscous outer shell is formed, which covers the liquid core of the particle. This outer shell is still fragile and with a rising vapor pressure of the solvent the shell can be ruptured, releasing parts of the enclosed liquid into the surrounding medium. This causes a high drug loss during processing. In former experiments even the precipitation of drug crystal needles could be observed (data not shown). Thus a certain rate of particle solidification is essential to minimize the length of this vulnerable stage of the solidification process and to obtain intact microspheres with a high drug load.

3.2.6 Influence of a subsequent resuspension of the particles with ethanol

In addition, we studied the effect of a terminal ethanolic resuspension step on the resulting particle characteristics. Ahmed et al. showed that the treatment of the wet microparticles with an organic solvent/water mixture and adding solvents into the external aqueous phase changed the microstructure of the particles [30]. It caused the reduction of pores and thus reduced burst release. After 5 hours of extraction at 35 °C the microspheres were filtrated, immediately suspended in an ethanol/water mixture (25:75 (v/v)), and heated up to 25 °C or 40 °C, respectively. Ethanol is a non-solvent for PLGA and only a poor solvent for the encapsulated drug. By diffusing into the polymer matrix it can act as a plasticizer and lower the T_g of the polymer. This was confirmed experimentally as a slight reduction of T_g from 33 °C to 29 °C after 1 hour was measured. Thus, depending on the applied preparation temperature, a further change in the structure of the polymer matrix can be expected.

In all samples which were treated with ethanol the degradation of the polymer was more pronounced in consequence of the prolonged processing time (Tab. 3). The treatment of the microparticles with 25% ethanol at 40 °C caused an extreme drug loss. Only about 60% of the drug substance employed was encapsulated. In contrast particles treated at 25 °C showed an encapsulation efficiency of more than 80%, comparable to the microspheres without ethanol treatment.

Table 3: Preparation parameters and characteristics of microparticles treated with ethanol/water mixture (25:75) at different temperatures

Temperature [°C]	Duration [min]	Encapsulation efficiency [%]	Molecular weight [Da]	Lag phase [d]
40	60	60.50	48930	17
40	120	61.44	45390	17
25	60	80.27	49750	14

The microspheres showed a lag phase of 14 days when treated with ethanol for 1 hour at 25 °C. Incubation at 40 °C caused a change to a triphasic pattern. A lag

phase of 17 days is followed by a slightly increased drug release up to 10% and finally a very fast release after 18 or 26 days, respectively (Fig. 13).

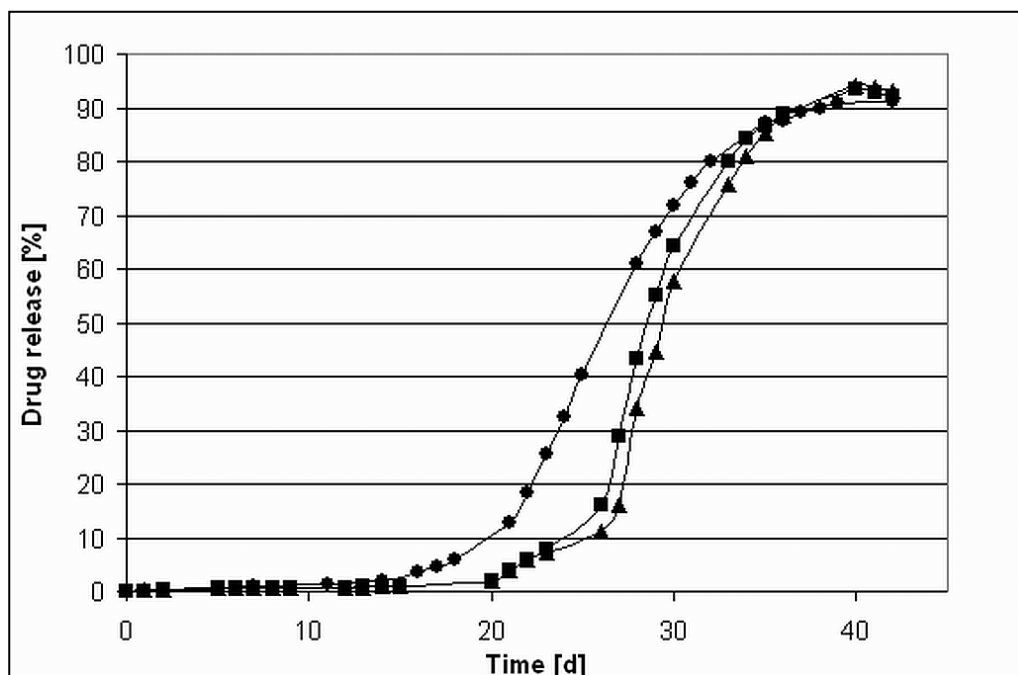


Figure 13: Drug release profiles of the microspheres treated with ethanol-water-mixtures for 1 hour at 40 °C (■-), 2 hours at 40 °C (◆-), and 1 hour at 25 °C (●-)

The particles treated with 25% ethanol at 25 °C had a similar shaped drug release profile as particles without this pretreatment. Due to the decreased molecular weight (49750 Da) the profile lies between the curves of non-incubated particles made from a 36510 Da PGLA and those made from a 58300 Da PLGA. At 25 °C the T_g was not exceeded by the process temperature and thus, besides the increased polymer degradation, no structural changes could occur.

Compared to the untreated microspheres those particles treated with ethanol at 40°C showed a thick and dense outer shell (Fig. 14). Chemical imaging revealed that this shell was almost completely free of drug (Fig. 15).

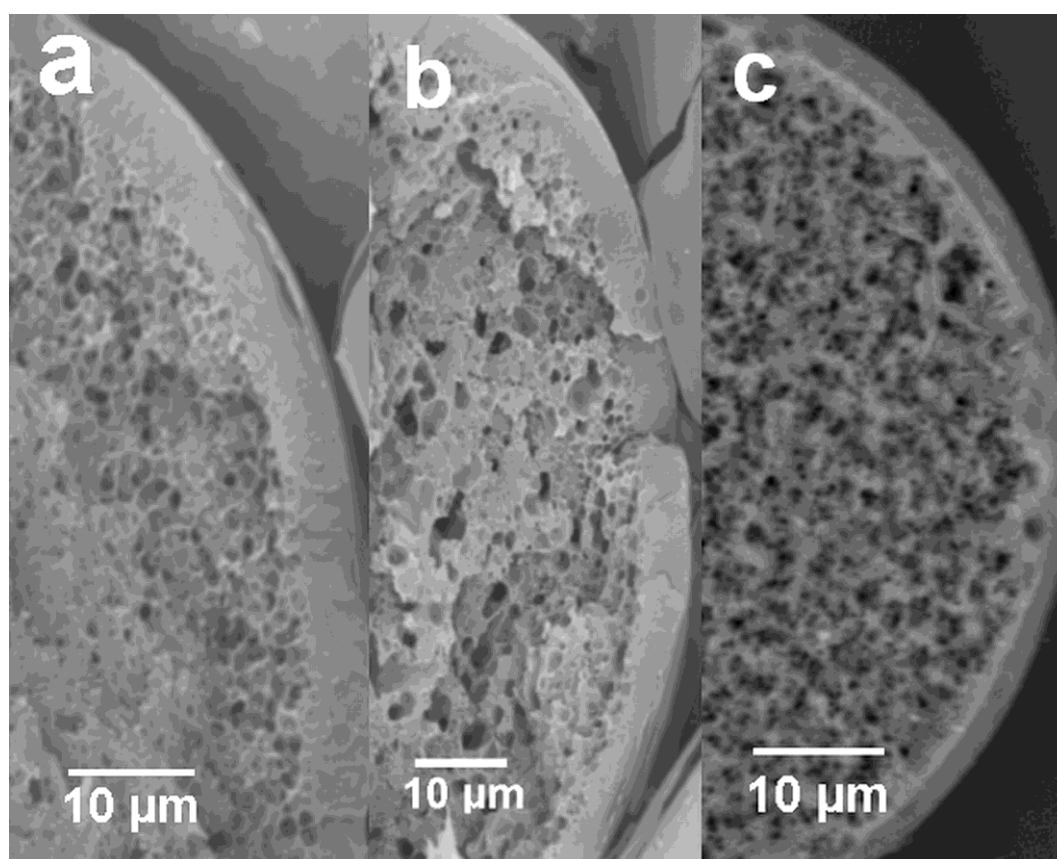


Figure 14: SEM micrographs of microparticles after treatment with ethanol (25%) at 40 °C after 1 (a) and 2 hours (b) and without treatment (right)

Hindrance of diffusion by this low porous shell is to be considered as the cause of the extended lag-phase after ethanol incubation at elevated temperature.

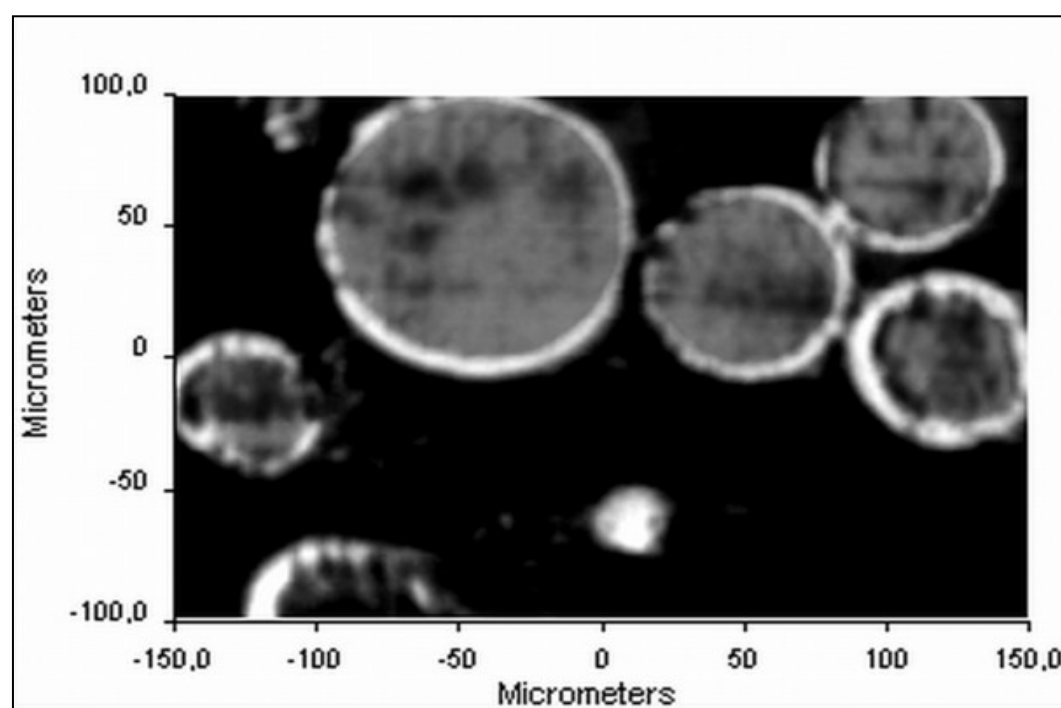


Figure 15: Chemical imaging of the microparticles: distribution of PLGA in the particles (white coloured area = high adsorption at 1747 cm⁻¹ (characteristic band for PLGA))

4 Conclusions

The effects of different process parameters on the characteristics of PLGA microspheres were investigated with a focus on the processing temperature. The T_g of the polymer was used to measure the flexibility of the polymer chains during processing. The T_g depends on the amount of organic solvent in the polymer matrix and can also be affected by other molecules like water or drug substance. A good correlation can be found for the concentration of organic solvent and the decrease of the T_g if no drug substance is present. A linear correlation cannot be found for drug loaded particles, indicating a synergistic effect of the solvent and the drug substance dissolved in the polymer phase.

The encapsulation efficiency and the drug release can be distinctly modified by changing the preparation temperature. This is due to the fact that particles prepared at 10 °C show an open porous structure, whereas a higher temperature leads to the formation of a dense matrix and a smooth surface, impeding a diffusive drug release at the beginning of the dissolution testing. Consequently, in case of a shell structure, the degradation products cannot diffuse out of the microspheres. This induces a significant pH-drop inside the particles with the occurrence of autocatalytic effects and enhanced drug solubility.

The time span during which the polymer chains remain flexible, which can be recognized by a T_g higher than the process temperature, can be modified by a slower removal of the organic solvent. If the solvent removal is carried out too slowly the process can become instable resulting in irregularly shaped and broken microspheres. A certain rate of solidification is essential to obtain spherical microspheres with efficiently encapsulated drug substance.

The slow release of a poorly soluble drug substance from a PLGA matrix is influenced by the chain length of the applied polymer. Further modifications can be obtained by the formation of different structures of the polymer matrix. For this reason a good control of the T_g during processing is essential, as its change has a strong influence on the resulting microsphere morphology. A precise control of the process temperature and the solvent removal rate are necessary which is often not possible on a laboratory batch scale. Depending on the process time during which the polymer chains remain flexible and mobile, the structure of the polymer matrix can be coarse- and open-porous or fine-porous with a dense outer shell. Thereby

the drug release varies between an almost zero-order-release to a sigmoidal type of the curve with a distinct lag-time. The latter mentioned profile was particularly marked for particles prepared with an additional suspension step in an ethanol water mixture. This caused a softening of the polymer matrix and the formation of a dense outer shell. However it should be pointed out, that this change of the morphology occurred on the expense of the drug load.

5 References

- [1] Wischke,C.; Schwendeman,S.P. Principles of encapsulating hydrophobic drugs in PLA/PLGA microparticles. *International Journal of Pharmaceutics* **2008**, *364* (2), 298-327.
- [2] Cavalier,M.; Benoit,J.P.; Thies,C. The Formation and Characterization of Hydrocortisone-Loaded Poly((+/-)-Lactide) Microspheres. *Journal of Pharmacy and Pharmacology* **1986**, *38* (4), 249-253.
- [3] Smith,A.; Hunneyball,I.M. Evaluation of Poly(Lactic Acid) As A Biodegradable Drug Delivery System for Parenteral Administration. *International Journal of Pharmaceutics* **1986**, *30* (2-3), 215-220.
- [4] Suzuki,K.; Price,J.C. Microencapsulation and Dissolution Properties of A Neuroleptic in A Biodegradable Polymer, Poly(D,L-Lactide). *J. Pharm. Sci.* **1985**, *74* (1), 21-24.
- [5] Conti,B.; Genta,I.; Modena,T.; Pavanetto,F. Investigation on Process Parameters Involved in Polylactide-Co-Glycolide Microspheres Preparation. *Drug Development and Industrial Pharmacy* **1995**, *21* (5), 615-622.
- [6] ODonnell,P.B.; McGinity,J.W. Preparation of microspheres by the solvent evaporation technique. *Advanced Drug Delivery Reviews* **1997**, *28* (1), 25-42.
- [7] Sato,T.; Kanke,M.; Schroeder,H.G.; Deluca,P.P. Porous Biodegradable Microspheres for Controlled Drug Delivery .1. Assessment of Processing Conditions and Solvent Removal Techniques. *Pharmaceutical Research* **1988**, *5* (1), 21-30.
- [8] Cheng,Y.H.; Illum,L.; Davis,S.S. A poly(D,L-lactide-co-glycolide) microsphere depot system for delivery of haloperidol. *Journal of Controlled Release* **1998**, *55* (2-3), 203-212.
- [9] Li,W.I.; Anderson,K.W.; Mehta,R.C.; Deluca,P.P. Prediction of solvent removal profile and effect on properties for peptide-loaded PLGA microspheres prepared by solvent extraction/evaporation method. *Journal of Controlled Release* **1995**, *37* (3), 199-214.
- [10] Lynn,D.M.; Amiji,M.M.; Langer,R. pH-responsive polymer microspheres: Rapid release of encapsulated material within the range of intracellular pH. *Angewandte Chemie-International Edition* **2001**, *40* (9), 1707-1710.
- [11] Reich,G. Use of DSC to study the degradation behavior of PLA and PLGA microparticles. *Drug Development and Industrial Pharmacy* **1997**, *23* (12), 1177-1189.
- [12] Blasi,P.; D'Souza,S.S.; Selmin,F.; Deluca,P.P. Plasticizing effect of water on poly(lactide-co-glycolide). *Journal of Controlled Release* **2005**, *108* (1), 1-9.

- [13] Hancock,B.C.; York,P.; Rowe,R.C. The use of solubility parameters in pharmaceutical dosage form design. *International Journal of Pharmaceutics* **1997**, *148* (1), 1-21.
- [14] Passerini,N.; Craig,D.Q.M. An investigation into the effects of residual water on the glass transition temperature of polylactide microspheres using modulated temperature DSC. *Journal of Controlled Release* **2001**, *73* (1), 111-115.
- [15] Okada,H.; Yamamoto,M.; Heya,T.; Inoue,Y.; Kamei,S.; Ogawa,Y.; Toguchi,H. Drug-Delivery Using Biodegradable Microspheres. *Journal of Controlled Release* **1994**, *28* (1-3), 121-129.
- [16] Vay,K.; Scheler,S.; Friess,W. New insights into the pore structure of poly(D,L-lactide-co-glycolide) microspheres. *International Journal of Pharmaceutics* **2010**, *402* (1-2), 20-26.
- [17] Fu,X.; Ping,Q.; Gao,Y. Effects of formulation factors on encapsulation efficiency and release behaviour in vitro of huperzine A-PLGA microspheres. *Journal of Microencapsulation* **2005**, *22* (7), 705-714.
- [18] Graves,R.A.; Freeman,T.; Pamajula,S.; Praetorius,N.; Moiseyev,R.; Mandal,T.K. Effect of co-solvents on the characteristics of enkephalin microcapsules. *Journal of Biomaterials Science-Polymer Edition* **2006**, *17* (6), 709-720.
- [19] Yang,Y.Y.; Chung,T.S.; Bai,X.L.; Chan,W.K. Effect of preparation conditions on morphology and release profiles of biodegradable polymeric microspheres containing protein fabricated by double-emulsion method. *Chemical Engineering Science* **2000**, *55* (12), 2223-2236.
- [20] Hakkarainen,M.; Albertsson,A.C.; Karlsson,S. Weight losses and molecular weight changes correlated with the evolution of hydroxyacids in simulated in vivo degradation of homo- and copolymers of PLA and PGA. *Polymer Degradation and Stability* **1996**, *52* (3), 283-291.
- [21] Alexis,F. Factors affecting the degradation and drug-release mechanism of poly(lactic acid) and poly[(lactic acid)-co-(glycolic acid)]. *Polymer International* **2005**, *54* (1), 36-46.
- [22] Zidan,A.S.; Rahman,Z.; Khan,M.A. Online Monitoring of PLGA Microparticles Formation Using Lasentec Focused Beam Reflectance (FBRM) and Particle Video Microscope (PVM). *Aaps Journal* **2010**, *12* (3), 254-262.
- [23] Yeo,Y.; Park,K.N. Control of encapsulation efficiency and initial burst in polymeric microparticle systems. *Archives of Pharmacal Research* **2004**, *27* (1), 1-12.
- [24] Bae,S.E.; Son,J.S.; Park,K.; Han,D.K. Fabrication of covered porous PLGA microspheres using hydrogen peroxide for controlled drug delivery and regenerative medicine. *Journal of Controlled Release* **2009**, *133* (1), 37-43.
- [25] Su,Z.X.; Sun,F.Y.; Shi,Y.N.; Jiang,C.J.; Meng,Q.F.; Teng,L.R.; Li,Y.X. Effects of Formulation Parameters on Encapsulation Efficiency and Release Behavior of Risperidone Poly(D, L-

- lactide-co-glycolide) Microsphere. *Chemical & Pharmaceutical Bulletin* **2009**, 57 (11), 1251-1256.
- [26] Burkersroda, F.v.; Schedl, L.; Gpferich, A. Why degradable polymers undergo surface erosion or bulk erosion. *Biomaterials* **2002**, 23 (21), 4221-4231.
- [27] Siepmann, J.; Elkharraz, K.; Siepmann, F.; Klose, D. How autocatalysis accelerates drug release from PLGA-based microparticles: A quantitative treatment. *Biomacromolecules* **2005**, 6 (4), 2312-2319.
- [28] Friess, W.; Schlapp, M. Modifying the release of gentamicin from microparticles using a PLGA blend. *Pharmaceutical Development and Technology* **2002**, 7 (2), 235-248.
- [29] Graves, R.A.; Pamujula, S.; Moiseyev, R.; Freeman, T.; Bostanian, L.A.; Mandal, T.K. Effect of different ratios of high and low molecular weight PLGA blend on the characteristics of pentamidine microcapsules. *International Journal of Pharmaceutics* **2004**, 270 (1-2), 251-262.
- [30] Ahmed, A.R.; Ciper, M.; Bodmeier, R. Reduction in Burst Release from Poly(D,L-Lactide-Co-Glycolide) Microparticles by Solvent Treatment. *Letters in Drug Design & Discovery* **2010**, 7 (10), 759-764.

CHAPTER 6

A novel method for the determination of the intraparticulate pore volume and structure of microspheres ‡

Abstract

The objective of this work was to develop a fast and significant method for the determination of the intraparticulate pore size distribution of microspheres. Poly(lactide-co-glycolide (PLGA) microspheres prepared with a solvent extraction/evaporation process were studied. From the envelope and the skeletal volume of the microspheres the porosity was calculated. The skeletal volume was determined with nitrogen and helium pycnometry and mercury intrusion porosimetry. Based on single particle optical sensing (SPOS) a novel method was developed by which the envelope volume is calculated from the particle size distribution (PSD), provided that all particles have a spherical shape. The penetration capacity of the applied intrusion media is limited by their atomic or molecular diameter or by the surface tension and the pressure in case of mercury. A classification of the pore structure was obtained by comparing these different skeletal values with the values for the envelope volume. Two well separated pore fractions were found, a nanoporous fraction smaller than 0.36 nm and a macroporous fraction larger than 3.8 µm. The total porosity and the ratio between both fractions is controlled by the preparation process and was shown to depend on the solvent extraction temperature.

‡Published in International Journal of Pharmaceutics 2010, 402 (1-2), 20-26. Vay,K.; Scheler,S.; Friess,W., New insights into the pore structure of poly(D,L-lactide-co-glycolide) microspheres.

1 Introduction

Porous materials have found widespread use in many pharmaceutical and also technical applications, such as ion exchangers, adsorbents, chromatographic packings, supports for heterogeneous catalysis or solid-phase synthesis. Because of rapid advances in controlled drug delivery and tremendous growth of fields like solid phase catalysis and separation science, research on these kinds of materials has experienced a considerable uptrend in recent years. In all these applications the pore texture of the material is a crucial factor for its functionality and has to be optimized for the intended purpose. In many applications, for example, a bimodal pore size distribution is desirable with a network of large pores providing the pathways for an efficient mass transport and small pores providing a large active surface [1, 2]. Numerous porous materials are designed in the form of microspheres, frequently manufactured via emulsification or spray drying processes. In case of microspheres for pharmaceutical use, the porosity has significant influence for example on drug release [3-8]. In other applications of microspheres where the pore texture is sometimes considered not to be a principal feature, porosity is at least an important quality characteristic and its significance is often underestimated.

In general the porosity describes the fraction of voids in a given volume of a material. Depending on the size and type of pores included by the measurement different values can be derived [9]. This fact is also reflected in the existence of different definitions of porosity. The American Society for Testing and Materials (ASTM) defines it as “the ratio, usually expressed as a percentage, of the total volume of voids of a given porous medium to the total volume of the porous medium” [10], whereas the British Standards Institution (BSI) describes it as “the ratio of open pores and voids to the envelope volume [11]. Thus a given porosity value has to be interpreted in consideration of (i) the range limits of the measuring method and (ii) the inclusion or exclusion of open pores. Especially in case of dispersed solids the precise determination of the particles' envelope volume is a difficult and often unsolved problem. Many intrusion media even mercury under low pressure were found to fill not only the interparticular voids but to penetrate also into open pores to a certain extent. Various approaches have been made to overcome this problem e.g. subtraction of the interparticular volume of crushed nonporous

glass beads from the total void volume of the porous sample particles, both measured by mercury intrusion [12].

Mercury intrusion porosimetry is a common method to determine the porosity of a material and provides also information about its pore size distribution [13]. Mercury is a non-wetting, non-reactive liquid, which will not penetrate into small pores until a certain pressure is applied. The relationship between the pressure and the pore size, into which mercury is able to intrude, is given by the Washburn equation. It permits to acquire data over a broad range of pore diameter up to 360 μm , but implies several problems as well. Besides the difficulty to distinguish between intra- and interparticulate porosity as aforementioned, the measurement requires a toxic substance, relatively large sample quantities and is time-consuming. Furthermore ink-bottle shaped pores and interconnected pores shift the pore size distribution to smaller pores and bias the results [14, 15].

Another technique to gain information about the porosity is nitrogen adsorption. Beyond the specific surface area of the sample further textural characteristics can be derived from adsorption-desorption isotherms of nitrogen at its boiling point. However, only the micro- and mesoporous range of the pore distribution is covered by this method. Further approaches to determine the porosity are the water saturation [16] and water evaporation technique [17]. In these methods the sample is allowed to equilibrate with an excess of water. The total volume minus the amount of the not absorbed water reflects the volume of the pore space. If water is able to cause swelling of the sample, these methods do not allow distinguishing between permanent and temporary porosity.

Despite their widespread use all these techniques lack in accuracy and/or simplicity and are not able to distinguish between intra- and interparticulate pores. As mentioned before, the porosity can be calculated from the envelope and the skeletal density of the material. Gas pycnometry is an accurate method to determine the latter parameter, whereas the measurement of the apparent density is often difficult in case of a dispersed material. For this reason we developed a novel method for the determination of the intraparticulate porosity using single particle optical sensing (SPOS). This particle sizing method enables to determine the envelope volume of dispersed particles with high accuracy, provided that all particles have a spherical shape. The intraparticulate porosity ε is defined as:

$$\varepsilon = \frac{V(\text{envelope}) - V(\text{skeletal})}{V(\text{envelope})} \times 100\% = 1 - \frac{\rho(\text{envelope})}{\rho(\text{skeletal})} \times 100\%$$

As mentioned before the use of different intrusion media allows gauging different fractions of the total pore volume. The different pore fractions in a material can be classified according to IUPAC into micropores, smaller than 2 nm, mesopores ranging from 2 to 50 nm and macropores, bigger than 50 nm [18]. The volume occupied by helium is assumed to be the total pore volume and the difference to the envelope volume is therefore the skeletal volume of the material. With nitrogen and mercury lower pore volumes are obtained corresponding to the diameter of the smallest pores into which the respective medium is able to penetrate. By comparing these values detailed information about the pore size distribution and the morphological structure can be gained. In the presented study this method was evaluated for porosity and structure analysis of poly(lactide-co-glycolide (PLGA) microspheres prepared via an emulsion solvent extraction/evaporation process.

2 Materials and Methods

2.1 Materials

Poly (D,L-lactide-co-glycolide) 75:25 (Resomer 755 S): Mw = 64710 Da was purchased from Boehringer Ingelheim, (Ingelheim, Germany); Poly (D,L-lactide-co-glycolide) 75:25 (Lactel) in granulated form was purchased from Durect Corporation (Pelham, USA); 3-{2-[4-(6-fluor-1,2-benzisoxazol-3-yl)piperidino]ethyl}-2-methyl-6,7,8,9-tetrahydro-4H-pyrido[1,2-a]pyrimidin-4-one was obtained by Jubilant Organosys (Mysore, India). Polyvinylalcohol 26-88 and methylene chloride analytical grade were obtained from Merck (Darmstadt, Germany), TRIS (Tris(hydroxymethyl)-aminomethan) from AppliChem (Darmstadt, Germany) and Polystyrene research particles (Mean diameter 98.7 $\mu\text{m} \pm 1 \mu\text{m}$) from microParticles GmbH (Berlin, Germany).

2.2 Microparticle preparation

The microparticles were prepared by an emulsification, solvent extraction/evaporation technique. 2.8 g drug substance and 3.2 g PLGA were dissolved in 40 ml of methylene chloride. The polymer solution was then emulsified

in 500 ml of the extraction medium consisting of an aqueous solution of 0.5% (w/v) polyvinylalcohol and 0.1 M Tris buffer (pH 9.0). The emulsion was then fed into a 5 L jacketed glass reactor containing 3.5 L of the aqueous phase. By stirring for 5 hours the particles were hardened by solvent extraction and evaporation with an air flow of 10 l/min through the headspace of the reactor. The particles were separated by filtration and dried under vacuum in a desiccator. Different particle batches were produced by varying the temperature of the extraction mix between 10 and 35 °C.

2.3 Analytical methods

2.3.1 Single particle optical sensing (SPOS) - light obscuration

The particle size distribution was measured with an AccuSizer 780 (Sensor: LE400-05SE; Particle Sizing Systems, Santa Barbara, CA). This instrument uses the principle of light obscuration to count and size particles from 0.5 to 400 µm. The data is obtained in 512 logarithmically spaced channels with a minimum and maximum fraction width of 1 to 5.54 µm. Per measurement about 10 mg of microparticles were weighed exactly into a particle free vessel and dispersed in 100 ml particle free 1% Polysorbate 80 solution. For exact results it is essential, that the complete suspension is analyzed. In the case of spherical particles the total volume of a sample can be calculated from the particle size distribution. For every particle size fraction the average volume of a single particle was calculated with the sphere volume formula from the average diameter d_i of each fraction range. The total volume of all particles within a fraction was obtained by multiplication with the number n_i of particles within the respective size class. With the sum of the volumes of all 512 size fractions and the sample weight m the envelope density ρ_{env} was computed.

$$\rho_{env} = \frac{3 \cdot m}{2 \cdot \pi \cdot \sum_{i=1}^{512} (d_i \cdot n_i)}$$

2.3.2 Gas pycnometry

The skeletal density was measured using helium pycnometry (Ultrapycnometer 1000, Quantachrome GmbH, Odelzhausen, Germany). The samples were dried in

an air flow of 3% r.h. for at least 72 hours and about 500 mg particles were weighed into the medium size sample holder (volume 1.8 cm³). The density of the sample was additionally measured with nitrogen.

2.3.3 Mercury intrusion porosimetry

In order to cover a wide pore range the mercury intrusion measurements were performed with both a high- and a low-pressure unit. As low-pressure-unit a Pascal 140 porosimeter (Thermo Fisher Scientific, I-Milano; pressure range: 0.01 to 400 kPa) and as high-pressure-unit a Porosimeter 2000 (Carlo-Erba, I-Milano; maximum pressure: 200 MPa) were utilized.

2.3.4 Specific surface area

The specific surface area was determined by analyzing a sample of approx. 350 mg by a BET method (multi-point measurement) using a Nova 2000e surface analyzer (Quantachrome GmbH, Odelzhausen, Germany). Before the measurement the samples were degassed for 1 hour at 40 °C.

2.3.5 Scanning electron microscopy

Cross sections of the microspheres were examined by scanning electron microscopy (JEOL JSM – 5310LV; JEOL Ltd., Tokyo, Japan). To study the internal structure, the particles were frozen in liquid nitrogen and cut with a razor blade. The specimens were sputtered with gold.

3 Results

A first impression of the inner structure of the microspheres can be obtained by gas pycnometry. Preliminary experiments showed that it is essential to dry the samples completely. By purging the sample for incremental periods with the measuring gas in the sample cell of the pycnometer the moisture is slowly removed and 10 hours of purging are necessary to reach constant readings (Fig. 1).

In many samples, due to their microporosity, densities measured with nitrogen were lower than those measured with helium, corresponding to different molecule and atom sizes of the gases. Without pre-drying the difference between both

measurements does not become apparent. Since the microspheres are not thermally stable an air flow of 3% r.h. was applied for at least 72 hours to dry the samples at room temperature prior to gas pycnometry.

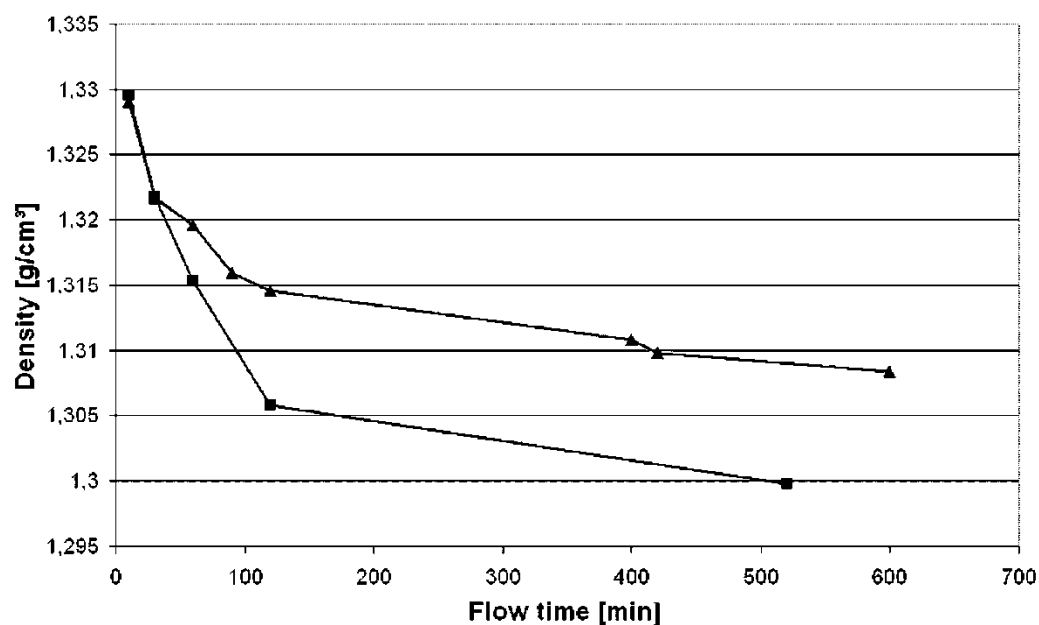


Figure 1: Density of PLGA-microspheres as a function of drying time with dry gas flow of helium (▲) and nitrogen gas (■)

In order to estimate the skeletal density of the polymer matrix, pure PLGA in different morphological forms was measured as a reference material with helium and nitrogen pycnometry (Tab. 1).

Table 1: Density of PLGA in different morphologies measured with helium and nitrogen pycnometry

Measuring gas	Helium	Nitrogen
Sample	Density [g/cm ³]	density [g/cm ³]
PLGA, powder	1.2468	1.3831
PLGA, tablet *	1.3071	1.2884
PLGA, granules	1.3018	1.2893
PLGA, microspheres (process temperature : 35 °C)	1.3046	1.2755
Polystyrol microparticles	1.0516	1.0536

* compressed with a compactor for IR spectroscopy

The values of the granulated and tableted PLGA and the placebo microspheres showed only slight differences between the measurements with both gases yielding a skeletal density of $1.3045 \pm 0.0027 \text{ g/cm}^3$ for helium and $1.2844 \pm 0.0077 \text{ g/cm}^3$ for nitrogen. Only the PLGA powder revealed a lower density for helium and an unexpected high value for nitrogen.

In the same way the microspheres prepared with varying process temperatures were analyzed (Tab. 2).

Table 2: Density and specific volume of PLGA microspheres prepared at different process temperatures

	Intrusion medium	Helium		Nitrogen		Mercury (at 350 kPa)	
Formulation	Process temperature [°C]	Density [g/cm ³]	Specific volume [cm ³ /g]	Density [g/cm ³]	Specific volume [cm ³ /g]	Density [g/cm ³]	Specific volume [cm ³ /g]
1	10°C	1.2834	0.7792	1.2784	0.7822	1.335	0.7491
2	20°C	1.2800	0.7813	1.2554	0.7966	1.236	0.8091
3	30°C	1.2719	0.7862	1.1827	0.8455	1.164	0.8591
4	32.5°C	1.2763	0.7835	1.1983	0.8345	1.178	0.8489
5	35°C	1.2853	0.7780	1.1841	0.8445	1.203	0.8313

The incorporated drug substance reduced the nitrogen pycnometric density more than 0.09 g/cm^3 below the density of the placebo microspheres. In contrast the densities measured with helium showed rather identical values differing only about 0.02 g/cm^3 from the placebo density. Using helium, the densities ranged between 1.2719 and 1.2853 g/cm^3 , whereas the nitrogen pycnometric values cover a larger range from 1.1827 to 1.2784 g/cm^3 . The differences between the helium and the nitrogen pycnometric results depend on the temperature applied in the preparation process and ranged from 0.005 g/cm^3 ($10 \text{ }^\circ\text{C}$) to 0.1 g/cm^3 ($35 \text{ }^\circ\text{C}$).

As a second parameter in equation 1 the envelope volume of the material is required for the calculation of the intraparticulate porosity. Taking advantage of the particles' spherical shape a method was developed to obtain the specific envelope volume and its reciprocal value, the envelope density, by optical particle counting and size fractionation of a known sample weight. In order to prove the accuracy monodisperse polystyrene microparticles with a mean diameter $98.7 \pm 1 \text{ }\mu\text{m}$ were analyzed. In case of these nonporous spherical particles the bulk density can be assumed to equal the true density of the particles. According to manufacturer's data the true density of the polystyrene particles is 1.05 g/cm^3 . By gas pycnometry a value of 1.0518 ± 0.0012 ($n = 5$) was obtained and with SPOS a density of 1.0427 ± 0.0149 ($n = 4$) was calculated, which means a deviation of less than 0.7% .

The PLGA microspheres of formulations 1 to 5 were found to have similar particle size distributions with median diameters (volume weighted) between 80 and $90 \text{ }\mu\text{m}$ (Tab. 3).

Table 3: Volume weighted median diameter measured with SPOS and calculated envelope volume and bulk density

Process temperature [$^\circ\text{C}$]	Median [μm]	Specific envelope volume [cm^3/g]	Envelope density [g/cm^3]
10	82.725	0.950	1.053
20	84.445	0.970	1.031
30	82.270	0.959	1.043
32.5	86.835	1.014	0.988
35	87.100	1.035	0.972

This corresponds well with the photomicrographs shown in Fig.2. The calculated envelope densities varied between 0.972 to 1.053 g/cm³ with higher values in case of smaller particles. The envelope density decreased with rising process temperatures, following a trend which can also be observed in nitrogen pycnometry.

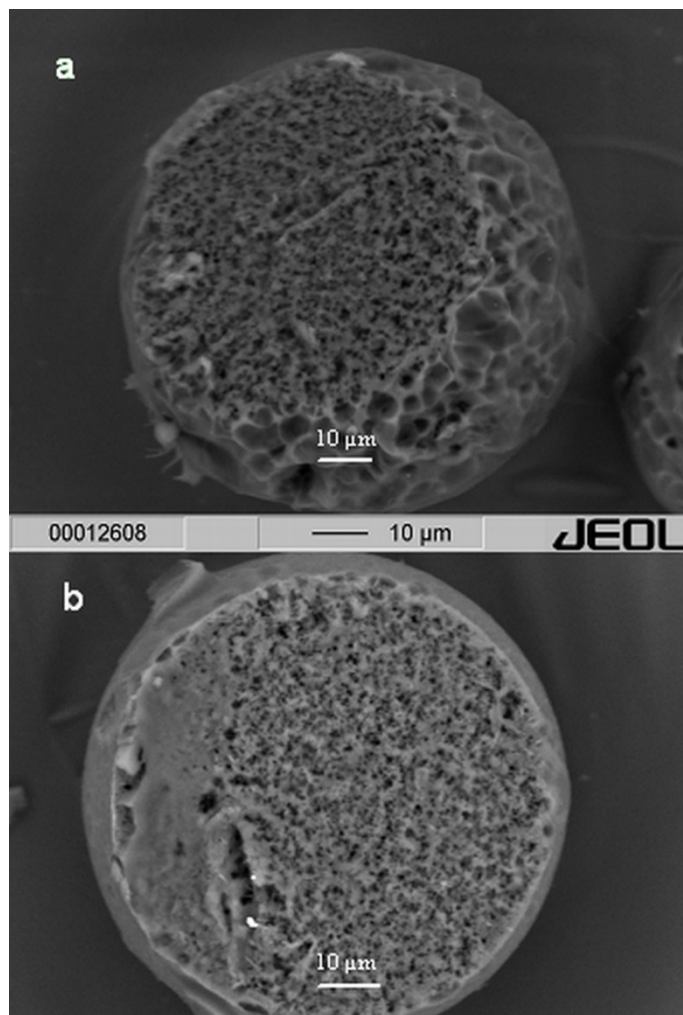


Figure 2: SEM of PLGA microspheres prepared at 10°C (top) and 35°C (bottom)

The density measured by low pressure mercury intrusion porosimetry did not show continuous temperature dependence. (Tab. 2) The values exceeded the envelope densities by about 0.1 to 0.3 g/cm³ thus indicating, that even under the conditions of low pressure Hg-porosimetry (350 kPa) mercury penetrates into the particles and consequently the values do not correctly represent the envelope volume of the microspheres.

The surface area of formulation 5 was determined by nitrogen adsorption. Although SEM photomicrographs revealed a highly porous structure, the value for the surface area of 0.41 m²/g was unexpectedly low.

4 Discussion

4.1 Interparticulate volume

The main focus of this investigation was the intraparticulate volume. However, a bulk material like microspheres contains also another type of voids: the interparticulate space. Figure 3 shows the mercury intrusion-extrusion curve of monodisperse polystyrene spheres with a diameter of 98.7 μm .

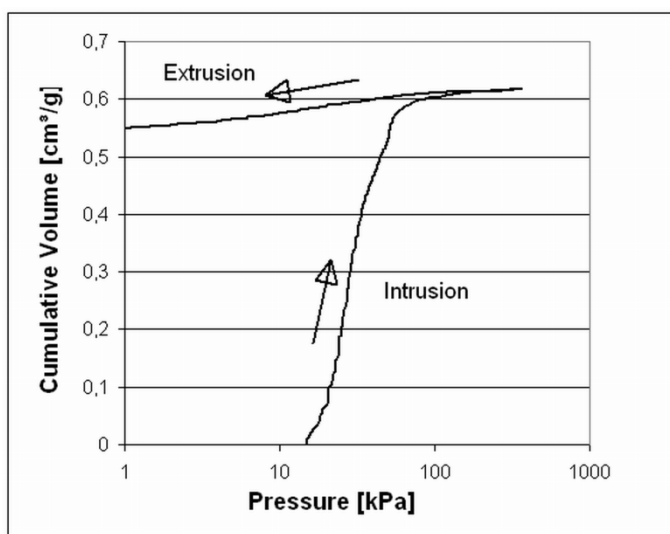


Figure 3: Intrusion - extrusion curve of monodisperse polystyrene microspheres ($\varnothing 98.7 \pm 1 \mu\text{m}$)

The intruded mercury fills the interparticulate space until its volume reaches a plateau value of $0.603 \text{ cm}^3/\text{g}$ at 100 kPa. This pressure corresponds to a pore diameter of 17 μm which is exactly 1/6 of the particle diameter, the value expected on basis of a consideration of Tonellier [12]. He reports that the diameter of voids between monodisperse spheres is about 1/6 of the particle diameter. It can be concluded that it is even smaller in case of a heterogenous size distribution where small particles fill the voids between larger ones. The small slope of the plateau can be attributed to a pressure-induced deformation of the polymer structure. It leads to an intrusion volume of $0.618 \text{ cm}^3/\text{g}$ at 350 kPa, the pressure which was found necessary to fill also the interparticulate voids between the smaller particles of the PLGA formulations. The sum of this intrusion volume and the specific volume of the polystyrene spheres measured at the same pressure of 350 kPa ($0.929 \text{ cm}^3/\text{g}$) is the bulk volume of the particle bed ($1.547 \text{ cm}^3/\text{g}$). Its packing density, 61.99%, is obtained as the ratio of the envelope volume, determined by the SPOS method

(0.959 cm³/g), and the bulk volume (0.959 cm³/g / 1.547 cm³/g = 61.99%). In case of non-porous particles about the same value can also be obtained from mercury porosimetry data only as the ratio of the specific volume and the bulk volume (0.929 cm³/g / 1.547 cm³/g = 60.05%). Both results are close to the maximum random packing density of monodisperse spheres which was calculated as 64.35% [19]. As discussed before, in case of porous PLGA microspheres the mercury intrusion volume covers the interparticulate voids in addition to a certain part of the intraparticulate pores (> 3.9 μm at 350 kPa). The specific volume measured at the same mercury pressure is the skeletal volume plus the remaining pore volume (< 3.9 μm). Table 4 shows the mercury intrusion volume, the specific volume (both determined at 350 kPa), and the bulk volume of formulation 1-5.

Table 4: Intrusion, specific and bulk volume for formulation 1-5 and the resulting packing density

Formulation	Intrusion volume [cm ³ /g]	Specific volume [cm ³ /g]	Bulk volume [cm ³ /g]	Packing density ¹ [%]
	at 350kPa	at 350 kPa		
1	0.5292	0.7491	1.2782	74.32
2	0.5159	0.8091	1.3249	73.21
3	—	0.8591	—	—
4	0.5478	0.8489	1.3968	72.59
5	0.6017	0.8313	1.4327	72.24

¹ Packing density = specific envelope volume (from Tab.3) / bulk volume

The difference to 100% is the share of the interparticulate voids in the total bulk volume. The particles of all formulations are about the same size and log-normal distributed with a standard deviation of 0.26 to 0.36. According to Farr the maximum packing fraction of a log-normal sphere distribution depends on its standard deviation σ_z and amounts to 67-68% for the mentioned range of σ_z . Because of the intraparticulate porosity it is not surprising to find values smaller than theoretically expected (58-61%) if the packing density is calculated as the ratio of the specific volume and the bulk volume, both determined with mercury at 350 kPa. If the

calculation is done with the envelope volume measured by SPOS, however, packing densities about 5% higher than predicted are obtained (72-74%). This can be explained by considering that the bulk volumes included in the calculation are determined with mercury under a pressure of 350 kPa. Due to the compression of the particle structure these values are smaller than they would be in an unpressurized state leading to an overestimation of the packing density.

4.2 Intraparticulate volume

According to their atomic or molecule diameters, the chosen intrusion media can penetrate to different degrees into the microspheres. They allow determining the intraparticulate volume, but rendering different results. There are several options to define the spatial dimensions of an atom or molecule. The kinetic diameter provides the most appropriate information for the estimation of the accessible pore size. This diameter - 0.36 nm for nitrogen and 0.26 nm for helium [20] - represents the diameter of the smallest pores into which the molecules or atoms can just penetrate. With these measuring gases the lower range of the microporosity can be determined. In case of mercury the intrusion capability depends on the applied pressure. Under the assumption of a cylindrical shape the minimum diameter d_p of mercury-accessible pores, can be calculated from the pressure p using the Washburn equation:

$$d_p = -4 \gamma \cos \theta / p$$

with a contact angle θ of 135° between mercury and PLGA and a surface tension γ of 485 mN/m [21]. At 350 kPa, the pressure applied during the low pressure measurement, pores with a minimum diameter of $3.9 \mu\text{m}$ are filled and sized and with a pressure of 200 MPa pores down to 6.9 nm are detected. This implies that the high pressure mode of mercury intrusion porosimetry is only suitable to determine pores in the meso- and macroporous range, whereas micropores can only be measured by gas pycnometry.

As reference the helium and nitrogen pycnometric densities were determined for the pure PLGA in different morphological forms, which showed consistent values. Only the PLGA powder shows different values ($\rho(\text{He}): 1.2468 \text{ g/cm}^3$ and $\rho(\text{N}_2): 1.3831 \text{ g/cm}^3$) which cannot be adequately explained.

Highest skeletal densities were found with pure PLGA granules and with the compressed polymer. The granules are transparent, which is an indication for a virtually pore-free, compact structure. A highly dense structure was also measured with particles prepared at 10°C. The He- and N₂-pycnometric densities are only slightly lower than the values obtained with PLGA granules (He: $\Delta\rho = 1.41\%$, N₂: $\Delta\rho = 1.27\%$) or compressed PLGA (He: $\Delta\rho = 1.81\%$, N₂: $\Delta\rho = 1.28\%$). Despite the similar gas pycnometric densities, formulation 1 clearly differs from PLGA granules and tablets in its morphology and internal microstructure. This demonstrates that the skeletal density alone does not allow distinguishing between a compact body and a porous material.

Different information on the intraparticulate volume is provided by the specific envelope volume, which is the reciprocal of the envelope density. Often it is assumed, that the specific envelope volume can be determined by low-pressure mercury intrusion porosimetry. Comparison of the specific volumes obtained by this method (0.7491 to 0.8591 cm³/g) (Tab. 2) with the envelope volumes calculated from SPOS (0.950 to 1.035 cm³/g) (Tab. 3) shows that, even under low pressure, mercury penetrates into the microspheres to a substantial degree. This is in accordance with Tonnellier [12] who found that mercury intrusion porosimetry is not an appropriate method to distinguish between intra- and interparticulate porosity. In order to measure the envelope volume of the spheres the intrusion medium must completely fill the interparticulate voids without infiltration of the porous particles. Because all the tested samples are particle fractions between 30 and 150 μm the smallest interspaces can be rated to about 5 μm (= 30/6 μm) according to the abovementioned consideration. According to the Washburn equation a pressure of about 350 kPa is necessary to guarantee that all these interparticulate pores (down to a theoretical diameter of 3.9 μm) are filled. As a consequence, however, mercury accesses also a certain fraction of intraparticulate pores which are in a similar size range (Fig. 2). Hence at least in case of samples with a broad size distribution, where the smallest interparticulate voids are similar in size to the largest intraparticulate pores, mercury intrusion is not a suitable method for determination of the particles' envelope volume. Provided that the sample consists of spherical particles only, the optical method we have developed allows a precise determination of this parameter.

4.3 Porosity profiles

The principle of the described method for studying the pore size distribution of microspheres is the combined application of three different intrusion media and an optical particle sizing method. The envelope volume is confined by a convex hull around the outer dimensions of each particle, whereas the specific volume determined with helium represents the volume of the mere polymer matrix. Thus the difference between both is the volume of voids within the material. Due to its smaller intrusion capacity a different pore volume is calculated when nitrogen is used instead of helium. Yet another value is obtained by mercury intrusion porosimetry. By combining these data porosity profiles can be obtained which provide information on the absolute pore volume and the pore size distribution. Figure 4 depicts the different types of the pore volume as percentages of the total particle volume, i.e. the envelope volume. The highest pore volume can be detected with helium, as its atoms have the smallest kinetic diameter of all applied intrusion media. An exception is formulation 1, which shows a pore volume filled by mercury of 21.2%, but a pore volume filled by helium of only 18%. This can also be interpreted as a result of a substantial collapse of the more fragile internal pore structure under the applied pressure during the mercury porosimetry measurement.

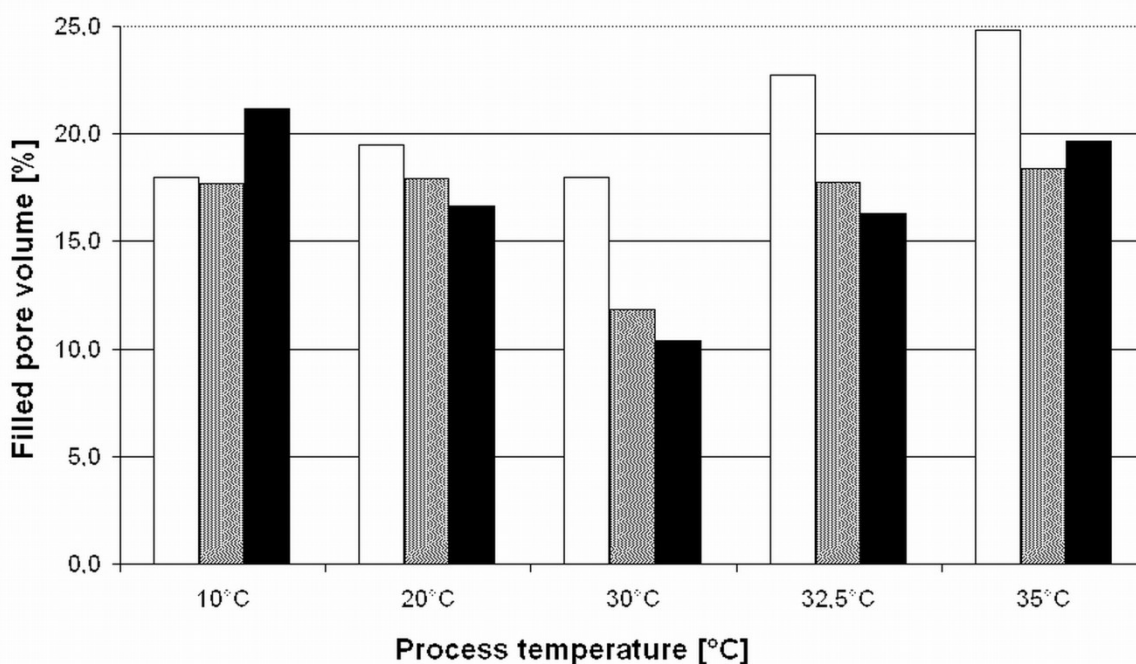


Figure 4: Pore volumes filled by helium (□), nitrogen (▨) and mercury (■)

The volume of these helium-accessible pores shows an increase from 18% for the sample prepared at 10 °C (formulation 1) to 24.8% for the microspheres prepared at 35 °C (formulation 5). Neither the pycnometric data nor the mercury porosimetric measurements reflect this trend because it is almost exclusively caused by the change of the envelope volume. This emphasizes once more the importance of this parameter. In case of formulation 1 and 2 (preparation temperature 10 °C and 20 °C, respectively) there is only little difference between the helium and nitrogen pycnometric data. This is an indication of a coarse pore structure with large pores, embedded in a tightly packed polymer matrix. These particles reveal an open macroporous structure which is highly accessible to all intrusion media (Fig. 2a) and microporosity is very low. Formulation 2 reveals a more graduated pore size distribution with a small fraction of microporosity but more than 85% of the total pore volume consists of voids larger than 3.9 μm .

The presence of a small fraction of micropores in formulations 1 and 2 can be attributed to an incomplete solvent extraction at low temperatures (3% methylene chloride remaining after 6 h extraction). As drying took place at room temperature and thus above the glass transition temperature (21 °C), the PLGA matrix could densify since the polymer chains were still flexible resulting in a loss of microporosity.

During extraction at higher temperatures a densified shell is formed around the particles as can be seen in Fig. 2b [22, 23]. At 30 °C the superficial solidification has to be regarded as a still relatively slow process which passes an extended transitional stage with a fragile polymer skin surrounding the solidifying droplets. Frequent disruptions of this skin resulting in a release of solvent portions and shrinkage of the particles could explain the porosity profile of formulation 3. The total porosity is similar to the one of formulation 1 and 2, but a substantial fraction of micropores is detected, whereas the macro- and mesoporosity is strongly reduced. With an increase in process temperature, the structure changes and the differences between helium and nitrogen measurements become more distinctive. Between 30 and 35 °C the total porosity increases from 18 to 24.8% and a fraction of micropores occurs at 30 °C which is only accessible to helium but not to nitrogen. Expressed as a proportion of the total pore volume, this subfraction of micropores smaller than 0.36 μm increases abruptly from 2-8% up to 22-34% as the preparation temperature reaches 30 °C. This suggests, that the structure becomes finely ramified, so that only small helium atoms can diffuse into the end sections of the pores, whereas they

are inaccessible to nitrogen. These “submicropores” are the main reason for the increase of total porosity at elevated extraction temperatures. At a process temperature above 30°C the polymer matrix is well hydrated and the concentration of residual solvent is very low at the end of the extraction process (< 0.7%). The glass transition temperature is therefore above room temperature (> 31 °C) and the polymer is dried in a rigid state. Under these conditions water acts as a porogen leaving sub-nanometer voids in the places from which water molecules are removed.

In case of all formulations tested nitrogen and mercury fill almost the same fraction of pores. Although nitrogen is able to penetrate into pores which are about 10000 times smaller than those accessible to mercury at 350 kPa the pore volume measured with nitrogen is not more than 1.4% higher than the volume determined with mercury. Helium, however, which atoms are only a little smaller than N₂ molecules with respect to their kinetic diameters, is able to reach an additional pore volume of up to 6.4% compared to nitrogen. This indicates the presence of two separate pore populations, one smaller than 0.36 nm and another larger than 3.8 μm, with not more than 6% of the total porosity lying inbetween. This is the reason for a rather low BET surface area of only 0.41 m²/g. From the particle size distribution the envelope surface area of the microspheres was calculated as 0.07 m²/g which amounts already to 17% of the total specific surface area. Although the microspheres exhibit pores to a substantial degree (Fig. 2) their internal surface area is only about 0.34 m²/g. This can be explained by the fact, that on the one hand macropores larger than 50 μm contribute only little to the surface area and on the other hand the majority of the micropores is smaller than the kinetic diameter of nitrogen and is therefore not accessible to the measuring gas used for the BET measurements.

The appearance of two separate intraparticulate pore populations suggests their formation by different mechanisms. The larger voids are obviously created by shrinkage and rupture of the drying polymer or are a result of larger channels and pockets in the material, which were initially filled with sequestered water [24, 25]. The micropores, by contrast, are the remaining vacancies which are formed when water molecules evaporate from the hydrated polymer [26].

5 Conclusions

As the porosity represents a central feature of microspheres for pharmaceutical use as well as for other applications it is a key to understanding the mechanisms of formation and behavior of such complex structured materials. So far the porosity is often estimated by SEM micrographs, but this method provides only information about the macroporous structures inside the microspheres. Mercury intrusion porosimetry is an established method to determine the specific pore volume and the pore size distribution of solid materials but (i) does not provide any information on the porosity as defined by ASTM, (ii) is not able to distinguish between inter- and intraparticulate porosity, and (iii) is often biased by compression induced structural changes of the specimen. Because of these limitations further techniques are needed to supplement these methods. Our novel combined method is able to determine the porosity according to the ASTM definition (pore volume per total volume) and provides “fingerprints” of the pore size distribution covering a larger size range than any single method. At least three different pore size fractions can be distinguished including micropores smaller than 0.36 nm, in which only helium can diffuse, pores ranging from 0.36 nm to 3.9 μm in which nitrogen, but not mercury can penetrate, and macropores larger than 3.9 μm which are accessible to all intrusion media. With this comprehensive information it is possible to uncover structural properties even in the submicroscopic scale thus gaining deeper insight into the application-specific functionalities of microparticles.

6 References

- [1] Zhang, Y. Preparation of alumina-silica bimodal pore catalysts for Fischer-Tropsch synthesis. *Catalysis Letters* **2005**, *99*, 193-198.
- [2] Leofanti, G.; Padovan, M.; Tozzola, G.; Venturelli, B. Surface area and pore texture of catalysts. *Catalysis Today* **1998**, *41*, 207-219.
- [3] Mao, S.R.; Shi, Y.; Li L.; Xu, J.; Schalper, A.; Kissel, T. Effects of process and formulation parameters on characteristics and internal morphology of poly(D,L-lactide-co-glycolide) microspheres formed by the solvent evaporation method. *European Journal of Pharmaceutics and Biopharmaceutics* **2008**, *68*, 214-223.
- [4] Ghaderi, R.; Stureson, C.; Carlfors, J. Effect of preparative parameters on the characteristics of poly(D,L-lactide-co-glycolide) microspheres made by the double emulsion method. *International Journal of Pharmaceutics* **1996**, *141*, 205-216.
- [5] Klose, D.; Siepmann, F.; Elkharraz, K.; Krenzlin, S.; Siepmann, J. How porosity and size affect the drug release mechanisms from PLGA-based microparticles. *International Journal of Pharmaceutics* **2006**, *314*, 198-206.
- [6] Lemaire, V.; Belair, J.; Hildgen, P. Structural modeling of drug release from biodegradable porous matrices based on a combined diffusion/erosion process. *International Journal of Pharmaceutics* **2003** *258*, 95-107.
- [7] Luan, X.S.; Bodmeier, R. In situ forming microparticle system for controlled delivery of leuprolide acetate: Influence of the formulation and processing parameters. *European Journal of Pharmaceutical Sciences* **2006**, *27*, 143-149.
- [8] Batycky, R.P.; Hanes, J.; Langer, R.; Edwards, D.A. A theoretical model of erosion and macromolecular drug release from biodegrading microspheres. *Journal of Pharmaceutical Sciences* **1997**, *86*, 1464-1477.
- [9] Webb, P. Volume and density determinations for particle technologists. Micromeritics Instrument Corp. **2001**, www.micromeritics.com.
- [10] American Society for Testing and Materials. *Compilation of ASTM Standard Definitions*, **1994**, 8th Edition, Philadelphia.
- [11] British Standards Institution. *British Standard BS2955 Glossary of Terms Relating to Particle Technology* **1991**, London.

- [12] Tonnellier, J. Online-Überwachung der Granulateigenschaften Wassergehalt und Partikelgröße in der Wirbelschicht mit der NIR-VIS-Spektroskopie und Untersuchung zur Porosität von Granulaten mit Quecksilberporosimetrie. **2008**, PhD Thesis. Bonn.
- [13] Webb, P. An introduction to the physical characterization of materials by mercury intrusion porosimetry with emphasis on reduction and presentation of experimental data. Micromeritics Instrument Corp. **2001**, www.micromeritics.com.
- [14] Allen, T. Particle size measurement. **1997**, 5th Ed., p. 251, Chapman&Hall, New York.
- [15] Dees, P.J.; Polderman, J. Mercury Porosimetry in Pharmaceutical Technology. Powder Technology. **1981**, *29*, 187-197.
- [16] Kate, J.M.; Gokhale, C.S.; A simple method to estimate complete pore size distribution of rocks. Engineering Geology **2006**, *84*, 48-69.
- [17] Krus, M.; Hansen, K.K.; Kunzel, H.M. Porosity and liquid absorption of cement paste. Materials and Structures **1997**, *30*, 394-398.
- [18] Burwell, R.L. Manual of Symbols and Terminology for Physicochemical Quantities and Units - Appendix 2 - Definitions, Terminology and Symbols in Colloid and Surface-Chemistry 2., Heterogeneous Catalysis, Pure and Applied Chemistry **1976**, *46*, 71-90.
- [19] Farr, R.S.; Groot, R.D. Close packing density of polydisperse hard spheres. Journal of Chemical Physics **2009**, 131.
- [20] Breck, D.W. Zeolite molecular sieves **1974**, p. 636, Wiley, New York.
- [21] Mikos, A.G.; Thorsen, A.J.; Czerwonka, L.A.; Bao, Y.; Langer, R.; Winslow, D.N.; Vacanti, J.P. Preparation and Characterization of Poly(L-Lactic Acid) Foams. Polymer **1994**, *35*, 1068-1077.
- [22] Jeyanthi, R.; Thanoo, B.C.; Metha, R.C.; Deluca, P.P. Effect of solvent removal technique on the matrix characteristics of polylactide/glycolide microspheres for peptide delivery. Journal of Controlled Release **1996**, *38*, 235-244.
- [23] Allison, S.D. Effect of structural relaxation on the preparation and drug release behavior of poly(lactic-co-glycolic) acid microparticle drug delivery systems. Journal of Pharmaceutical Sciences **2008**, *97*, 2024-2037.
- [24] Nihant, N.; Stassen, S.; Grandfils, C.; Jerome, R.; Teyssie, P.; Goffinet, G. Microencapsulation by Coacervation of Poly(Lactide-Co-Glycolide) 3. Characterization of the Final Microspheres. Polymer International **1994**, *34*, 289-299.
- [25] Li, W.I.; Anderson, K.W.; Mehta, R.C.; Deluca, P.P. Prediction of solvent removal profile and effect on properties for peptide-loaded PLGA microspheres prepared by solvent extraction/evaporation method. Journal of Controlled Release **1995**, *37*, 199-214.

- [26] Yang, Y.Y.; Chia, H.H.; Chung, T.S. Effect of preparation temperature on the characteristics and release profiles of PLGA microspheres containing protein fabricated by double-emulsion solvent extraction/evaporation method. *Journal of Controlled Release* **2000**, *69*, 81-96.

CHAPTER 7

Summary of the Thesis

The objective of this work was to investigate the role and the interactions of the process parameters in a solvent extraction / evaporation process for the preparation of PLGA microspheres containing a poor water soluble drug substance.

For the preparation of the emulsion which is fed into the extraction medium, the solubility of both the drug substance and PLGA play a crucial role for the solidification rate and the crystalline or amorphous state of the drug in the resulting particles. Methylene chloride is one of the most common solvents utilized for in the solvent extraction / evaporation process. On basis of the determined partial solubility parameters of the drug substance and those of PLGA, benzyl alcohol and butanol were chosen as co-solvents for the preparation process. Benzyl alcohol reduced the encapsulation efficiency of the drug substance and rendered crystalline drug substance in the microparticles because its solubility parameters are similar to the ones of the drug substance. This is reflected in a better solubility of the drug substance and its extraction along with the solvent from the particles. In microspheres prepared with butanol the drug substance was present in a completely amorphous state. Despite of the different drug substance morphology, the particles showed an almost identical drug release profile, suggesting that the amorphous drug substance re-crystallizes when aqueous medium diffuses into the particles upon dissolution or in vivo.

The size of the emulsion droplets, respectively of the resulting particles, has also a strong influence on their degradation and drug release rate. The droplet size is mainly determined by the primary emulsion and the parameters used for its preparation. Applying a static mixer these are the pump rates of the organic and the aqueous phase and the number of mixing elements, which split up and recombine the emulsion stream. An efficient way to investigate this process is to plan the study by applying Design of Experiments (DoE). Having a defined composition of the organic and aqueous phase the droplet size is influenced only by the pump rates of both phases and the numbers of mixing elements. The higher the velocities of both

phases are the finer become the resulting emulsion droplets. The number of mixing elements influences strongly the width of the droplet size distribution.

During processing the droplets and forming particles can undergo size and morphological changes. The Focused beam reflectance measurement is a versatile tool to monitor especially the transformation of liquid emulsion droplets to solid particles and occurring surface changes. Furthermore events like the leakage of drug substance into the external medium and its precipitation therein can be detected by this online-measuring technique.

The extraction of the organic solvent and thus the solidification of the emulsion droplets to hardened microparticles are strongly influenced by varying the process temperature of the external phase. As long as the polymer chains stay flexible due to (i) a sufficient amount of organic solvent in the polymer matrix or (ii) a sufficiently high process temperature, above the glass transition temperature of the polymer matrix, the morphology of the particles can change during processing. The rate of solidification in turn has major impact on the final particle size, the encapsulation efficiency and the drug release. A slow removal of the organic solvent from the hardening particles leads to irregularly shaped or broken microspheres and to a leakage of the drug substance into the extraction medium. A certain solidification rate is necessary to encapsulate the drug substance efficiently and to obtain spherical shaped microparticles. A dense microparticle structure is obtained by applying a process temperature, which is above the glass transition temperature of the hydrated and solvated particles. Another process modification is the resuspension of the resulting microspheres in an ethanol-water-mixture, which resulted in a very dense outer shell around a fine porous interior structure.

As the porosity of the polymer matrix strongly determines the degradation rate and the degradation mechanism, it has a major impact on the drug release rate from microparticles. So far it is often estimated by SEM micrographs, a method which provides only information about the macroporous structures inside the microspheres. The mercury intrusion porosimetry is an established method to determine the specific pore volume and the pore size distribution of solid materials but it is not able to distinguish between inter- and intraparticulate porosity, and in case of microspheres structural changes due to compression during the measurement can bias the results of this analytical method. With a novel method, combining the calculation of the envelope volume obtained by a particle sizing measurement based on light obscuration and the skeletal volumes determined by

nitrogen and helium pycnometry and mercury intrusion porosimetry three different pore size fractions could be distinguished. With these porosity “fingerprints” structural properties even in the submicroscopic scale can be detected. This helps to gain deeper insight into the underlying formation mechanisms and the application-specific functionalities of microparticles.

This work describes the structure formation in a solvent removal process and demonstrated different possibilities to modify the particle morphology and functional characteristics at the various process steps. The correlation of different morphologies and the decisive properties of the microspheres, amongst others release of the drug substance, were shown. With special analytical methods a deeper insight into the encapsulation process of a poor water soluble drug substance in a PLGA matrix and the transformation from liquid emulsion droplets to solid particles was obtained.

Annexes

Abbreviations

API	Active pharmaceutical ingredient
ASTM	American Society for Testing and Materials
BET	Brunauer Emmett Teller
BSI	British Standards Institution
CCF	Central composite face-centered
CLD	Chord length distribution
CO ₂	Carbon dioxide
DAD	Diode array detector
DoE	Design of Experiments
DSC	Differential scanning calorimetry
e.g.	for example
GAS	Gas antisolvent process
FBRM	Focused Beam Reflectance Measurement
FDA	Food and Drug Administration (US)
Fig.	Figure
h	hour
i.e.	that is
IUPAC	International union of pure and applied chemistry
Mw	Molecular weight
PAT	Process Analytical Technology
PGSS	Particles from Gas Saturated Solutions process
PLA	polylactide acid
PLG	polyglycolid acid
PLGA	poly(lactide-co-glycolid) acid
PVA	polyvinyl alcohol

PVC	polyvinylchloride
PSD	particle size distribution
RED	Relative Energy Difference
r.h.	relative humidity
resp.	respectively
RT	room temperature
SAS	Supercritical antisolvent process
SCF	supercritical fluid
SEDS	Solution Enhanced Dispersion by Supercritical Fluids
SEM	Scanning electron microscopy
SPOS	Single Particle Optical Sensing
Sqr. wt	Square weighted
Tab.	Table
T_g	Glass transition temperature
Tris	tris(hydroxymethyl)aminomethane
XRPD	X-ray powder diffraction

List of publications and presentations

JOURNALS

Vay,K.; Scheler,S.; Friess,W. New insights into the pore structure of poly(D,L-lactide-co-glycolide) microspheres. *International Journal of Pharmaceutics* **2010**, *402* (1-2), 20-26.

Vay,K.; Scheler,S.; Friess,W. Application of Hansen solubility parameters for understanding and prediction of drug distribution in microspheres. *International Journal of Pharmaceutics* **2011**, *416* (1), 202-209.

Vay,K.; Friess,W.; Scheler,S. A detailed view of microparticle formation by in-process monitoring of the glass transition temperature. *European Journal of Pharmaceutics and Biopharmaceutics* **2012**, *81* (2), 399-408.

Vay,K.; Friess,W.; Scheler,S. Understanding reflection behavior as a key for interpreting complex signals in FBRM monitoring of microparticle preparation processes. *International Journal of Pharmaceutics* **2012**, *437* (1-2), 1-10.

POSTER AND PRESENTATIONS

Vay,K.; Scheler,S.; Friess,W. In-process particle size analysis with FBRM for monitoring a microparticle preparation process, poster presentation, International Graz Congress for Pharmaceutical Engineering, Graz, 2009.

Vay, K. Scheler, S. A novel method for the determination of the intraparticle pore volume of microspheres, poster presentation, 1st Sandoz R&D Day, Holzkirchen, 2009.

Vay, K. A novel method for determination of the intraparticle pore volume of microspheres, oral presentation, International Graz Congress for Pharmaceutical Engineering, Graz 2010.